Runoff simulation using the SWAT model for flood frequency analysis and design flood estimations in the Luvuvhu River catchment, South Africa

by

Mulalo Precious Thavhana

submitted in fulfilment of the academic requirements of the degree of

Master of Science in Agriculture

in Agrometeorology

Soil-Plant-Atmosphere-Continuum Research Unit

School of Agricultural, Earth and Environmental Sciences

College of Agriculture, Engineering and Science

University of KwaZulu-Natal

Pietermaritzburg

South Africa

Supervisor: Professor MJ Savage

Co-supervisor: Dr ME Moeletsi

March 2018

PREFACE

The research contained in this dissertation was completed by the candidate while based in the Discipline of Agrometeorology, School of Agricultural, Earth and Environmental Sciences of the College of Agriculture, Engineering and Science, University of KwaZulu-Natal, Pietermaritzburg, South Africa. The research was financially supported by the Agricultural Research Council Professional Development Program and the Water Research Commission.

The contents of this work have not been submitted in any form to another university and, except where the work of others is acknowledged in the text, the results reported are due to investigations by the candidate.

Signed: Professor MJ Savage

Date: _20th March 2018_____

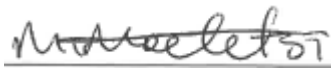

Signed: Dr ME Moeletsi

Date: __8th March 2018_____

DECLARATION 1: PLAGIARISM

I, Mulalo Precious Thavhana, declare that:

(i) the research reported in this dissertation, except where otherwise indicated or acknowledged, is my original work;

(ii) this dissertation has not been submitted in full or in part for any degree or examination to any other university;

(iii) this dissertation does not contain other persons' data, pictures, graphs or other information, unless specifically acknowledged as being sourced from other persons;

(iv) this dissertation does not contain other persons' writing, unless specifically acknowledged as being sourced from other researchers. Where other written sources have been quoted, then:

a) their words have been re-written but the general information attributed to them has been referenced;

b) where their exact words have been used, their writing has been placed inside quotation marks, and referenced;

(v) where I have used material for which publications followed, I have indicated in detail my role in the work;

(vi) this dissertation is primarily a collection of material, prepared by myself, published as journal articles or presented as a poster and oral presentations at conferences. In some cases, additional material has been included;

(vii) this dissertation does not contain text, graphics or tables copied and pasted from the Internet, unless specifically acknowledged, and the source being detailed in the dissertation and in the References sections.

Signed: Mulalo Precious Thavhana

Date: __8th March 2018_____

DECLARATION 2: PUBLICATIONS

My role in each paper and presentation is indicated. The * indicates corresponding author.

1. Thavhana MP, Savage MJ*, Moeletsi ME. 2016. Simulation of runoff for the Luvuvhu catchment of South Africa using the SWAT model. Poster presentation to the 17th WaterNet/WARFSA/GWP-SA symposium, 26th to 28th October 2016, Gaborone, Botswana. Poster presented by MP Thavhana.
2. Thavhana MP, Savage MJ*, Moeletsi ME. 2017. Runoff Simulation using the SWAT Model for Flood Frequency Analysis and Design Flood Estimations in the Luvuvhu River Catchment, South Africa. Oral presentation to the 33rd Annual Conference of South African Society for Atmospheric Sciences, 21st to 22nd September 2017, Limpopo, South Africa. Oral presentation by MP Thavhana.

Signed: Mulalo Precious Thavhana

Date: __8th March 2018_____

ABSTRACT

Fatal flood events around the world have led to the execution of many projects in an attempt to solve some of the prevailing flood control problems. These studies have identified an increase in the frequency of flood events over the years. The increases accompanied by hydrological alteration and rainfall variation may have great effects on future flood design and planning. This study focuses on the Luvuvhu river catchment in the Limpopo province of South Africa, which has been identified and considered vulnerable to flooding.

The soil and water assessment tool (SWAT) was used to simulate daily streamflows (runoff) of the Luvuvhu River catchment. The model was executed through an interface between SWAT and QGIS desktop 2.6.1 software, QSWAT 1.3 2016. The model was run for a 33-year period of 1983 to 2015. Having compared observed streamflow data with the simulated data, the initial streamflow evaluation was unsatisfactory and the model needed to be calibrated and validated.

Sensitivity analysis, calibration and validation were conducted using the SUFI-2 algorithm through its interface with SWAT calibration and uncertainty procedure (SWAT-CUP). The calibration process was conducted for the period 1986 to 2005 while the validation process was from 2006 to 2015 inclusive. A minimum of 300 simulations were performed for each run. The model performance to simulate runoff was based on four objective functions coefficient of determination (R^2), Nash–Sutcliffe efficiency (NSE) index, root mean square error (RMSE)-observations standard deviation ratio (RSR) and percent bias (PBIAS) and two performance indices probability (*P*)-factor and correlation coefficient (*R*)-factor.

During the calibration period, the model produced a *P*-factor of 0.64, 0.52, 0.67, and 0.45 and an *R*-factor of 0.59, 1.81, 0.68 and 0.91 for the four sub-catchments. The objective function results revealed an R^2 of 0.61, 0.73, 0.63 and 0.75, an NSE index of 0.35, -16.46, 0.66 and -0.36, an RSR of 0.62, 3.23, 0.56 and 0.71 and a PBIAS of 1.18, -7.60, 16.30 and -2.10 for the sub-catchments. During the validation period, the model produced a *P*-factor of 0.59, 0.34, 0.69 and 0.41 and an *R*-factor of 0.46, 2.67, 0.53 and 0.75 for the sub-catchments. The objective function results revealed an R^2 of 0.34, 0.63, 0.52 and 0.62, an NSE index of 0.35, -0.45, 0.48 and 0.31, an RSR of 0.86, 1.14, 0.72 and 2.10 and a PBIAS of 65.0, -12.30, 19.90 and -14.60 for the sub-catchments.

Predominantly, parameter ranges of the *P*-factor and *R*-factor reached desired limits indicating considerable parameter uncertainties results, which were acceptable. Moreover, model uncertainties were falling within the permissible limits, which signified the capability of SUFI-2 to capture the model's behaviour. Objective functions analysed performed well during both calibration and validation. For this reason, results obtained in this study demonstrated acceptable model performance and acceptable accuracy of the model in runoff simulation. It can be concluded that SWAT simulation results were satisfactory for runoff simulation in the Luvuvhu catchment.

Flood frequency analysis and design flood estimation were completed following model validation. This was accomplished using a 30-year period of simulated flood discharge from the SWAT model. A log-normal probability distribution was used to fit the maximum annual peak data to estimate flood frequencies. Focusing on a sub-catchment, the Luvuvhu catchment outlet, 50, 100 and 200-year floods revealed flood magnitudes of 960.70, 1121.02 and 1281.35 m^3 s^{-1} respectively. The results obtained from the frequency analysis would assist in the planning and designing purposes of the catchment, to mitigate and adapt during flooding season.

ACKNOWLEDGMENTS

To my Father, my Lord and Saviour Jesus Christ. This would have been impossible without you. You have been my constant help and faithful guide when the road seemed too narrow and too dark to see. You were the light that kept shinning even when the goal appeared to be extremely difficult to reach, you remained the God of possibilities. Your unfailing love and unshakable word kept me strong and full of hope. In this, may your name be glorified. Thank you.

I would like to thank my supervisors, Professor MJ Savage and Dr ME Moeletsi for your support and supervision. Your leadership and efforts in this study have been impeccable and I am grateful. May God continue to bless you both.

A great thank you to my mother, NG Maguga for being the source of inspiration that keeps me going when I start to fear and waver. I am grateful to all the sacrifices and prayers you make each day for me to succeed. Thank you to my aunt, FD Maguga for the encouragements and the constant phone calls. All your advices I have heeded in my heart. Thank you to my brother Nnyambe and my sisters Mbavhi, Vhoni and Tendi for always being there for me to lend an ear when I got frustrated and anxious.

Thank you to all my friends who have supported me ever since I started with this journey. I appreciate all the efforts you have made to emotionally support and cheer me.

Thank you to the Agricultural Research Council, Institute for Soil Climate and Water (ARC-ISCW) agrometeorology division for your support.

Thank you to Dr M Tsubo for finding time to look through my dissertation and correct the mistakes. Your time and efforts are highly appreciated.

A special thank you to the ARC Professional Development Program for funding my studies and giving me the opportunity to study further.

Finally yet importantly, I would like to thank the Water Research Commission for funding the project.

TABLE OF CONTENTS

Page

LIST OF TABLES

Table **Page**

LIST OF FIGURES

Figure **Page**

CHAPTER 1: INTRODUCTION

1.1 General background

Flooding has often been identified as a natural, climatic and recurring event, during which an area of land is covered with an extensive amount of water, over a short period of time (Gichere *et al*., 2013). This occurs depending on the parameters that govern the flood phenomena such as: rainfall amount, catchment area and soil antecedent moisture content, to name a few (Alexakis *et al*., 2012; Gichere *et al*., 2013). In some cases, this type of event is not natural in its cause, but rather, anthropogenic (Tshikolomo *et al*., 2013). For example, the bursting of a dam wall or a water pipeline in an impervious area, may also lead to flooding (Kozlovac, 1995; Etuonovbe, 2011). In most cases flooding is caused by an event whereby heavy and continuous rainfall occurs for an extended period of time, which then exceeds the infiltration capacity of soil or flow capacity of rivers, streams, and coastal areas, thus resulting in runoff (Hirschboeck *et al*., 2000; Ezemonye and Emeribe, 2011; Singo *et al*., 2012; Tshikolomo *et al*., 2013). The runoff produced from this climatic condition (heavy rainfall) may then cause the catchment to respond in a manner that results in flooding (O'Connell *et al*., 2007; Warburton *et al*., 2010).

The geographical distribution of river flood plains may also have an influence on flood occurrence (Smith, 2001) and according to Hart *et al*. (2013) and Wetterhall *et al*. (2015), South Africa's rainfall distribution varies considerably both spatially and temporally, which has led to more floods across the country (Kane, 2009). The frequency and distribution of floods is usually defined by the cycle of El-Niño southern oscillation (ENSO) events where ENSO is an irregular phenomenon that recurs every 2 to 7 years (Kane, 2009; Trenberth, 2011). The phenomenon accounts for the extreme variability of climate in the global climate system (Allan, 2000). ENSO is often associated with rainfall in most parts of the southern African region, interchanging between two extremes known as El Niño (drought) and La Niña (floods) events (Allan, 2000; Moeletsi *et al*., 2011). The two events, El Niño and La Niña differ in magnitude, area of impact, onset, duration and cessation (Davis and Joubert, 2011).

Although some floods may be accounted for by climate change, documentation and classification of the different types of floods exists, including among others river floods, flash floods, structural failure, urban drainage and coastal flooding (**Table 1.1**) (DePue, 2010; Sauer, 2011). According to the South African Weather Service (SAWS), examples of floods that have occurred throughout South Africa over the past years displaying some characteristics

mentioned in (**Table 1.1**) include floods which occurred in the years: 1980, 1984, 1987, 1995, 2000, 2007 and 2010/2011(Dyson, 2009; Zuma *et al*., 2012).

Table 1.1 Different types of flooding and their characteristics (DePue, 2010)

FLOOD TYPE	CAUSE	IMPACT	DURATION
River floods	Inability of the river system to carry certain amount of flows due to heavy rains or prolonged rains.	Floodplain areas along the river banks.	Slow onset and may last for a short or long period depending on rainfall characteristics.
Flash floods	Heavy and localised rainfall over a short period of time, in a steep or impervious catchment. Closely linked with structural failure.	Destruction of infrastructures such as bridges and roads.	Quick onset and last over a short period of time, but impacts are severe.
Structural failure	Structure failure after periods of heavy rainfall in a catchment due to inadequate structure design, or the dam design structure capacity has been exceeded.	Area along the structure and downstream residence if it is a dam.	Quick onset, occurring without warning and over a short period of time.
Urban drainage	The drainage is unable to handle the floods due to heavy and localised rainfall, or the design has been exceeded.	Urban areas and residence.	Bursting of pipes, without warning over a short period of time.
Coastal flood	Hurricanes and tropical cyclones along the coastal lines.	Impacts along the coastal area and may extend into the inland.	Quick onset and flooding may last for a long period.

Fatal flood events around the world have led to the execution of many projects in an attempt to solve some of the prevailing flood control problems (Krzhizhanovskaya *et al*., 2011). These studies have identified an increase in the frequency of flood events over the years, with climate change being one of main root causes (Millington *et al*., 2011; Aronica *et al*., 2012; Norouzi and Taslimi, 2012; Xie *et al*., 2012). The increases accompanied by hydrological alteration and rainfall variation may have great effects, not only on dam and bridge designs, but also on future food security production due to reduced yield (Lauer, 2008; Millington *et al*., 2011 Sauer, 2011; Syaukat, 2011). Floods usually occur with no warning, and under future climate conditions, flood frequency is expected to increase even further (Kang *et al*., 2009). For this reason, it is essential for hydrologists and engineers to be able to predict the magnitude and frequency of floods for planning and mitigation (Chetty and Smithers, 2005; Geoscience Australia, 2013).

This study focuses on the Luvuvhu river catchment in the Limpopo province of South Africa, which has been identified and considered vulnerable to flooding (Muinga, 2004). As much as flood events have been occurring more frequently in the world (Xie *et al*., 2012), the Luvuvhu catchment is no exception. The catchment's vulnerability to flooding is said to be caused by tropical depressions and the geographical distribution of river floodplains (Smith, 2001; Muinga, 2004; Wetterhall *et al*., 2014). This has led to the catchment experiencing extreme flooding events over the past years; washing away some of the crops and thus resulting in crop failure and reduced crop yield (**Figure 1.1**). A large portion of the catchment is under subsistence agriculture, and the remainder of the catchment is woodlands, mining and communal lands (**Table 1.2**) (Jewitt *et al*., 2004; Warburton *et al*., 2010). Intensive irrigation farming is practiced in the catchment, where vegetables, citrus and a variety of fruits such as bananas, mangoes, avocados and nuts are grown (Hall, 2008). State and privately owned forestry plantations (pine, eucalyptus and wattle) are located at the south of the Soutpansberg (Jewitt *et al*., 2004).

The Luvuvhu river catchment, along with the Letaba river catchment, forms part of the Luvuvhu/Letaba Water Management Area (WMA), which is one of the 19 WMAs in South Africa, delineated and acknowledged by the South African Department of Water and Sanitation (DWS) (Jewitt *et al*., 2004; Masereka *et al*., 2015). The catchment consists of 14 Water Management Units (WMU), which are demarcated according to quaternary catchments (QCs)

and have been adjusted to account for streamflow gauging stations (Warburton *et al*., 2010). The Luvuvhu catchment is subdivided into 14 DWS QCs (Jewitt *et al*., 2004) (**Figure 1.2**).

Figure 1.1 Sanari area in the Luvuvhu catchment experiencing 2016/2017 flooding (Photo: Teboho Masupha)

Table 1.2 Land use/cover in the Luvuvhu River catchment according to Jewitt *et al.* (2004) and Warburton *et al.* (2010)

Land use (% of area)	Jewitt *et al*. (2004)	Warburton *et al*. (2010)
Natural vegetation	-	62.5
Water bodies	-	0.2
Degraded areas	-	8.1
Commercial forestry	4.0	6.0
Commercial agriculture (Irrigated)	-	3.0
Subsistence agriculture	-	15.8
Informal residential areas	-	4.4
Protected game reserve areas	30	-
Urban areas	3	-
Cultivated lands	13	-
Subsistence agriculture and grazing	50	-

1.2 Technical background

1.2.1 Hydrological models

Hydrological models have been developed over the years in order to understand the different aspects that occur in a hydrological system (**Figure 1.3**) (Chow *et al*., 1988). When designing a hydrological model, the main aim is to improve the understanding of the hydrological system on how changes, such as climate, land use and soil changes, may affect the system (Xu, 2002). In order to understand the phenomenon of a hydrological system, hydrological models are used

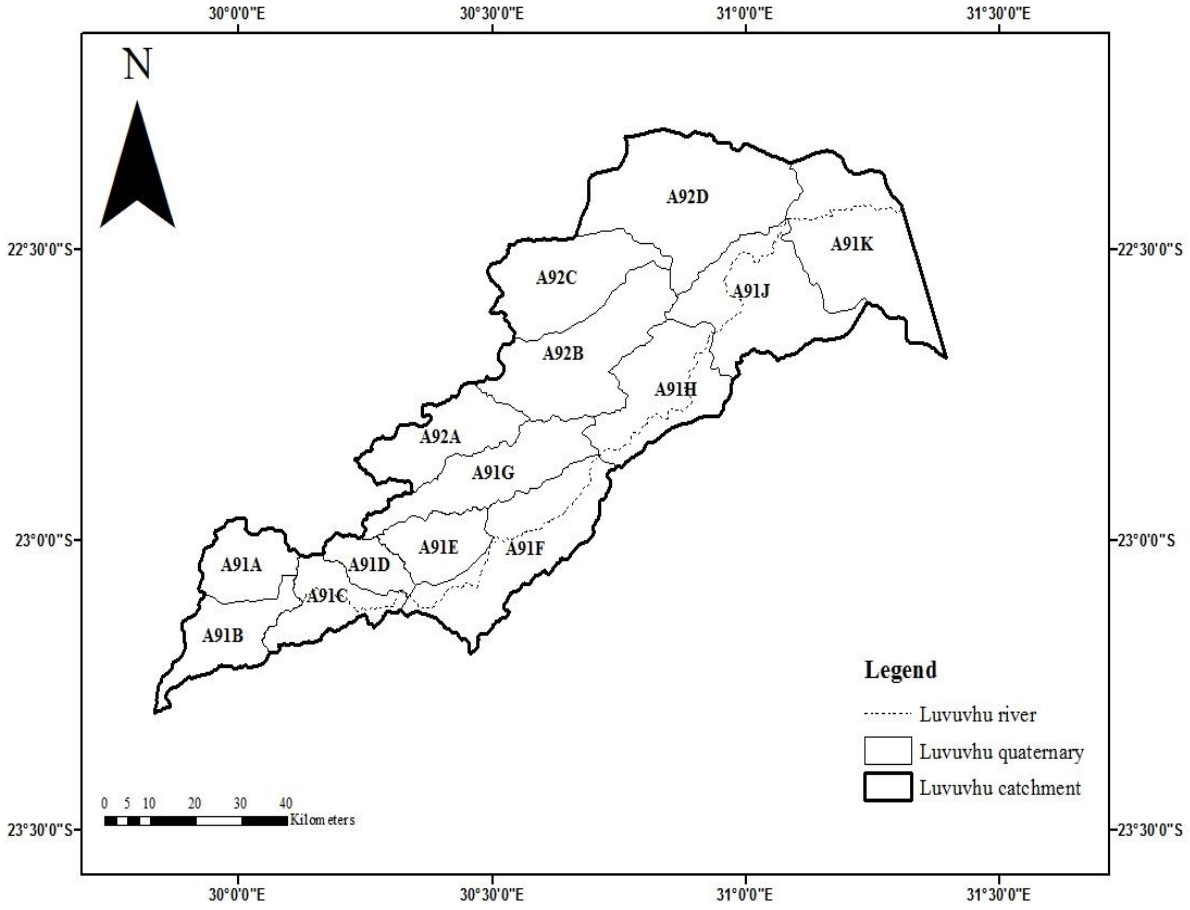

Figure 1.2 Luvuvhu River and quaternaries

to simulate the catchment's responses to the various changes of climate, land use and soil (Leavesley *et al*., 1983; Viessman *et al*., 1989). Hydrological simulation may be used in flood frequency studies by modelling how the climate, land use and soil changes may affect flood occurrence in the future (McCuen, 2003). When modelling, one needs to be cognisant that the simulations are not real, but rather projected values to better understand and predict future scenarios (Smithers *et al*., 1997; McCuen, 2003; Chetty and Smithers , 2005).

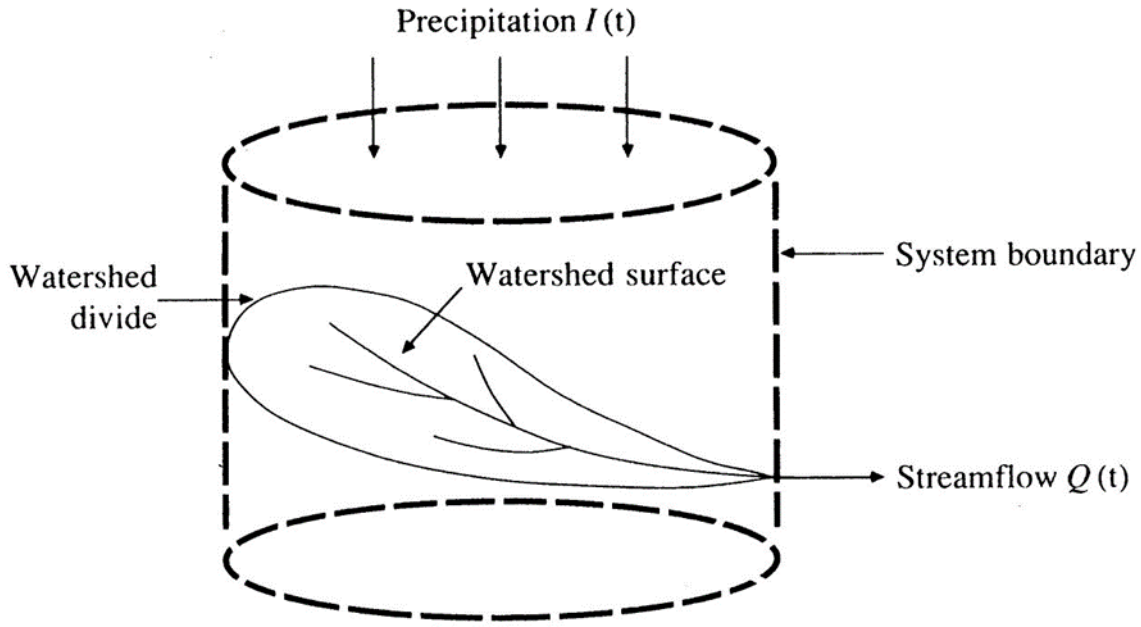

Figure 1.3 A catchment as a hydrological system (Chow *et al.*, 1988)

Choosing the appropriate model to use in hydrological studies requires full knowledge of expected results, and hence assistance from experts and specialists is required (Viessman *et al*., 1989; Lundin *et al*., 2000). Apart from expert knowledge, most hydrological models do not operate on their own, but require other software to operate (de Jong van Lier *et al*., 2005). In most cases geographic information system (GIS) is a system that is most relevant and highly used to complement hydrological applications (Fadil *et al*., 2011). A 2012 version of the SWAT model was used in this study to simulate runoff in order to estimate flooding in the Luvuvhu catchment. The SWAT model was run through an interface with a QGIS desktop 2.6.1 software, QSWAT 1.3 2016.

1.3 Main objectives

This study aims to estimate design flood peaks in the Luvuvhu River catchment in Limpopo province, South Africa. This will be conducted through the simulation of runoff using QSWAT 1.3 2016, an interface between the 2012 version of the SWAT model and QGIS 2.6.1 software.

1.4 Specific objectives

- To choose a hydrological model (QSWAT) that will best simulate streamflow using observed climate, land use and soil data.

- To conduct streamflow simulation from historical climate data using QSWAT to check how best the model mimics the Luvuvhu River catchment.
- To conduct calibration and validation of the model using observed data of Luvuvhu river catchment for a better model representation of the catchment.
- To conduct flood frequency analysis and design flood estimation for the Luvuvhu River catchment using simulated data from the SWAT model in order to estimate flooding in the catchment.

1.5 Thesis layout

Chapter 1 focuses on introducing the concept of a flood, its impacts and why the phenomenon should be studied. The study area is also introduced, giving reasons for the choice of the study area. Some historical background on hydrological models is also reviewed in this chapter.

Chapter 2 informs the reader about hydrology, hydrological models and hydrological modelling. Different hydrological models that have been applied in previous studies are reviewed. A review on calibration process and sensitivity analysis is also presented.

Chapter 3 is an in-depth record of the methods taken to achieve the objectives of the study. Here the method focuses mostly on the application of the SWAT model, the SWAT-CUP and the SUFI-2 algorithm. The use of log-normal distribution for flood frequency analysis is explained in this chapter.

Chapter 4 presents the results obtained in the execution of SWAT model in the form of reports, tables and graphs. Furthermore, flood frequency analysis results are expressed in this chapter.

Chapter 5 accounts for and explains the results obtained through a discussion and also gives recommendations for future research and application.

CHAPTER 2: LITERATURE REVIEW

2.1 Climate change

South Africa is considered a semi-arid region with greatest rainfall vulnerability in provinces such as the Eastern Cape, KwaZulu-Natal, North-West and Limpopo (Zuma *et al*., 2012; Hart *et al*., 2013). High intra-seasonal and inter-annual rainfall variability has led to extreme events such as floods occurring more frequently (Davis and Joubert, 2011). There have been several natural disaster events in South Africa between 1980 and 2014, and within these decades, flooding has occurred many times including the years 1981, 1987, 1994, 2000 and 2013 (Moodley, 2014).

Numerous studies have been conducted to identify the connection between rainfall anomalies that could lead to flooding in South Africa and the El Niño-southern oscillation (ENSO) phenomenon (Tennant and Hewitson, 2002; Kane, 2009). Furthermore, it has been established that South African rainfall is not equally distributed spatially and temporally (Hart *et al*., 2013) and according to Moeletsi *et al*. (2011) this causes extreme rainfall in La Niña years and may lead to flooding. A study done by Warburton *et al*. (2011) revealed that such climate change phenomena have a significant impact on hydrological responses of a catchment. This was further confirmed by a study done by Gaur (2013) where even small changes in climate variables showed results of significant impact on hydrological characteristics of a catchment. According to such findings, it can be ascertained that climate change continues to be one of the greatest challenges in terms of hydrological responses with an annual risk of flooding of 83.3% in South Africa (Zuma *et al*., 2012).

Climate change alters the magnitude, spatial and temporal distribution of storms that produce flood events (Davis, 2011). This is through increases in air temperature and rainfall which thus influence the increase in frequency and magnitude of flood occurrences (Tadross M *et al*., 2009; Millington *et al*., 2011). According to Kang *et al*. (2009), these frequencies will continue to increase under future climatic conditions. Therefore, continuous studies to predict magnitude and frequency of floods remain essential (Chetty and Smithers, 2005).

2.2 Hydrology

Hydrology is the study of water and its movement in a catchment (Tessema, 2011). The study focuses on various pathways such as the occurrence, distribution and disposal of water in a

hydrological system (Raghunath, 2006). Hydrology focuses on processes such as runoff that may occur in a hydrological system (Tessema, 2011). Understanding of the hydrology concept is achieved through monitoring water movement, speed and discharge in a catchment (Els, 2011). Processes and interactions that govern the hydrological system are considered, bearing in mind the physical characteristics of the catchment (Els, 2011). It is important to study hydrology especially under changing climate caused by global warming since hydrology plays a great role in factors affecting human life (Pilgrim *et al*., 1988; Seibert, 1999). Moreover, hydrology plays an important role in the estimation of flood occurrence probability and frequency, which are essential for planning, and management purposes (Rogger *et al*., 2012; Gericke and du Plessis, 2013).

In a hydrological system, input variables such as rainfall interact with the physical, chemical and/or biological processes to produce output variables such as runoff (Xu, 2002). These interactions are referred to as the hydrologic cycle (**Figure 2.1**) (Raghunath, 2006). The hydrological cycle is expressed through the hydrologic equation, a law of conservation explaining processes in the hydrological system, (Raghunath, 2006):

$$I = O + \Delta S \tag{2.1}$$

where I is the total inflow (m^3) in a given area, O is the total outflow (m^3) from that area and ΔS is the change in storage (m^3).

The hydrologic equation is generally influenced by the water balance, (Rasiuba, 2007):

$$P = R + ET + {}^{\Delta S}/_{\Delta t} \tag{2.2}$$

where P is precipitation in mm a^{-1}, R is the runoff in mm a^{-1}, ET is the evapotranspiration in mm a^{-1} and ${}^{\Delta S}/_{\Delta t}$ is the storage changes per time step in mm a^{-1}. In this hydrological equation, events such as evapotranspiration and runoff that play a great role in the hydrologic cycle are captured and expressed through equations of their own (Latha *et al*., 2010):
Evapotranspiration is represented in the shortened surface energy balance equation (Ncube, 2006):

$$R_n = \lambda E + H + G \tag{2.3}$$

where R_n is the net radiation, λE is the latent heat (evapotranspiration; ET), H is the sensible heat flux and G is the soil heat flux.

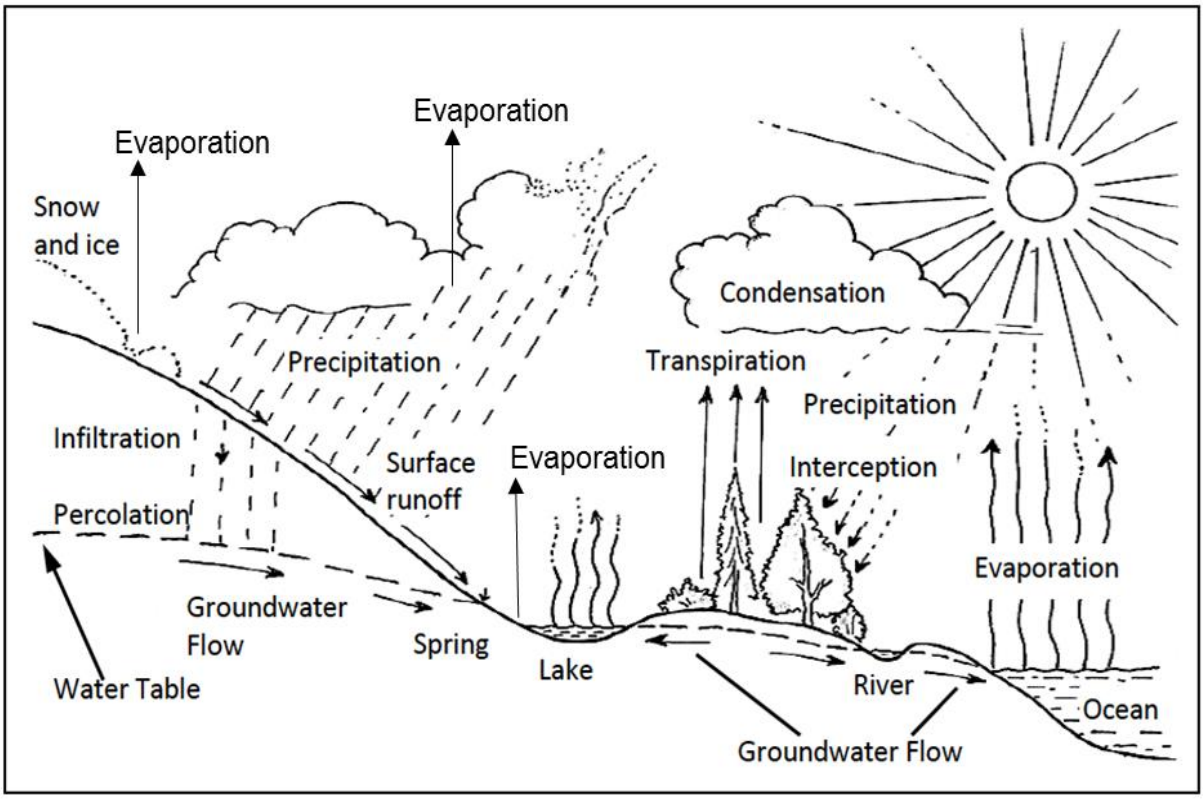

Figure 2.1 The hydrological system and the water cycle (Source: Zhang *et al*., 2002)

Runoff is expressed through the SCS curve number (Xiao *et al*., 2011; Soulis and Valiantzas, 2012):

$$Q_{surf} = \frac{(R_{day} - I_a)^2}{(R_{day} - I_a + S)} \tag{2.4}$$

where Q_{surf} is the accumulated runoff (mm), R_{day} is the rainfall depth (mm), I_a is the initial abstraction (surface storage, interception and infiltration) (mm) and S is the retention parameter (varies due to change in soils, land use and management) (mm).

The above equations are essential for hydrological modelling since they are drivers of most hydrological models that have been developed over the past years (Ncube, 2006). Hydrological modelling has become a well-used technique in hydrology to improve the understanding of processes that occur in a hydrological system (Praskievicz and Chang, 2009).

2.3 Hydrological modelling

Hydrological systems are very complex and not easily understood; hence, to overcome this, hydrologists have resorted to hydrological modelling which is a much simpler way of representing the hydrological system (Xu, 2002; Woessner, 2012). Hydrological modelling entails the use of mathematical equations to present the hydrological system and the processes that occur in the hydrological cycle (Woessner, 2012). Investigations on hydrological factors such as design flood, flood frequency and water quality may be achieved by the many ways of hydrological modelling (Todini, 2007; Smithers, 2012; Ahn *et al*., 2014). Due to data availability or lack thereof, different methods of hydrological modelling have been developed around the world and their applications vary (Chetty and Smithers, 2005; Ball, 2012). For example, in order to estimate for design flood, certain paths according to Smithers and Schulze (2001) can be followed (**Figure 2.2**).

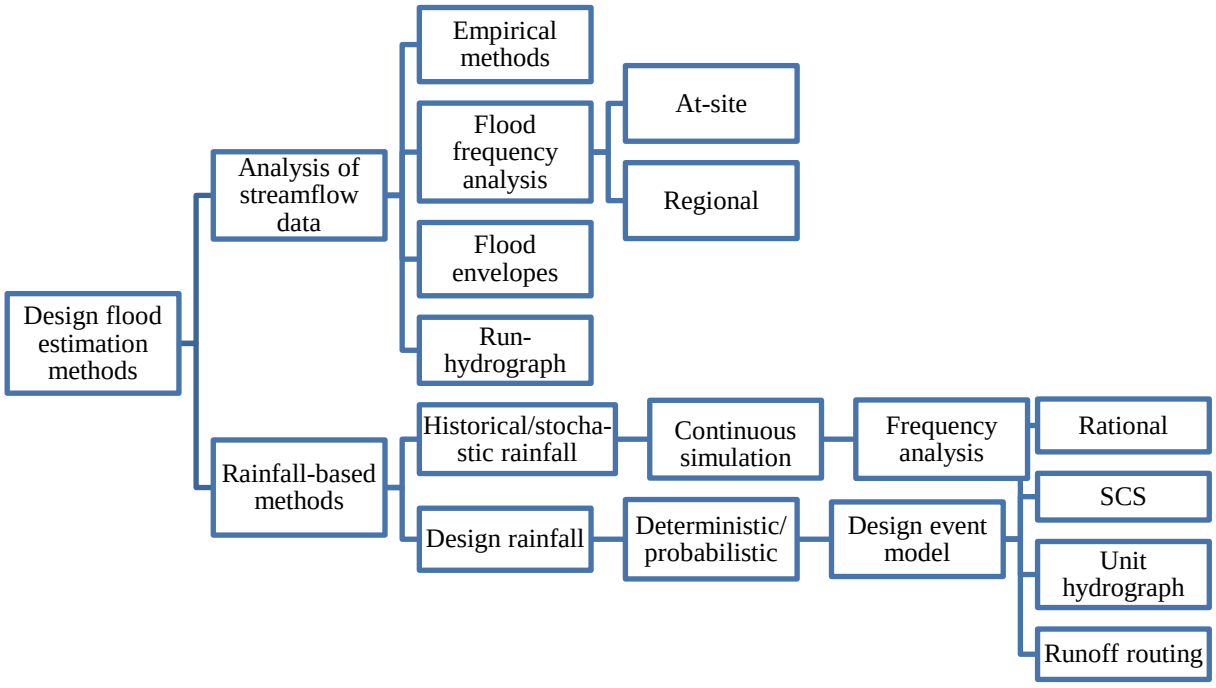

Figure 2.2 Different methods for estimating design flood in South Africa (Source: Smithers and Schulze, 2001)

2.3.1 Flood frequency analysis and design flood estimation

Flood estimation approaches are usually twofold: an analysis of observed floods, and rainfall-based methods (Smithers, 2012). A number of probabilistic approaches including flood frequency statistics and design storm method can estimate design floods for a given location at a stream (Rogger *et al*., 2012). These probabilistic methods are most applicable where there

are sufficient streamflow data, and in such cases use of empirical equations, unit hydrograph and/or flood frequency analysis methods are applied (Chetty and Smithers, 2005; Smithers, 2012) (**Figure 2.2**). Alternatively, in the case where there is inadequate streamflow data, for example, short duration recorded streamflow data, rainfall-runoff models (rainfall based methods) are thus more applicable (Smithers *et al*., 1997; Chetty and Smithers, 2005).

Flood frequency analysis method is more of a statistical procedure whereby flood frequency distribution is fitted to observed flood peaks (Rogger *et al*., 2012). The procedure analyses the statistics of observed flood events by means of determining and estimating flood magnitudes at different exceedance probability or recurrence intervals (Hirschboeck *et al*., 2000; Atroosh and Moustafa, 2012; Waghaye *et al*., 2015). The probability of exceedance is the percentage chance that a given flood magnitude will be exceeded in any year while the recurrence interval is the reciprocal of percent probability of exceedance divided by 100 (Walker and Krug, 2003). Flood magnitude with a return period of *T* years is expected to equal or be exceeded, on average, once every *T* years (Kay *et al*., 2009).

According to Smithers *et al*. (2013), design flood estimates and flood frequency analysis are important for planning and design purposes. Therefore, it is essential that peak flow estimates for varying return periods be accurate in order for the planning to reduce flood damage (Viviroli *et al*., 2009). Hydrologists have been using annual flood-peak data to monitor flooding and to evaluate the probability of occurrence of flood of a given magnitude (Hirschboeck *et al*., 2000). The problem with flood frequency method is that it requires long and continuous streamflow data, which is generally unavailable in most cases (Stedinger, 2000). It is thus important to use statistical techniques and available historic information to improve estimated flood and flow frequency relationship (Baker, 2000). This entails determining distribution pattern and estimating cumulative distribution functions to calculate extreme flood values that may occur in the future (Millington *et al*., 2011; Atroosh and Moustafa, 2012).

It is essential that a probability distribution that provides a good fit for streamflow data be established in order to attain and interpret the probability occurrence and return period results (Mzezewa *et al*., 2010; Gamage *et al*., 2013; Waghaye *et al*., 2015). There are two most widely used probability distributions in hydrologic analysis, and they are the log normal and log-Pearson Type 3 distributions (McCuen, 2003). Frequency curve provides a probabilistic description of the likelihood of occurrence or non-occurrence of variables (McCuen, 2003). For concave and upward curve, a log normal distribution is more applicable while a large

sample requires an estimate of the skew coefficient distribution such as the log-Pearson type 3 distribution (McCuen, 2003). Frequency analysis is used for data record more than 10 years (Viessman *et al*., 1989; Walker and Krug, 2003).

2.4 Classification of hydrological models

Hydrological models are said to be the application of scientific methods to represent and quantify hydrological processes in the hydrological system (Lundin *et al*., 2000; Woessner, 2012). There are different types of models used in hydrological modelling and flood predictions and they are classified based on model input, parameters and extent to which physical principles are applied (Viessman *et al*., 1989; Gayathri *et al*., 2015). Hydrological models are classified and differentiated between *empirical, conceptual* and *theoretical* models, between *lumped* and *distributed* models and between *deterministic* and *stochastic* models (Refsgaard, 1996).

2.4.1 Distinction between empirical, conceptual and theoretical models

2.4.1.1 Empirical models

The empirical model is commonly known as the black box or the input-output model. This is because the model's properties do not resemble any physical characteristics nor do they consider any physical laws that govern the processes in a hydrological catchment (Leavesley *et al*., 1983; Refsgaard, 1996; Xu, 2002). Simple mathematical equations fall under this model category and the main advantage is that the model is very simple and parameter-efficient (Ye *et al*., 1997). However, the disadvantages are that the model does not have any physical representation and neither does it capture the essential response characteristics of a catchment (Ye *et al*., 1997). Examples of an empirical model is a unit hydrograph for streamflow routing and the SCS runoff curve number method in equation 2.4 (Refsgaard, 1996; Aghakouchak and Habib, 2010).

2.4.1.2 Conceptual models

A conceptual model is usually referred to as a grey box, mostly because it captures some parts of the physical elements of the catchment by averaging the catchment's parameters and variables (Refsgaard, 1996; Xu, 2002). Hence, conceptual models rely on probability to interpret the processes that occur in the catchment which do not fully represent the physical

processes (Viessman *et al.*, 1989; Woessner, 2012). Although too much theory and assumptions may over-simplify the physical laws, according to Ramirez (2000), conceptualisation can still be useful in producing adequate estimates of flood hydrograph.

Advantages

- Few input data requirements
- Computationally fast
- Interface easily with GIS databases
- Use simple inputs and hence can be easily developed without much understanding of the modelled phenomenon

Disadvantages

- Sometimes assumptions may be false
- Physical interpretation is often unclear

Example of a conceptual model is the topography based hydrological model (TOPMODEL) (Seibert, 1999). The underlying assumptions governing the TOPMODEL are (Beven, 1997):

(a) that the dynamics of the water table can be approximated by uniform subsurface runoff production per unit area over the area draining through a point, and

(b) that the hydraulic gradient of the saturated zone can be approximated by the local surface topographic slope.

The TOPMODEL is based on the following equations (Tarboton, 2003):

Assuming an exponential decrease in hydraulic conductivity with depth z:

$$K(z) = K_o e^{-fz} \tag{2.5}$$

the down slope transmissivity of the saturated part of the soil profile can be written in terms of the depth of water table (z_w):

$$T(z_w) = \int_{z_w}^{\infty} K(z)dz = \int_{z_w}^{\infty} K_o\, e^{-fz} dz = \frac{K_O}{f} e^{-fz_w} = T_O e^{-fz_w} \tag{2.6}$$

where K_O is the hydraulic conductivity at the surface, f is the sensitivity of parameter that quantifies how rapidly hydraulic conductivity decreases with depth and $T_O = \frac{K_O}{f}$ is the transmissivity of the soil profile.

Assuming effective porosity θ_e, the soil moisture deficit $D(m)$ can be approximated:

$$D = \theta_e z_w \tag{2.7}$$

and this assumes moisture content at the residual moisture content above the water table, thus,

$$T(D) = T_o e^{-fz_w} = T_o e^{-fD/\theta_e} = T_o e^{-D/m} \tag{2.8}$$

where $m = \theta_e/f$

2.4.1.3 Theoretical models

A theoretical model is physically-based and represents the actual catchment (Lundin *et al*., 2000). The model resembles the real world and details the hydrological processes that take place in the catchment (Viessman *et al*., 1989;). The model's ability to detail most process and changes that occur in a catchment is an advantage since catchment parameters such as climate, land-use and soils are never stationary but continuously change time and space (Xu, 2002). Due to the model's ability to capture laws that govern hydrological processes, it is commonly known as a "white-box" model (Viessman *et al*., 1989). Although every mathematical model is effective depending on the objective at hand, how complex the problem is and the degree of accuracy that the modeller desires, Leavesley *et al*. (1983) argue that it is imperative that physically-based models be applied in hydrological research because of their ability to simulate catchments' hydrological processes in their entirety. However, simulating streamflow is a challenging process due to the numerous uncertainties that exist in the form of input parameter inaccuracies, processes unaccounted for by the model, and processes occurring in the catchment that are unknown to the modeller.

Advantages

- Details most processes occurring in the catchment
- Best at simulating the catchment's hydrological system

Disadvantages

- Extensive data requirement

- Time-consuming and needs a specialist to operate

Examples of a physically-based white box model are, the WEPP model, the MIKE-SHE model and the SWAT model which have been described in detail in the following sections. The water balance equation is the main driver of the SWAT model:

$$SW_t = SW_0 + \sum_{t=1}^{t}(R_i - Q_i - ET_i - W_i - QR_i) \quad (2.9)$$

where SW_t is the final soil water content ($cm^3\ cm^{-3}$), SW_0 is the initial soil water content ($cm^3\ cm^{-3}$) on day i and $R_i, Q_i, ET_i, W_i\ and\ QR_i$ (mm) are precipitation, surface runoff, evapotranspiration, seepage flow and return flow on day *i* respectively (Mutenyo *et al*., 2013).

2.4.2 Distinction between lumped and distributed models

2.4.2.1 Lumped models

Lumped models treat catchments as single entities, and do not take into consideration both spatial and temporal variability of the catchment parameters such as climate, land cover, slopes and soils management practices, but rather average input variables and parameters within the whole catchment (Ramirez, 2000; Pechlivanidis *et al*., 2011). Lumped models are usually applied in situations where there is lack of streamflow data (Refsgaard, 1996). Continuous models which require continuous data may apply lumping parameters since the volume of the continuous data becomes too great to manage (Viessman *et al*., 1989). Disadvantages of a lumped model are that it implies that the catchment does not change both spatially and temporally, and that the catchment's hydrological response is direct, which is not correct because there will always be catchment variability and the hydrological rule "there is no linearity" will always apply (Schulze, 1998). Although the lumped model has been discredited in some research, it can assist in accounting for natural variability of a catchment while preserving the main feature (Ponce and Hawkins, 1996).

2.4.2.2 Distributed models

In contrast to lumped models, distributed models to some extent are capable of accounting for the spatial and temporal variability of hydrologic processes and catchment parameters (Ramirez, 2000). Distributed models use average variables and parameters at small grid scales to account for process variations from grid to grid throughout the entire catchment (Viessman

et al., 1989; Ramirez, 2000; Pechlivanidis *et al*., 2011). An example of the application of the distributed model is the "event-based simulation model" which uses distributed parameters and shorter time increments (Viessman *et al*., 1989).

Both lumped and distributed models can further be classified as conceptual and physically-based respectively (Ramirez, 2000). The lumped conceptual models try to mimic or capture parts of the physical processes in the catchment while distributed physically-based models actually model the physical processes when representing the hydrological processes (Refsgaard, 1996; Xu, 2002).

2.4.3 Distinction between deterministic and stochastic models

2.4.3.1 Deterministic models

A deterministic model divides the hydrological cycle into parts and then outlines the different interactions that occur in each part (Viessman *et al*., 1989). In so doing, the model produces results which are uniquely determined from known interactions between processes in the hydrological cycle and data input (Pechlivanidis *et al*., 2011). A deterministic model is a model based on physical processes such as precipitation, evaporation and runoff (Viessman *et al*., 1989). However, in the case where data are missing or for example, rainfall data need to be extended, stochastic methods are then used and incorporated to produce rainfall values, which are then converted into streamflow data (Viessman *et al*., 1989).

2.4.3.2 Stochastic models

Stochastic models depend on probabilities of existing data records rather than physical catchment characteristics and processes (Refsgaard, 1996). This is through the use of random variables representing catchment process uncertainty, which then leads to different results being generated from one set of input data (Pechlivanidis *et al*., 2011). The difference between these models is that a deterministic model produces the same output for the same set of input values while a stochastic model is less consistent, producing different random values of output from the same set of inputs (Gayathri *et al*., 2015). Although a significant part of hydrological processes, both spatial and temporal distinctions of hydrological parameter and variables are described using deterministic models, lack of data requires the hydrologist to apply the joint stochastic-deterministic approach (Refsgaard, 1996).

2.5 Weather generation

A major obstacle facing research nowadays, in this event, in the field of hydrology is the absence of a complete and continuous data record; the data are either incomplete or not reliable (Viessman *et al*., 1989; McCuen, 2003; Smithers, 2012). This challenge has therefore led to researchers and hydrological modellers depending on weather generators to produce artificial (synthetic) data, in order to have meaningful research (Viessman *et al.*, 1989). Due to limited historical data (less than 30 years), a hydrologist possesses limited knowledge to determine the magnitude of risk involved in the event of any future changes (Viessman *et al*., 1989). Hydrological models require observed long-term daily climatic data such as daily rainfall, air temperature, relative humidity, solar radiation and wind speed for them to run or be applied (Clemence, 1997; McKague *et al*., 2003; McKague *et al*., 2005; Tingem *et al*., 2007; Safeeq and Fares, 2011). This becomes a limitation since observed climatic data records are not readily available or are insufficient for good estimations of probability of extreme events such as floods (Tingem *et al*., 2007; Safeeq and Fares, 2011). Due to this limitation, there has been the formation of deterministic mathematical models known as stochastic weather generators, which in turn have addressed the situation and also reduced the time required to prepare weather input data (McKague *et al*., 2005; Tingem *et al*., 2007). As previously mentioned, these stochastic models are known to simulate time series climatic variables such as air temperature and rainfall data to improve on the existing record and to provide climate information where measured data are not available (McKague *et al*., 2003; Tingem *et al*., 2007; Ailliot *et al*., 2015). Stochastic models use existing observed historical climatic data to generate statistically similar synthetic weather data to that of observed data when simulating variables (McKague *et al*., 2003; McKague *et al*., 2005; Tingem *et al*., 2007).

There has been the development of different weather generators to account for missing data, weather generators such as WGEN by Richarsdon and Wright (1984), TAMSIM by McCaskill (1990), and WXGEN by Sharpely and Williams (1990) have been developed (Muthuwatta, 2004). The WXGEN model uses the Markov chain model, where the input values include the probability of rain on a given condition of the day, not minding the state of the previous day (Hayhoe and Stewart, 1996). A wet day is defined as a day with rainfall greater than 0.1 mm (Muthuwatta, 2004). Having obtained wet-dry probabilities, WXGEN stochastically determines the occurrence of rainfall on the particular day. When the rain occurs, the amount is determined by generation from a skewed normal daily rainfall distribution. Simulations requiring four transition probabilities are depicted (**Table 2.1**).

Table 2.1 Transition probabilities for WXGEN simulations (Source: Muthuwatta, 2004)

Day (*i*-1)/Day (*i*)	Wet	Dry
Wet	P_i *(W/W)*	P_i *(W/D)*
Dry	P_i *(D/W)*	P_i *(D/D)*

- P_i *(W/W)* is the probability of a wet day on day *i* given a wet day on day *i* -1
- P_i *(W/D)* is the probability of a wet day on day *i* given a dry day on day *i* -1
- P_i *(D/W)* is the probability of a dry day on day *i* given a wet day on day *i* -1
- P_i *(D/D)* is the probability of a dry day on day *i* given a dry day on day *i* -1

WXGEN requires only two of the above transition probabilities, deriving the remaining two using the following:

$$P_i\left({}^{D}/_{W}\right) = 1 - P_i\left({}^{W}/_{W}\right) \tag{2.10}$$

$$P_i\left({}^{D}/_{D}\right) = 1 - P_i\left({}^{W}/_{D}\right) \tag{2.11}$$

In order to delineate the day as wet or dry, the model generates random number (**X**) between 0 and 1, where the random number is then compared to the appropriate wet-dry probability, P_i *(W/W)* or P_i *(W/D)* (Muthuwatta, 2004).

If **X** ≤ wet-dry probability, the day is regarded as wet
If **X** > wet-dry probability, the day is regarded as dry
The amount of rainfall in a wet day is thus calculated using:

$$R_{day} = \mu_{month} + 2\sigma_{month}\left\{\frac{\left[\left(SND_{day} - \frac{g_{month}}{6}\right) \times \left(\frac{g_{month}}{6}\right) + 1\right]^3 - 1}{g_{month}}\right\} \tag{2.12}$$

where R_{day} is the amount of precipitation on a given day in mm, μ_{month} is the mean daily precipitation for the month in mm, σ_{month} is the standard deviation of daily precipitation for the month in mm, SND_{day} is the standard normal deviation calculated for the day and g_{month} is the coefficient of skewness for daily precipitation in the month (Muthuwatta, 2004).

Mean daily precipitation for the month by:

$$\mu_{month} = \frac{PCPMM}{PCPD} \quad (2.13)$$

where $PCPMM$ and $PCPD$ are average amount of precipitation falling in a month (mm month^{-1}) and average number of days of precipitation in month (days) respectively.

The standard normal deviation is expressed by:

$$SND_{day} = \cos\ (6.283 \times rnd_1) \times \sqrt{-2\ln(rnd_2)} \quad (2.14)$$

where rnd_1 and rnd_2 are random numbers between 0 and 1.

2.6 A review on selected hydrological models

Five hydrological models were selected for review. The water erosion prediction project (WEPP) model, MIKE-système hydrologique européen (SHE) model, Soil and water assessment tool (SWAT), TOPography based hydrological MODEL (TOPMODEL) and Agricultural catchment research unit (ACRU) Model. The models were selected because they are physically based and their ability to account for spatial variability. Moreover, these are hydrological models which can be used for streamflow simulations.

2.6.1 Water erosion prediction project (WEPP) model

The WEPP model is a physically- (process) based, distributed parameter, continuous simulation, water erosion prediction model (Bhawan, 1998; Bowen *et al*., 1998; Conroy *et al*., 2006; Pieri *et al*., 2007; Wu, 2011). The WEPP model was developed in 1985 for soil and water conservation and environmental assessment by the United Nations Department of Agriculture-Agricultural Research Service (USDA-ARS) (Wu, 2011). The WEPP model's main application is the estimation of soil erosion (Wu, 2011). The WEPP model main input requirements are data files from climate, topography, soil and management (Bowen *et al*., 1998; Conroy *et al*., 2006; Pieri *et al*., 2007; Wu, 2011). The model operates on a daily time step, and requires from the climate data file daily values of precipitation, air temperature, relative humidity, wind speed and solar radiation (Laflen *et al*., 1994; Bowen *et al*., 1998; Pieri *et al*., 2007).

The WEPP model is composed of weather generation, winter processes, irrigation, surface hydrology and water balance, subsurface hydrology, soils, plant growth, residue decomposition, overland-flow hydraulics, and erosion (Pieri *et al*., 2007). The WEPP model divides the catchment into homogeneous properties, where the soil properties and vegetation

conditions are regarded uniform and unique. These properties are known as overland flow elements (OFE) (Pieri *et al*., 2007).

The WEPP model simulates infiltration, runoff, rain drop and flow detachment, sediment transport, deposition, plant growth, and residue decomposition (Laflen *et al*., 1994; Bhawan, 1998; Bowen *et al*., 1998; de Jong van Lier *et al*., 2005). Reference ET is estimated from the Penman equation (Penman, 1963) or Priestley-Taylor method (Priestley and Taylor, 1972) depending on the availability of wind speed and relative humidity data (Pieri *et al*., 2007). Climgen weather generator is embedded in the model and is used to generate climate data to be used for climate scenarios (Laflen *et al*., 1994; Bhawan, 1998; Pudasaini *et al*., 2004; de Jong van Lier *et al*., 2005; Pieri *et al*., 2007).

One of the disadvantages of the WEPP model is that it is limited to small catchments (Bhawan, 1998). Two other limitations of the model are that the WEPP model does not explicitly include hydrodynamic channel network flood flow routing or sediment transport algorithms but rather uses a simplified hydrologic model and single sediment transport capacity equation (Conroy *et al*., 2006). The model uses the soil conservation service curve number to simulate water routing from hillslope and this limits the accuracy of runoff simulations, since the method only determines the peak flow and volume but ignores the physical processes governing open channel flow (Conroy *et al*., 2006). The WEPP model is freely available online from the USDA-ARS website.

2.6.2 MIKE-système hydrologique européen (SHE) model

The MIKE-SHE is a deterministic, physically-based, fully distributed model used to simulate the different hydrological processes, such as, surface water flow, evapotranspiration, base channel flow and groundwater. (Refsgaard and Storm, 1996; El-Nasr *et al*., 2005; Golmohammadi *et al*., 2014). The MIKE-SHE model has been used and applied widely in research over the past years, developed to substitute for the incompetency of lumped conceptual rainfall-runoff models such as the Stanford model (Refsgaard and Abbott, 1996). The MIKE-SHE model uses suitable concepts that detail the physical processes in the catchment and further capture the processes on various temporal and spatial scales (Refsgaard and Abbott, 1996).

To account for the spatial variations in catchment properties, Mike-SHE represents the basin horizontally by an orthogonal grid network and uses a vertical column at each horizontal grid square to describe the variation in the vertical direction (El-Nasr *et al*., 2005). This is achieved by dividing the catchment into a large number of discrete elements or grid squares, then solving for the state variables in every grid square (El-Nasr *et al*., 2005; Golmohammadi *et al*., 2014). The polygons or grid networks are divided according to land use, soil type and precipitation (Golmohammadi *et al*., 2014). It is essential that a large time step be used for this model because it has high computational demands (Golmohammadi *et al*., 2014).

The Mike-SHE model can be used for any catchment size, small or large (Golmohammadi *et al*., 2014). The Mike-SHE system has been built in such a way that its digital post-processor is able to calibrate and evaluate for current conditions and for management alternatives where climate, soil and land use keep changing (Golmohammadi *et al*., 2014). Because of the distributed nature of the Mike-SHE model, it requires a large amount of input data to run the model. This is the model's main disadvantage since it is unlikely or rare to find a catchment where all input data required to run the model are available and this may limit the model's results (El-Nasr *et al*., 2005; Golmohammadi *et al*., 2014). The MIKE-SHE model is not freely available online and one needs licencing to have access to the software.

2.6.3 Soil and water assessment tool (SWAT)

SWAT is a conceptual physically-based hydrological model which has been developed to measure land management practices' impacts on water, among other applications (Arnold *et al*., 1998; El-Nasr *et al*., 2005; Gassman *et al*., 2007; Fadil *et al*., 2011; Golmohammadi *et al*., 2014). The SWAT model has been built and developed in a semi-distributed way, where the catchment is sub-divided into sub-catchments and further sub-divided into hydrological response units (HRUs), which then allows the model to account for soil, land use and climate changes (El-Nasr *et al*., 2005; Gassman *et al*., 2007; Golmohammadi *et al*., 2014). HRUs are categorised units, delineated to account for homogeneous regions. This is done by overlying digitized maps of soil, slope and land use (Golmohammadi *et al*., 2014). The water balance of each HRU is represented by four storage volumes including snow, soil profile (0–2 m), shallow aquifer (typically 2–20 m) and deep aquifer (>20 m) (Rostamian *et al*., 2008).

The SWAT model uses a daily time step and is able to conduct continuous simulations over long time periods (Arnold *et al*., 1998; Gassman *et al*., 2007; Golmohammadi *et al*., 2014).

The main components of SWAT include among others climate, surface runoff, return flow, evapotranspiration, crop growth and irrigation, groundwater flow, and water transfers (Arnold *et al*., 1998; Gassman *et al*., 2007; Fadil *et al*., 2011). The SWAT model input requirements consist of information on climate, soil properties, topography, vegetation, and land management practices (Gassman *et al*., 2007; Golmohammadi *et al*., 2014).

The SWAT model has been extensively used and applied for climate change impacts and hydrological processes (Gassman *et al*., 2007). Climatic inputs which are accepted by the SWAT model are daily precipitation, maximum and minimum air temperature, solar radiation, relative humidity, and wind speed (Gassman *et al*., 2007). Three methods for estimating potential evapotranspiration (ET) are provided: Penman-Monteith, Priestly-Taylor, and Hargreaves in the SWAT model (Golmohammadi *et al*., 2014). Relative humidity is required when using Priestly-Taylor ET routines, and when Penman-Monteith method is used both relative humidity and wind speed are required (Golmohammadi *et al*., 2014). ET values estimated outside the SWAT model can also be used as inputs for a simulation run (Gassman *et al*., 2007). According to Gassman *et al*., (2007), the Penman-Monteith option must be used for climate change scenarios that account for changing atmospheric CO_2 levels. The maximum and minimum air temperature inputs are used in the calculation of daily soil and water temperatures (Golmohammadi *et al*., 2014).

SWAT uses GIS tools to process the input data. It has been coupled with a number of GIS software products such as ArcSWAT for ArcGIS, QSWAT for QGIS and MWSWAT for Map-Window (Fadil *et al*., 2011). Spatial data needed for the ArcSWAT and QSWAT interface are DEM, soil type and land use, and the temporal data required are the weather and river discharge data (Fadil *et al*., 2011). Generated weather inputs are calculated from tables derived from long-term measured weather records (Gassman *et al*., 2007).

The advantage of the SWAT model is that it is computationally efficient to operate on large catchments in a practical time scale (El-Nasr *et al*., 2005). One other advantage of the model is that a user can choose an auto-calibration option which reduces labour, frustration and minimises uncertainties which come with the manual calibration (Fadil *et al*., 2011). Another advantage is that, because it is supported by the USDA Agricultural Research Service at the Grassland, Soil and Water Research Laboratory in Temple, Texas, they have made it freely accessible for anyone from the USDA or online http://www.brc.tamus.edu/swat/swatmod.html.

As with other hydrological models, one of the limitations when it comes to application of the SWAT model is the scarcity of historical data (Fadil *et al*., 2011). The SWAT model assumes that the catchment dimensions remain static, which is unrealistic since simulations are made over 100 years or more and in that time-period a catchment could have changed greatly (Arnold *et al*., 1998). The SWAT model is freely available with no registration required.

2.6.4 TOPography based hydrological MODEL (TOPMODEL)

The TOPMODEL is a rainfall-runoff, physically-based and semi-distributed hydrological catchment model (Nourani *et al*., 2011; Beven, 2012). The model represents a set of modelling tools that combines the computational and parametric efficiency of a lumped modelling approach with the link to physical theory (Nourani *et al*., 2011), and due to this, Franchini *et al*. (1996) argues that the TOPMODEL is more of a lumped conceptual model rather than the physically-based model that it is purported to be. TOPMODEL simulates hydrological fluxes such as the infiltration-excess overland flow, saturation overland flow, infiltration, sub-surface flow, and evapotranspiration throughout the catchment (Nourani *et al*., 2011).

The model reads the data in ASCII format, where the data inputs include rainfall, potential evapotranspiration which is averaged over the whole catchment and mean soil surface transmissivity (Famiglietti *et al*., 1992; Franchini *et al*., 1996). TOPMODEL has been successfully applied for flood forecasting purposes and has been linked with different random rainstorm simulators for flood frequency predictions (Nourani *et al*., 2011). Many studies have been done using TOPMODEL relating the interaction of longer term climate change and hydrology (Famiglietti *et al*., 1992; Beven, 2012). An advantage of TOPMODEL is that versions for demonstrations and teachings are freely available (Beven, 2012).

2.6.5 Agricultural catchment research unit (ACRU) Model

The ACRU is a physical, conceptual, agro-hydrological model which operates on daily time step (Warburton *et al*., 2010). ACRU was developed in the early 1970s for the application of design hydrology, crop yield modelling and reservoir yield simulation (Smithers *et al*., 1997). Model input requirement includes daily rainfall, air temperature, and reference evaporation (Smithers *et al*., 1997, 2013).

According to Smithers *et al*. (1997), the ACRU model simulates all major processes of the hydrological cycle which affect the soil-water budget and this includes simulation of

streamflow volume, peak discharge and hydrograph, among others. The model thus uses past rainfall data to simulate and to develop hydrographs that show variations in peak discharges (Chetty and Smithers, 2005). The ACRU model may also be used for risk analysis and modelling by means of exceedance probability plots, for example flood exceedance probability (Smithers *et al*., 1997).

The ACRU model is structured in such a way that it is highly sensitive to changes, for example climate, land cover/use and soil, hence it may be used for future predictions where there are changes involved (Jewitt *et al*., 2004). This is an advantage and thus, the ACRU model has been used extensively in flood estimation and climate change impacts (Smithers *et al*., 1997). The ACRU model may be applied as a point or as a lumped catchment model, and in a catchment where physical characteristics and processes are more complex, the model can be treated as a distributed model (Smithers *et al*., 1997). This is done by dividing the catchment into sub-catchments of less than 30 km^2 (Chetty and Smithers, 2005). A disadvantage of the ACRU model is that it is not user-friendly, hence it requires a model expert to fully run the model. The ACRU model is freely accessible from the University of KwaZulu-Natal website, under the Centre for Water Resources Research page (http://cwrr.ukzn.ac.za/acru).

2.7 Model sensitivity analysis, calibration and validation

Hydrological testing such as sensitivity/uncertainty analysis, calibration, validation and statistical measures are required to test the authenticity of a model's results (Gassman *et al*., 2014; Gyamfi *et al*., 2016). Therefore, before using a model for hydrological analysis, one should conduct a sensitivity analysis, calibrate and validate for the catchment parameters in which the model is to be applied (Refsgaard and Storm, 1996; Golmohammadi *et al*., 2014). This is because each study area or catchment is different from the other, and depending on the environment, land use and soil, some parameters may differ from catchment to catchment (Arnold *et al*., 1998). A model is thus calibrated and verified by means of comparing results of the simulation with existing observed data, and then by adjusting parameters so that the simulation results may fit the known period of data (Viessman *et al*., 1989; Mutenyo *et al*., 2013).

2.7.1 Parameter sensitivity analysis

Catchment processes are influenced by a large number of parameters, which leads to distributed hydrological models being subjected to a great number of uncertainties (Rostamian *et al*.,

2008). Therefore, researchers have developed various uncertainty analysis techniques such as the Markov chain Monte Carlo (MCMC) method (Metropolis *et al*., 1953; Hastings, 1970; Geyer, 1992); the generalized likelihood uncertainty estimation (GLUE) (Beven and Binley, 1992); the parameter solution (ParaSol) (van Griensven and Meixner, 2006); and the sequential uncertainty fitting version 2 (SUFI-2) (Abbaspour *et al*., 2007) to account for such uncertainties (Rostamian *et al*., 2008; Manaswi and Thawait, 2014; Narsimlu *et al*., 2015).

These techniques have been interfaced with SWAT into a package known as the SWAT calibration uncertainty procedure (SWAT-CUP) (Rostamian *et al*., 2008; Narsimlu *et al*., 2015). SWAT-CUP is a freeware program developed by Abbaspour *et al*. (2007) which allows the use of the above-mentioned different algorithms (SUFI-2, GLUE, MCMC and ParaSol) for the optimisation of the SWAT model. This allows for sensitivity analysis, calibration, validation and uncertainty analysis looking at the variable at hand (for example, streamflow) (Mamo and Jain, 2013; Manaswi and Thawait, 2014; Szezesniak and Piniewski, 2015).

2.7.2 Description and operation of SUFI-2

SUFI-2 is an algorithm used to account for different types of uncertainties driving the model, parameters and observed data (Singh *et al*., 2013; Khalid *et al*., 2016). In SUFI-2, uncertainty is defined as the difference between measured and simulated variables (Rostamian *et al*., 2008). The input parameter uncertainty is represented by a uniform distribution, while the output uncertainty is computed at the 95% prediction uncertainty (95PPU) (Szezesniak and Piniewski, 2015). The cumulative distribution of an output variable is obtained through the Latin hypercube sampling method calculated at the level of prediction limit of 2.5 and 97.5% (Abbaspour, 2015).

The SUFI-2 model starts by assuming a large parameter uncertainty and then decreases this uncertainty through *P*-factor and *R*-factor performance statistics (Narsimlu *et al*., 2015). *P*-factor and *R*-factor are performance indices used by SUFI-2 to evaluate the model performance (Narsimlu *et al*., 2015). The *P*-factor is the percentage of measured data bracketed in the 95% prediction uncertainty (95PPU) indicating how much of the uncertainty is being captured (Rostamian *et al*., 2008; Mamo and Jain, 2013; Singh *et al*., 2013). The *R*-factor is the average thickness of the 95PPU band divided by the standard deviation of the measured data and quantifies the strength of the calibration uncertainty analysis (Mamo and Jain, 2013; Khalid *et al*., 2016).

How good the model calibration is and the prediction uncertainties are quantified and judged on the basis of the *P*-factor approaching 100% while the *R*-factor approaches 1, which indicates a very high model perfomance and efficiency (Singh *et al*., 2013). The *P*-factor ranges from 0 to 100% and the *R*-factor ranges from 0 to infinity (Narsimlu *et al*., 2015). A *P*-factor of 1 and *R*-factor of zero is a simulation that exactly corresponds to measured data and the degree to which simulation *P*-factor and *R*-factor results are different from these numbers can be used to judge the strength of the calibration (Mamo and Jain, 2013).

2.7.3 Calibration

Due to complex processes that occur in a catchment and uncertainties from modelling parameters, models require to be calibrated to minimise predictive errors (Gyamfi *et al*., 2016). Therefore, calibration is used to adjust the parameters until the simulated results and recorded data of streamflow correspond (McCuen, 2003; El-Nasr *et al*., 2005). The calibration procedure (**Figure 2.3**) determines the best values for parameters specified by the user through estimation of values for parameters which cannot be measured directly from field data (Refsgaard and Storm, 1996; Fadil *et al*., 2011). The process of calibration can be done manually or automatically based on a defined optimisation algorithm, which tries to minimise the objective function in order to illustrate the deviation between a measured and a simulated stream flow series (Abbaspour, 2015). The auto-calibration option is less labour-intensive and can be used to reduce the uncertainties that come with manual calibration (Fadil *et al*., 2011).

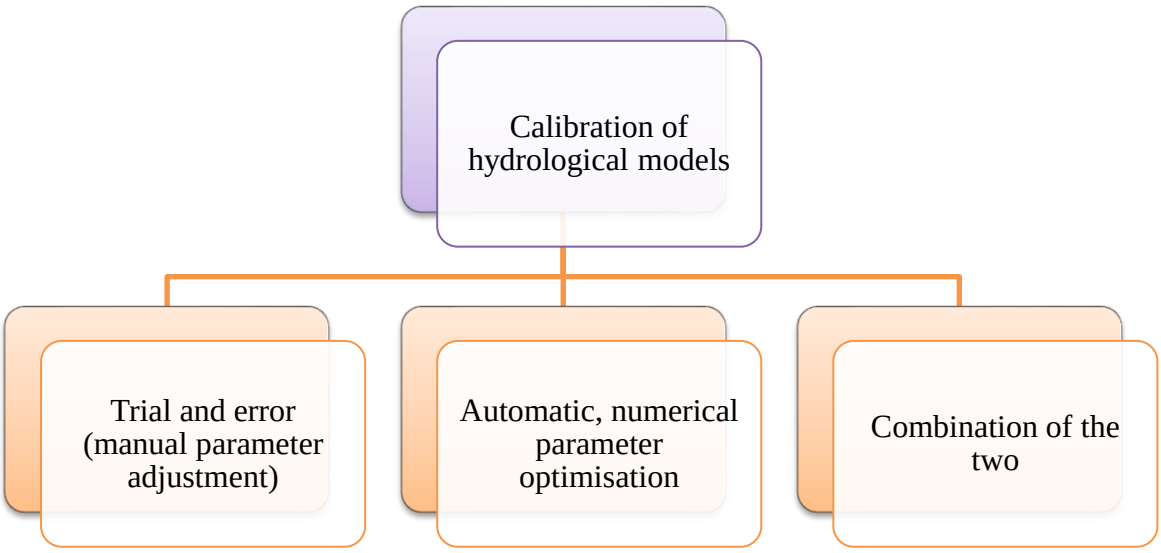

Figure 2.3: Calibration of hydrological models (Refsgaard and Storm, 1996)

When calibrating, the total data period is divided into three parts where the first few years are used for calibration, the second part used for validation and the final few years are used to run the model (Viessman *et al*., 1989; Golmohammadi *et al*., 2014). The more complex the model is, the more it requires time, knowledge and experience to set up data correctly (McCuen, 2003). Therefore, when selecting a model, one needs to understand that the model cannot substitute for lack of knowledge and neither can the model create new data but can only assume the possibility that simulated conditions indeed do occur (Smithers *et al*., 1997).

There are three different types of calibration according to Refsgaard and Storm (1996) (**Figure 2.3**). The trial and error method of calibration involves the manual adjustment of parameters, and assessing the parameters through a number of simulation runs (McCuen, 2003). According to Refsgaard and Storm, (1996), this type of calibration is widely used, especially for the more complex models. One disadvantage of this type of calibration is that the results are more subjective to the user unlike the automatic, numerical parameter optimisation type, thus it requires a more experienced user (Viessman *et al*., 1989). SWAT uses SWAT-CUP for both calibration and validation, which is semi-automatic (Abbaspour, 2015). SWAT calibrates by applying one of the most widely used algorithm, SUFI-2, which operates based on the Latin Hypercube sampling (Gyamfi *et al*., 2016) (**Figure 2.4**).

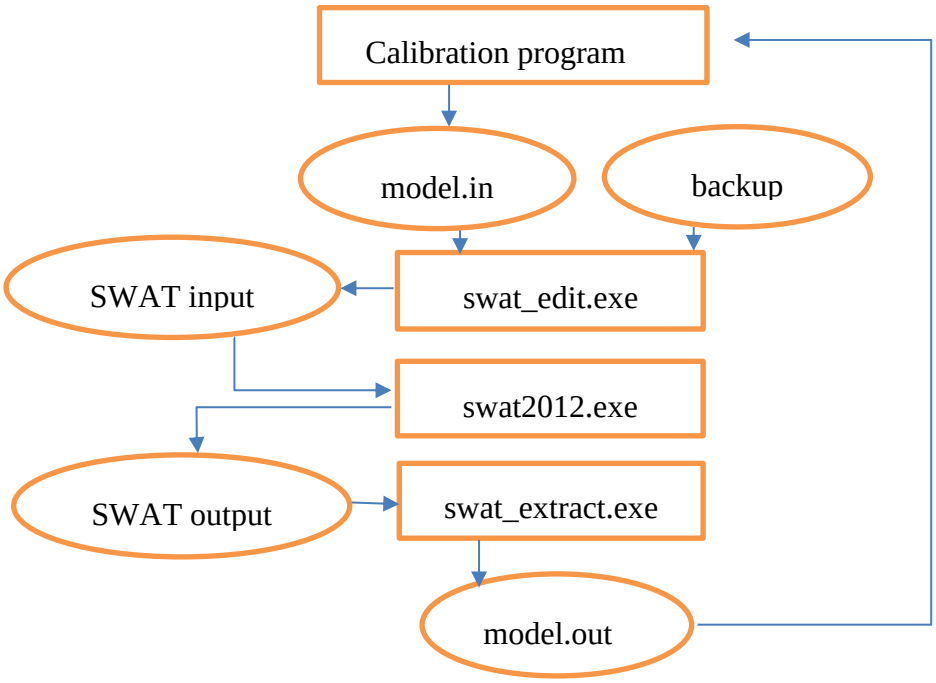

Figure 2.4 Interaction between a calibration program and SWAT in SWAT-CUP (Rostamian *et al*., 2008)

2.7.4 Validation

To ensure that a calibrated model is considered for later use, it must be tested against data different from that used for calibration, and this is called validation (Refsgaard and Storm, 1996). The model validation is a process that demonstrates that the model is capable of making accurate simulations depending on the project aims (Mutenyo *et al*., 2016). Therefore, a second period of record is taken to conduct validation, for control and to confirm the accuracy of the parameters derived from the calibration with the first period of record (Manaswi and Thawait, 2014). According to Refsgaard and Storm (1996), validation thus implies that a model which is site-specific can produce simulation results which are accurate for a particular study area.

2.7.5 Statistical testing

The most reported upon statistical measures used in hydrological modelling are the coefficient of determination (R^2), Nash-Sutcliffe modelling efficiency (NSE), percent bias (PBIAS) and RMSE-observations standard deviation ratio (RSR) (Gassman *et al*., 2014; Gyamfi *et al*., 2016). The R^2 represents the fraction of data that are closest to the line of best fit and thus allows one to determine the certainty of predictions; the NSE is used to quantify and assess the predictive accuracy of hydrological models output relative to the mean; PBIAS measures the average tendency of modelled output to be larger or smaller than the corresponding measured data with positive and negative values representing underestimation bias and overestimation bias respectively; and the RSR is the ratio of root mean square error between simulated and observed values to the standard deviation of the observations (Golmohammadi *et al*., 2014; Narsimlu *et al*., 2015). The R^2 and the NSE may also be used as probability measures through the comparison between observed and predicted streamflow (Narsimlu *et al*., 2015).

R^2 ranging from 0 to 1, below 0.5 is considered unsatisfactory while 0.5 to 0.75 are acceptable results and greater than 0.75 is considered good model simulation (Gassman *et al*., 2007). NSE ranges from $-\infty$ to 1; 1 being the optimal value, below 0 considered unsatisfactory, 0 to 0.5 considered acceptable, 0.5 to 0.75 considered satisfactory and above 0.75 considered good simulation results (Gassman *et al*., 2014; Szezesniak and Piniewski, 2015). The optimal value of PBIAS is 0, PBIAS greater than 0 is positive bias and less than 0 is negative bias, and low magnitude values indicate accurate model simulation (Narsimlu *et al*., 2015). RSR varies from an optimal value of 0 to a large positive value with lower values of RSR indicating good model simulation performance (Golmohammadi *et al*., 2014). According to Moriasi *et al*. (2007) and

Mutenyo *et al*. (2013), a model should aim at achieving a satisfactory model efficiency of concurrently having NSE greater than 0.5, PBIAS of ± 25% and RSR of less than 0.7.

According to Singh *et al*. (2013), streamflow is more sensitive to HRU definition thresholds than sub-catchment delineation. Therefore, *t*-test and *p*-value are variables used to rank the various parameters considered to influence the streamflow (Abbaspour, 2015). The *t*-test and the *p*-value are used to provide a measure and the significance of the sensitivity respectively (Narsimlu *et al*., 2015). The *t*-test gives a measure of sensitivity of a parameter while *p*-value gives the significance of the sensitivity of that parameter (Gyamfi *et al*., 2016). Large *t*-test and smaller *p*-value shows great sensitivity on streamflow. Hence, for *p*-value < 0.05, the parameters are considered to be more sensitive to streamflow (Jha, 2011). On the other hand, if $p > 0.05$, the parameter is considered to be statistically insignificant and has no effect on streamflow (Gyamfi *et al*., 2016).

CHAPTER 3: MATERIALS AND METHODS

3.1 Study area

The Luvuvhu catchment is located in the Limpopo province of South Africa, adjacent to and shares watercourses with Zimbabwe and Mozambique (Maré *et al*., 2007; Hall, 2008). The catchment is located between latitudes -22.292658° and -23.299253° and between longitudes 29.829489° and 31.392228° covering an area of about 5941 km^2 on a plateau of 1312 m above sea level (Singo *et al*., 2012).The Luvuvhu catchment encompasses the Luvuvhu River which rises as a steep mountain stream in the south-easterly slopes of the Soutpansberg Mountain range and then flows 200 km in an easterly direction toward and through the Kruger National Park before reaching the confluence with the Limpopo River at the border of South Africa and Mozambique (Jewitt *et al*., 2004; Warburton *et al*., 2010; Singo *et al*., 2012). The Limpopo River then finally drains into the sea at the northern part of Mozambique (Jewitt *et al*., 2004) (**Figure 3.1**).

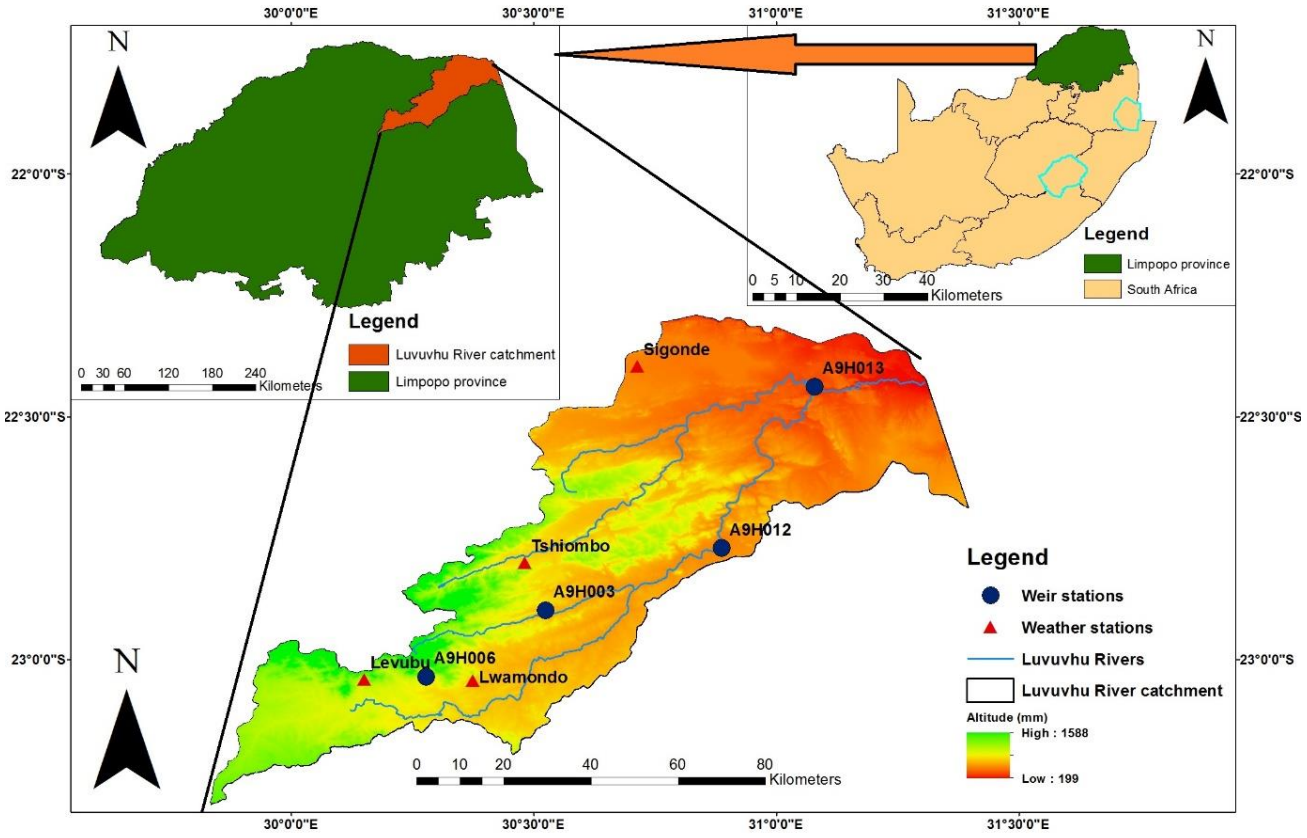

Figure 3.1 The Luvuvhu River catchment

Rainfall in the Luvuvhu catchment is strongly seasonal and is influenced by the topography and therefore variable both spatially and temporally (Jewitt *et al*., 2004; Hall, 2008; Warburton *et al*., 2010) (**Figure 3.2**). The Luvuvhu catchment has a mean annual precipitation of 608 mm varying from 300 mm in the drier, lower regions of the catchment to 1870 mm in the mountainous upper regions of the catchment (Soutpansberg mountain range) (Jewitt *et al*., 2004). The Luvuvhu catchment also experiences a high rate of evaporation with a mean annual evaporation of 1678 mm varying from 1905 mm to 2254 mm respectively (Warburton *et al*., 2010). Catchment rainfall occurs mainly in the summer months, October to April (Hall, 2008; Singo *et al*., 2012). The Luvuvhu catchment experiences mean annual runoff of about 520×10^6 m^3 (Jewitt *et al*., 2004; Maré *et al*., 2007). Mean annual air temperatures range from 17 ^oC in the mountainous regions to 24 ^oC towards the catchment outlet (Warburton *et al*., 2010) (**Figure 3.3**).

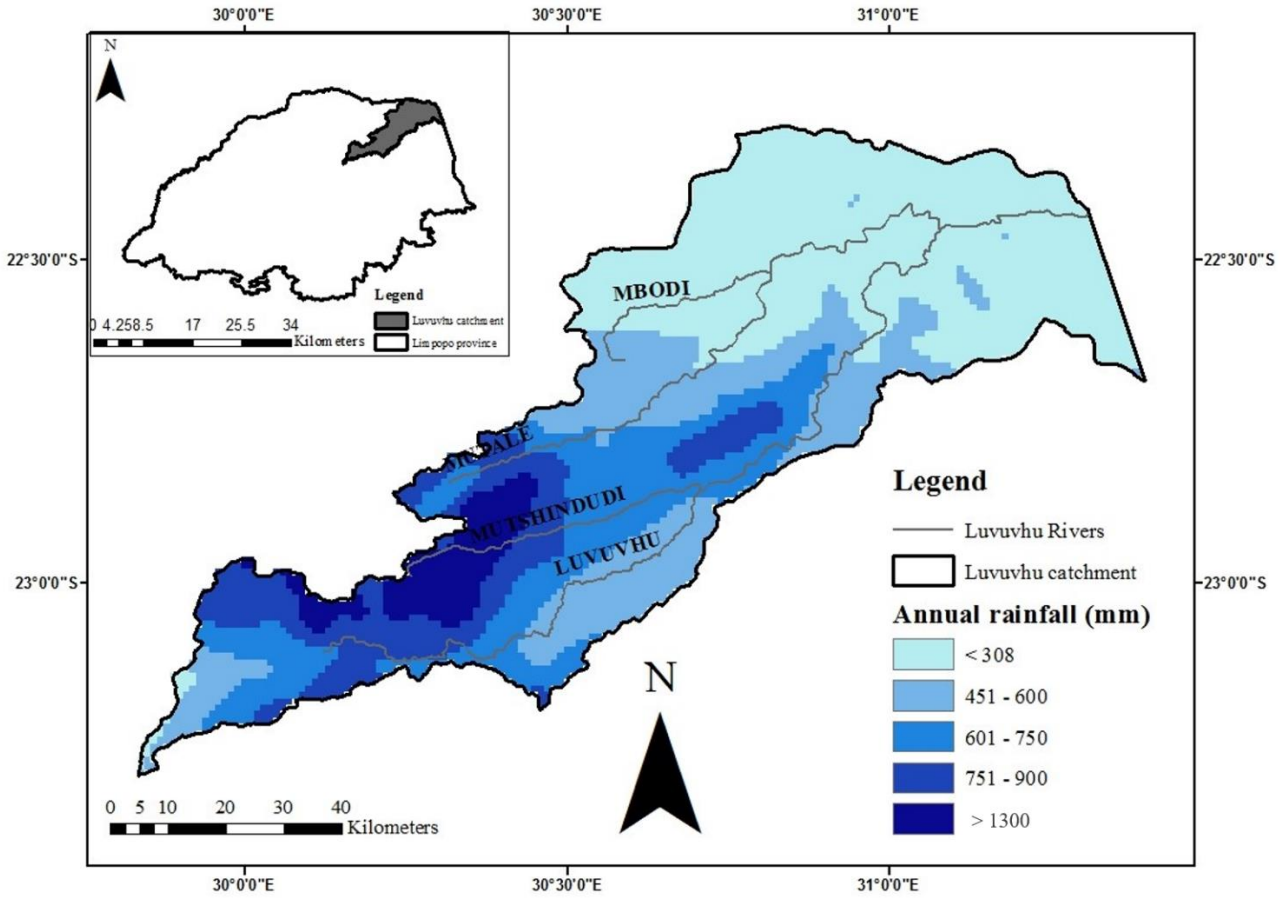

Figure 3.2 Rainfall variability in the Luvuvhu River catchment

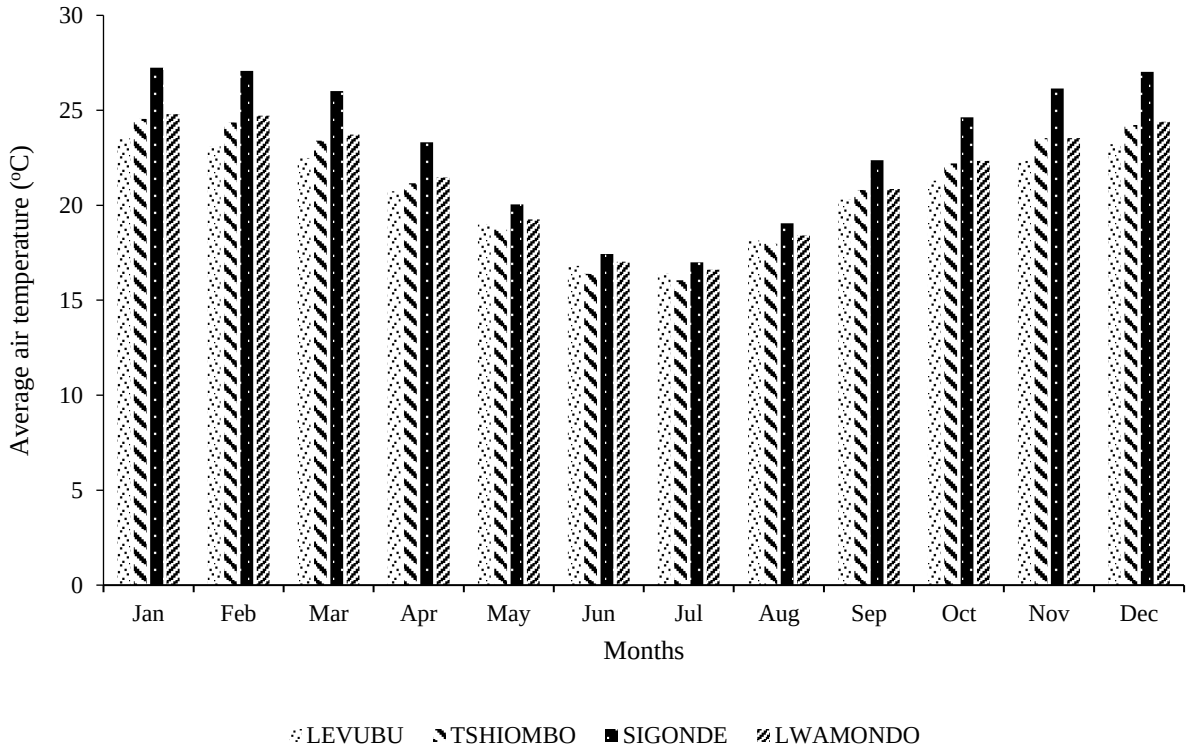

Figure 3.3 Average monthly air temperature for the four selected stations over the Luvuvhu River catchment

3.2 Soil and water assessment tool (SWAT)

The SWAT model was chosen for the purpose of this study among the other models which were reviewed (**Figure 3.4**). The reasons for this choice are expressed in (**Table 3.1**). The purpose of using SWAT for this study was to model spatial and temporal variation of surface runoff in the Luvuvhu River catchment. Based on the literature and previous studies, the model was considered to be best in simulating past data. The choice of model was also based on its surpassing capabilities, such as:

- ability to delineate the interactions of the different parts in the hydrological cycle through the model's deterministic nature (Viessman *et al*., 1989);
- ability to express and represent the actual catchment, detailing hydrological and physical processes that take place in the catchment (Viessman *et al*., 1989; Lundin *et al*., 2000);

Table 3.1 Advantages and disadvantages of hydrological models reviewed (Chapter 2)

Models	Description	Advantages	Disadvantages
ACRU	• Physical, conceptual agro-hydrological model	• Accounts for climate, land use and soil changes • Applied as a point, lumped or distributed model	• Cannot simulate confined groundwater flow and storage • Operatively less user friendly
MIKE-SHE	• Physically based, deterministic, fully distributed model	• Used for any catchment size • Can provide a water budget for the full hydrologic cycle	• High computation demand • Large input data
SWAT	• Physically based, deterministic, semi-distributed model	• Computationally efficient • The model has an inbuilt weather generator to simulate missing weather information. • Option for auto-calibration reduces labour and uncertainties • Freely accessible	• Assumes catchment dimensions remains static
TOPMODEL	• Physically based, lumped, conceptual model	• Freely accessible	• Does not take into account heterogeneity of the catchment
WEPP	• Physically based, distributed, continuous simulation model	• Allows spatial variability in land use and soil properties	• Limited to smaller catchments • Does not explicitly include hydrodynamic channel networks flood flow routing

- ability to account for spatial variability of hydrologic processes and changes in the catchment (Ramirez, 2000). This is applicable through sub-dividing the catchment into sub-catchments and further sub-dividing the sub-catchments into hydrological response units (HRUs) (El-Nasr *et al*., 2005; Jha, 2011; Arnold *et al*., 2012; Gyamfi *et al*., 2016);
- the model has not been applied in the Luvuvhu River catchment and this gives an opportunity to test the model parameters for the area.

SWAT is based on the principle that the water balance equation drives all processes that occur in a catchment (Arnold *et al*., 2012; Mutenyo *et al*., 2013). Therefore, the water balance for each sub-catchment is based on (Mutenyo *et al*., 2013; Kuhn, 2014):

$$SW_t = SW_0 + \sum_{t=1}^{t} (R_i - Q_i - ET_i - W_i - QR_i) \quad (3.1)$$

where SW_t is the final soil water content ($cm^3\ cm^{-3}$), SW_0 is the initial soil water content ($cm^3\ cm^{-3}$) on day i and $R_i, Q_i, ET_i, W_i\ and\ QR_i$ (mm) are precipitation, surface runoff, evapotranspiration, seepage flow and return flow on day *i* respectively. The parameters for the water balance equation are estimated using acquired past data.

Surface runoff is computed using a modification of the SCS curve number given by (Singh *et al*., 2013):

$$Q_i = \frac{(R_i - I_a)^2}{R_i - I_a - S}, \qquad R_i > I_a \quad (3.2)$$

where I_a is the initial abstraction of rainfall through interception, infiltration and surface storage before runoff and S is the potential retention (maximum depth of storm rainfall that could potentially be abstracted by a given site) (Liu and Li, 2008).

There is a linear relationship between the two parameters, where the amount of initial abstraction I_a becomes a fraction of a potential maximum retention S (Xiao *et al*., 2011) where:

$$I_a = \lambda S \quad (3.3)$$

where λ is an initial abstraction ratio of 0.2 (Singh *et al*., 2013).

Therefore runoff will occur when $R_i > 0.2\ S$ (Fennessey and Hawkins, 2001). The retention parameter S varies spatially due to soil, land use, management and slope changes, and varies temporally due to changes in soil water content (Silveira *et al*., 2000):

$$S = \frac{25400}{CN} - 254 \quad (3.4)$$

where CN is the curve number corresponding to soil type, land use and land management conditions which is obtainable from the National Engineering Handbook, Section 4: Hydrology (NEH-4) (Fennessey and Hawkins, 2001; Soulis and Valiantzas, 2012).

3.3 Data collection

3.3.1 Climate station data

Although acquiring historical data is very difficult, be it climatological or hydrological, it is still essential to obtain such data and make sure that it undergoes quality and homogeneity checks using scientifically proven gap-filling techniques (Chen and Liu, 2012). This is because hydrological simulation models require observed long-term daily climatic data such as daily rainfall, maximum and minimum air temperature, relative humidity, solar radiation and wind speed for modelling purposes (Clemence, 1997; McKague *et al*., 2003; McKague *et al*., 2005; Tingem *et al*., 2007; Safeeq and Fares, 2011). Four of the ARC-ISCW weather stations in the Luvuvhu catchment from the ARC-ISCW climatic weather database were chosen for this study. Their locations and station information are shown in **Figure 3.1** and **Table 3.2**. The weather stations chosen were selected according to the availability of data and position in the catchment, so that there would be a proper representation of the whole Luvuvhu catchment. Stations with fewer years of data were disregarded.

Table 3.2 Summary of climate stations

Station name	Latitude (degrees)	Longitude (degrees)	Elevation (m)	Start date	End date	Years
Levubu	-23.04175	30.1505	880	1983/01/01	2015/06/30	32
Lwamondo	-23.044008	30.37361	648	1978/01/01	2015/06/30	37
Sigonde	-22.3965	30.71308	416	1983/01/01	2015/06/30	32
Tshiombo	-22.80147	30.48145	650	1983/01/01	2015/06/30	32

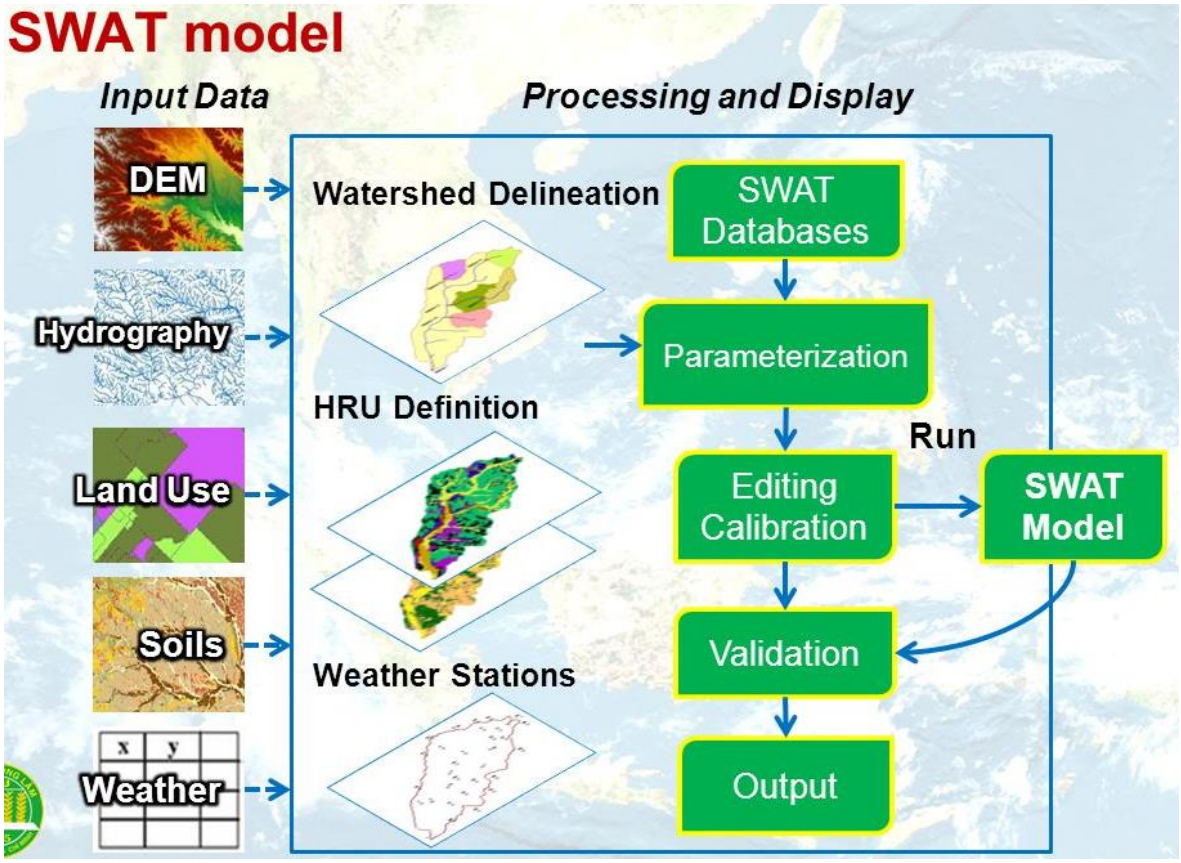

Figure 3.4 SWAT model (source: Garrison, 2012)

Rainfall data was patched using an inverse distance weighting (IDW) method that is based on the concept of Tobler's law of geography (Chen and Liu, 2012, Moeletsi *et al*., 2016). The method assigns a value to the missing data using neighbouring stations with known values that are within a certain radius from the weather station to be patched (Chen and Liu, 2012). Three closest weather stations were considered to implement the IDW method using the adjustment of power of two ($\propto = 2$):

$$\hat{R}_p = \sum_{i=1}^{N} w_i R_i \tag{3.2}$$

$$w_i = \frac{d_i^{-\propto}}{\sum_{i=1}^{N} d_i^{-\propto}} \tag{3.3}$$

where $\hat{R}_p$ is the estimated rainfall data value in mm for the missing value, R_i is the measured rainfall from the closest rainfall stations in mm, N is the number of rainfall stations used, w_i is the weighting of each rainfall station, d_i is the distance from each rainfall station to that with the missing rainfall and $\propto$ is the power or control parameter.

Minimum and maximum air temperatures were patched using the method known as the multiple linear regression (MLR) (Moeletsi *et al*., 2016). The method considers the best correlated stations (Montgomery *et al*., 2006). In this case, five best correlated stations were chosen. With the stations chosen, a linear regression line that best defines the five stations was identified. Thus the regression equation (**Equation 3.4**) obtained from the regression line was then used to estimate the missing air temperature values (**Equation 3.5**):

$$y = \beta_0 + \beta_1 x_1 + \beta_2 x_2 + \varepsilon \tag{3.4}$$

$$y = \sum_{i=1}^{N} \beta_i x_i + \beta_0 \tag{3.5}$$

where y is the estimated value, β_0 is the intercept of the regression plane, β_i $(\beta_1, \beta_2 \ldots)$ is the slope coefficient, x_i $(x_1, x_2 \ldots)$ are the known variables, N is the number of stations and ε is the error term (Montgomery *et al*., 2006).

Since daily shortwave radiation measurements were not available, daily sunshine hours were used to calculate solar radiation. Solar radiation was calculated using the equation developed by Ångström (1924) (**Equation 3.6**), where solar radiation is related to radiation received at the top of the atmosphere (extra-terrestrial radiation) R_a and the fraction of actual to maximum possible sunshine hours n (Ncube, 2006).

$$R_s = \left[a + b\frac{n}{D}\right] R_a \tag{3.6}$$

where R_s is the daily solar radiation in (MJ m^{-2}), a, b are the regression constants for estimation of shortwave radiation from sunshine duration and the general values for southern Africa are 0.24 and 0.53 respectively (Ncube, 2006). The constants vary seasonally, regionally and depend on the time scale (i.e. daily, weekly or monthly); n is the actual sunshine duration in hours; D is the day length in hours, varying with latitude and day of year; R_a is the solar radiation received on a horizontal plane at the top of the atmosphere (i.e. extra-terrestrial solar irradiance in MJ m^{-2}).

Table 3.3 summarises the interpolated values for D and R_a obtained from **Table B.1** and **Table B.2** in **Appendix B** by Wilson 1(990) (cited by Ncube, 2006). The values together with the sunshine hour time series were used to calculate the solar radiation using the solar radiation equation above. The latitude for the study area is 22 degrees south of the equator. Average

daily solar radiation estimated for the four weather stations over the Luvuvhu River catchment depicted high solar radiation over the mountainous region of the catchment (**Figure 3.5**).

Table 3.3: Daily interpolated values for day length *D* and extra-terrestrial solar irradiance R_a for 22 °S

	Jan	Feb	Mar	Apr	May	Jun	Jul	Aug	Sep	Oct	Nov	Dec
D **(h)**	13.35	12.90	12.30	11.65	11.05	10.75	10.85	11.40	12.0	12.65	13.20	13.50
R_a **(MJ m^{-2})**	40.79	42.44	34.10	29.72	24.17	22.88	23.30	27.30	33.46	36.98	41.36	41.27

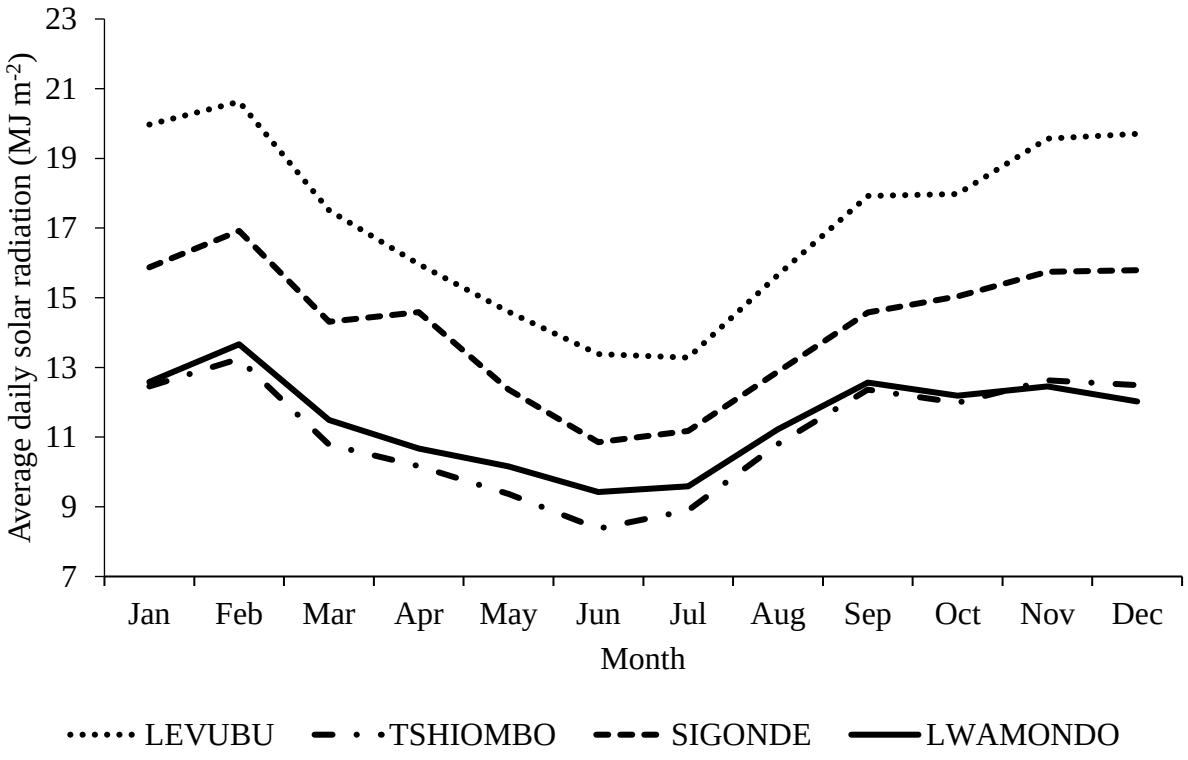

Figure 3.5: Average daily solar radiation of four selected stations from the Luvuvhu River catchment

Relative humidity (RH) missing values were filled by using a method by Eccel (2012). For this method, estimations of water vapour pressures at the maximum (*Tx*) and minimum (*Tn*) air temperatures were required. This meant that the dew point temperature had to be estimated through the following assumptions:

(a) the minimum air temperature was assumed to equal the dew point temperature;

(b) correction of the first assumption was carried out depending on either the presence or absence of precipitation or the water balance of the previous day (Eccel, 2012).

From the two assumptions, RH was estimated using air temperature using the following ratio:

$$RH = \frac{e}{e_s} \times 100 \quad (3.7)$$

where e is the actual water vapour pressure (kPa), and e_s the saturation water vapour pressure (kPa).

The water vapour pressure was calculated using a common exponential function:

$$e_s(T_n) = 0.61078\ exp^{17.269\frac{T}{T+237.3}} \quad (3.8)$$

where e_s is the water vapour pressure (kPa) at the daily minimum air temperature (T_n) (°C) (Allen *et al*., 1998).

Wind speed gaps were patched with a 2.0 m s^{-1} value since it is a standard acceptable average wind speed infilling value for most locations (Pasi, 2014).

3.3.2 Streamflow data

Daily flow data from the Department of Water and Sanitation (DWS) were used in this study. Stations with 20 years or more of data were selected. Out of the streamflow weir stations located inside the Luvuvhu catchment only four weir stations were chosen: A9H003, A9H006, A9H012 and A9H013 (**Figure 3.1 and Table 3.4**). The stations were chosen based on the following: availability of data; representation of the catchment (location); and that the data set included recent years. The streamflow data were used to calibrate simulated runoff.

3.3.3 GIS data (soil, land use and digital elevation model (DEM) data)

Shape files were obtained from the ARC-ISCW GIS data library. The dataset contains catchment delineation shape files of the Luvuvhu catchment (Luvuvhu secondary, quaternary and river shape files), digital elevation model (DEM), land use map and soils map. Soil and land use data were taken from the national land type and land cover maps respectively; however, a new and rarely researched "flow path improved STRM_90 DEM" was used for DEM. The data were modified according to model requirements. The soil and land use were converted to raster files and together with the DEM were re-projected from WSG 84 to WSG 84/UTM zone 36S projection which was recommended as an improved projection since the

study area has a north-south orientation. The soil, land use and DEM were projected into the same projection so that they would be accepted by the model.

Table 3.4 Summary of the weir stations

Station no	Location	Catchment area (km^2)	Latitude (degrees)	Longitude (degrees)	Data available	Years
A9H003	Tshinane River in haTshivhase	62	-22.89828	30.52391	1931-09-02 2015-04-15	84
A9H006	Livhungwa River in Barotta	16	-23.03577	30.27752	1961-11-13 2014-08-28	53
A9H012	Luvuvhu River in haMhinga	1758	-22.7705	30.88672	1987-11-04 2015-03-03	28
A9H013	Mutale River in Kruger National Park	1776	-22.43775	31.07832	1988-11-02 2013-02-14	25

3.4 Data processing and preparation

The processing tools used were: MS Excel using pivot tables; pcpSTAT (Stefan Liersch, 2003) for precipitation data manipulation; and QGIS desktop 2.6.1 for all GIS data. All maps generated were projected into the same projection (**Table 3.5**).

Table 3.5 Universal transverse Mercator for the Luvuvhu river catchment

Parameters	WSG 84/UTM zone 36S
Projection	Transverse Mercator
Spheroid	WGS_1984
Datum	D_WGS_1984
Zone	36
Central meridian	33
Reference Latitude	0
Northing (m)	10000000
Easting (m)	500000
Scale factor	0.9996

3.4.1 DEM Preparation

A DEM is required to facilitate the delineation of the catchment into multiple hydrologically connected sub-catchments (Dile *et al*., 2015). As mentioned previously, a flow-path improved 90 m DEM from the Shuttle Radar Topography Mission (SRTM) was used. Although the 90-m resolution is considered to be inadequate, the study area catchment is large and using a less detailed DEM was advisable. The created DEM for the study area is depicted (**Figure 3.6**).

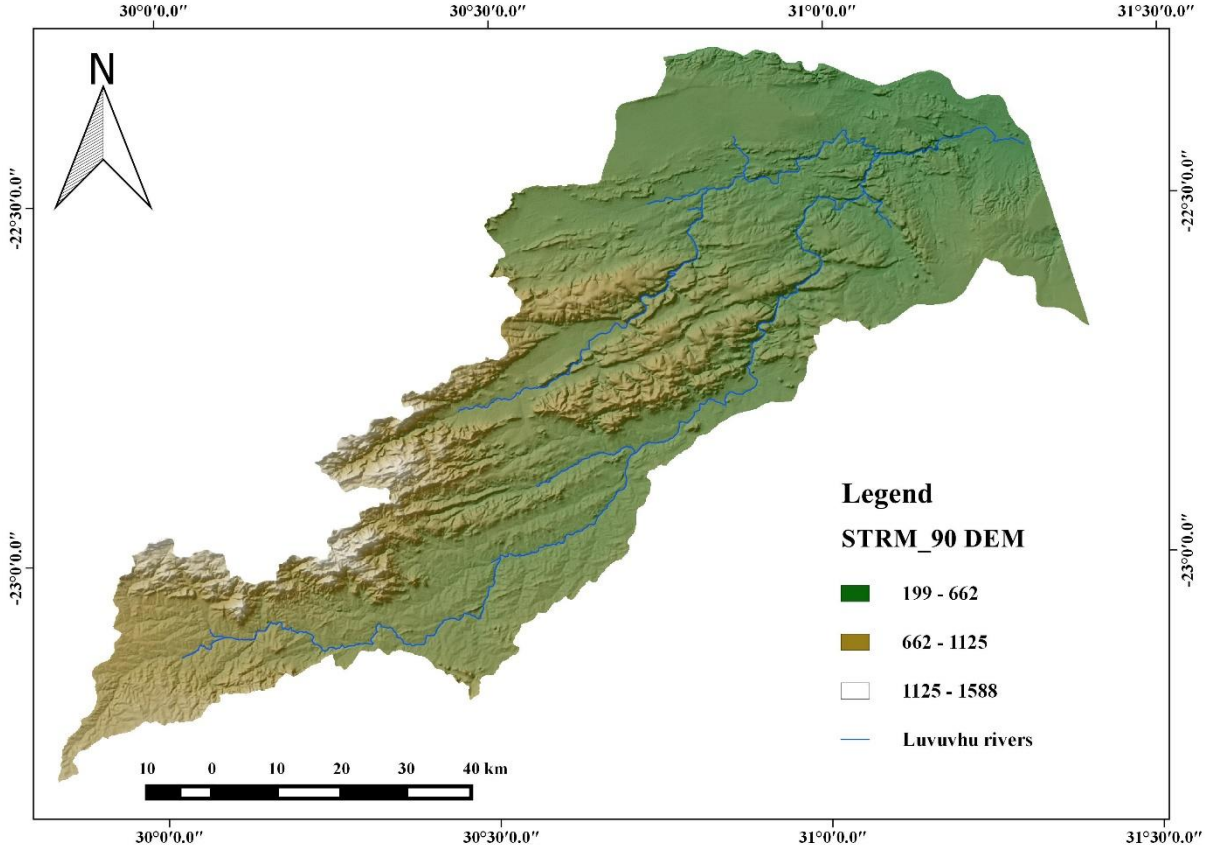

Figure 3.6: DEM for the study area (flow-path improved STRM_90m)

3.4.2 Land use and soil data preparation

Land use and soil data are important in determining soil and land use hydrologic parameters for the creation of hydrological response units (HRUs) (Ncube, 2006; Golmohammadi *et al*., 2014). The land use and soil shapefile maps which were obtained from the ARC-ISCW GIS data library were clipped to fit the Luvuvhu River catchment.

The model requires that a table be created for land use and soil maps. The prepared tables should be copied to either the QSWAT project database which is created when SWAT Editor software is installed or the project database that is created for every new project. In the case of the former, the tables are copied into every new project database created. For the latter, the

tables are only for the particular project. For this study, the prepared tables were copied to the QSWAT project database.

Soils

In the case of the soil map, the table which is created needs to have a string soil in its name thus allowing the table to be recognised by the model and be offered as an option for soil table on the dropdown menu. The table should contain the soil identity and the soil name. All the soil names used should also be available on the *usersoil* table found in the SWAT reference database. The soil map created is depicted in **Figure 3.7** while the table created is depicted in **Table B.3** in **Appendix B**.

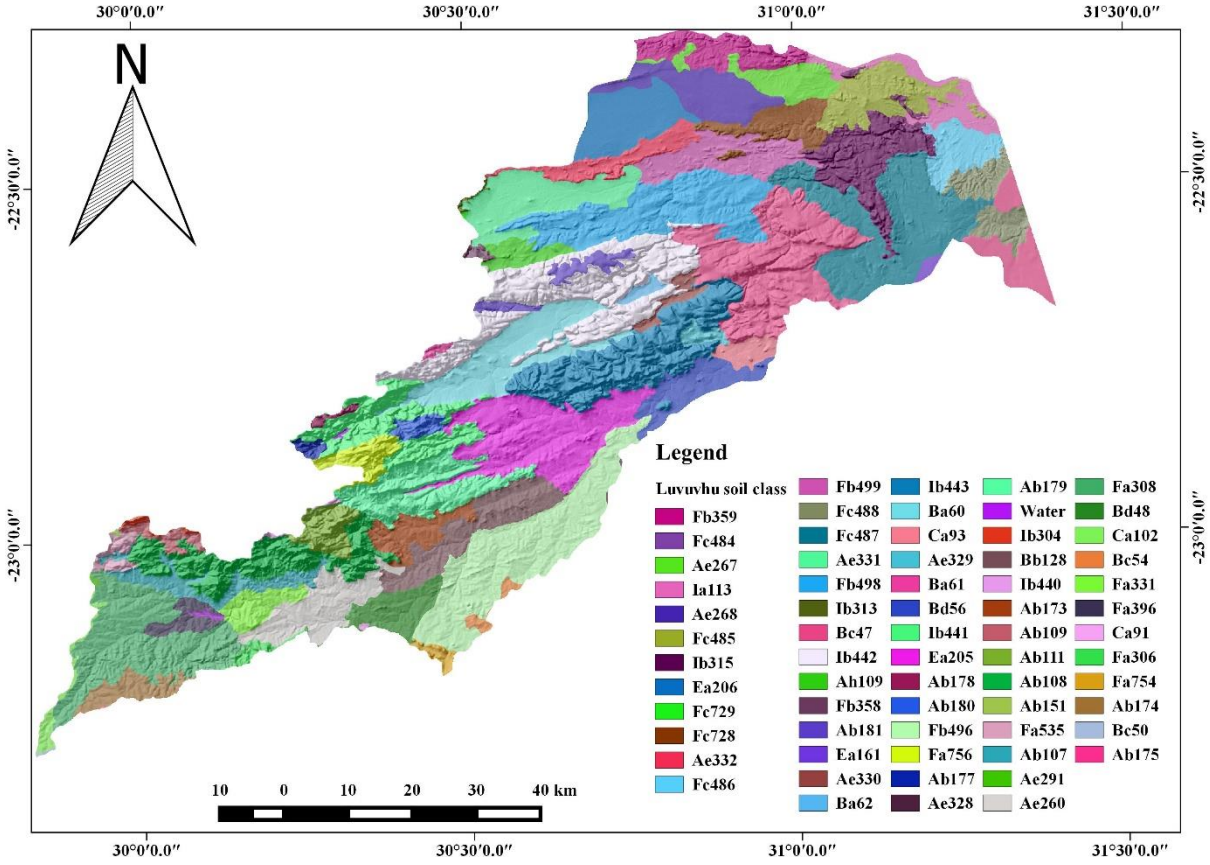

Figure 3.7 Soil map for the Luvuvhu River catchment

The SWAT model requires soil physical properties for simulation purposes (**Table 3.6**) and since there were no available data for different soil layers, it was assumed that there was only one layer. One of the soil physical properties required is the soil hydrologic group. The different groups are defined by grouping soils with same infiltration rates, soil depths, and drainage capacity and runoff potential under storm and cover conditions (Ponce and Hawkins, 1996). The soil hydrologic group were assigned to each soil class in the catchment according to the

information obtained from the soil map and soil inventory datasets from the ARC-ISCW (**Table B.3**). Soil albedo (0.1) was taken from default value.

Table 3.6: Soil physical properties required by SWAT model

PARAMETER	DEFINITION
HYDGRP	Soil hydrologic group (**A**, **B**, **C** and **D**).
SOL_ZMX	Maximum rooting depth of soil profile.
ANION_EXCL	Fraction of porosity (void space) from which anions are excluded.
SOL_CRK	Crack volume potential of soil.
TEXTURE	Texture of soil layer.
SOL_Z	Depth from soil surface to bottom of layer.
SOL_BD	Moist bulk density.
SOL_AWC	Available water capacity of the soil layer.
SOL_K	Saturated hydraulic conductivity.
SOL_CBN	Organic carbon content.
CLAY	Clay content.
SILT	Silt content.
SAND	Sand content.
ROCK	Rock fragment content.
SOL_ALB	Moist soil albedo.

The available water capacity (θ_a) parameter was attained by taking the difference between field capacity (θ_{fc}) and permanent wilting point (θ_{pwp}). Field capacity is the index of water content that can be held against the force of gravity thus corresponding to the pressure head of -3.4 m while the permanent wilting point is calculated as soil water content corresponding to -150 m since plants cannot exert suctions stronger than -150 m (Karkanis, 1983; Muthuwatta, 2004). These parameters are thus computed as follows:

field capacity (θ_{fc}):

$$\theta_{fc} = \emptyset(\frac{\varphi_{ae}}{340})^{1/b} \quad (3.9)$$

permanent wilting point (θ_{pwp}):

$$\theta_{pwp} = \emptyset(\frac{\varphi_{ae}}{15000})^{1/b} \quad (3.10)$$

and therefore:

$$\theta_a = \theta_{fc} - \theta_{pwp} \quad (3.11)$$

where $\emptyset$ is the porosity, φ_{ae} is the air entry water content in m, and *b* the exponent describing the soil water characteristic relationship.

Values for the different variables above are expressed (**Table 3.7**) including the saturated hydraulic conductivity (K_h) values. Other soil parameters required by the SWAT model such as bulk density and organic carbon are expressed in **Appendix C**.

Land use

In the case of preparing a land use table, there should be a string *landuse* in the file name so that it would be recognised by the model and be offered as an option for the land use table on the dropdown menu. The land use table should contain at least columns land use ID and SWAT code, where the SWAT code strings are four letters and should be found in the *crop* table contained in the SWAT reference database. The created land use table is depicted in **Table 3.8** while the map is depicted in **Figure 3.8**.

3.4.3 Climate data preparation

The model requires that the station information of all climate variables available be prepared before it can be implemented. The information needed includes station ID, station name, latitude, longitude and elevation. Missing values in the data were replaced with -99. Data format of all climate variables: solar radiation (MJ m^{-2}), wind speed (m s^{-1}), relative humidity (decimal fraction) and precipitation (mm) were the same, while the difference was when preparing minimum and maximum air temperature, where the minimum and maximum air temperature had to be separated by a comma.

Table 3.7 Parameter for estimating the available water capacity in different soils (Muthuwatta, 2004)

Soil Texture	ϕ	K_h (m s^{-1})	φ_{ae} (m)	b
Sand	0.395	1.76×10^{-4}	121	4.05
Loamy sand	0.410	1.56×10^{-4}	90	4.38
Sandy loam	0.435	3.47×10^{-5}	218	4.90
Silt loam	0.485	7.20×10^{-6}	786	5.30
Loam	0.451	6.95×10^{-6}	478	5.39
Sandy clay loam	0.420	6.30×10^{-6}	299	7.12
Silty clay loam	0.477	1.70×10^{-6}	356	7.75
Clay loam	0.476	2.45×10^{-6}	630	8.52
Sandy clay	0.426	2.17×10^{-6}	153	10.40
Silty clay	0.492	1.03×10^{-6}	490	10.40
Clay	0.482	1.28×10^{-6}	405	11.40

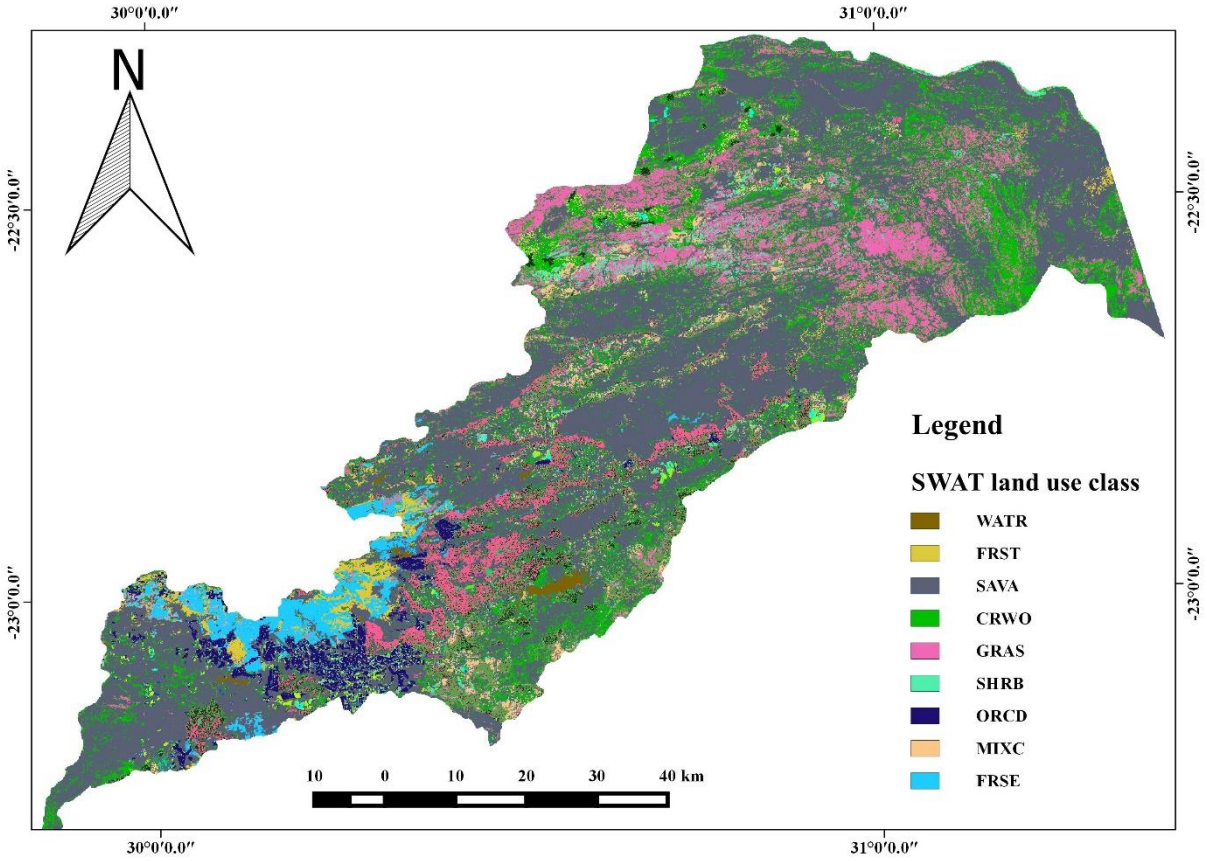

Figure 3.8 Land use map for the Luvuvhu River catchment

Table 3.8 SWAT land use name convention

Land-use	SWAT code	Physical name
1	WATR	Water
2	FRST	Forest-mixed
3	SAVA	Savana
4	CRWO	Cropland/woodland mosaic
5	GRAS	Grassland
6	SHRB	Shrubland
7	ORCD	Orchard
8	MIXC	Mixed dryland/irrigated crop
9	FRSE	Forest-evergreen

3.4.4 Weather generation and preparation

The SWAT model requires observed long-term daily climatic data such as daily rainfall, air temperature, relative humidity, solar radiation and wind speed for it to run or be applied (Clemence, 1997; McKague *et al*., 2003; McKague *et al*., 2005; Tingem *et al*., 2007; Safeeq and Fares, 2011). In the case where there are no measured data available, SWAT model uses data which is simulated by a weather generator model WXGEN. The WXGEN model generates precipitation data for the day and is thus able to generate data for other parameters (min/max air temperature, solar radiation and relative humidity) based on the availability of daily rainfall (Muthuwatta, 2004).

SWAT was able to generate rainfall using the WXGEN model based on historical statistics of weather elements like precipitation. The estimated parameters expressed in **Table 3.9** were tabulated in a weather generator table required by SWAT. The weather generator table contained parameters for all the weather stations where each weather station was represented by one line in the table. The weather generator table was created using statistical parameter data of daily precipitation obtained from the precipitation statistics (pcpSTAT) software while other parameters such as air temperature, RH, solar radiation and wind speed were obtained using the Excel pivot tables.

Table 3.9 Climate and statistical parameters needed by the SWAT model for the weather generator table

PARAMETER	MIN_	MAX_	DEFAULT	UNITS	DEFINITION
RAIN_YRS	5	100	14	Numeric	The number of years of maximum monthly 0.5 h rainfall data.
TMPMX	-30	50	0	ºC	Average maximum air temperature for month.
TMPMN	-40	40	1	ºC	Average minimum air temperature for month.
TMPSTDMX	0.1	100	2	ºC	Standard deviation for maximum air temperature in month.
TMPSTDMN	0.1	30	3	ºC	Standard deviation for minimum air temperature in month.
PCPMM	0	600	4	mm $month^{-1}$	Average amount of precipitation falling in month.
PCPSTD	0.1	50	5	mm $month^{-1}$	Standard deviation for daily precipitation in month.
PCPSKW	-50	20	6	na	Skew coefficient for daily precipitation in month.
PR_W1	0	0.95	7	fraction	Probability of a wet day following a dry day in the month.
PR_W2	0	0.95	8	Fraction	Probability of a wet day following a wet day in the month.
PCPD	0	31	9	days	Average number of days of precipitation in month.
RAINHHMX	0	125	10	Mm	Maximum 0.5 hour rainfall in entire period of record for month.
SOLARAV	0	750	11	MJ m^{-2}	Average daily solar radiation in month.
DEWPT	-50	25	12	ºC	Average dew point temperature in month.
WNDAV	0	100	13	m s^{-1}	Average wind speed in month.

The created weather generator table was added to the QSWAT reference database starting with a string *WGEN* so that whenever a new project is created the table would be available. The SWAT Editor allocates to each sub-catchment the nearest weather generation from the selected table. **Figure 3.9** depicts a snapshot of the window that appears in SWAT Editor when selecting the appropriate weather generator table.

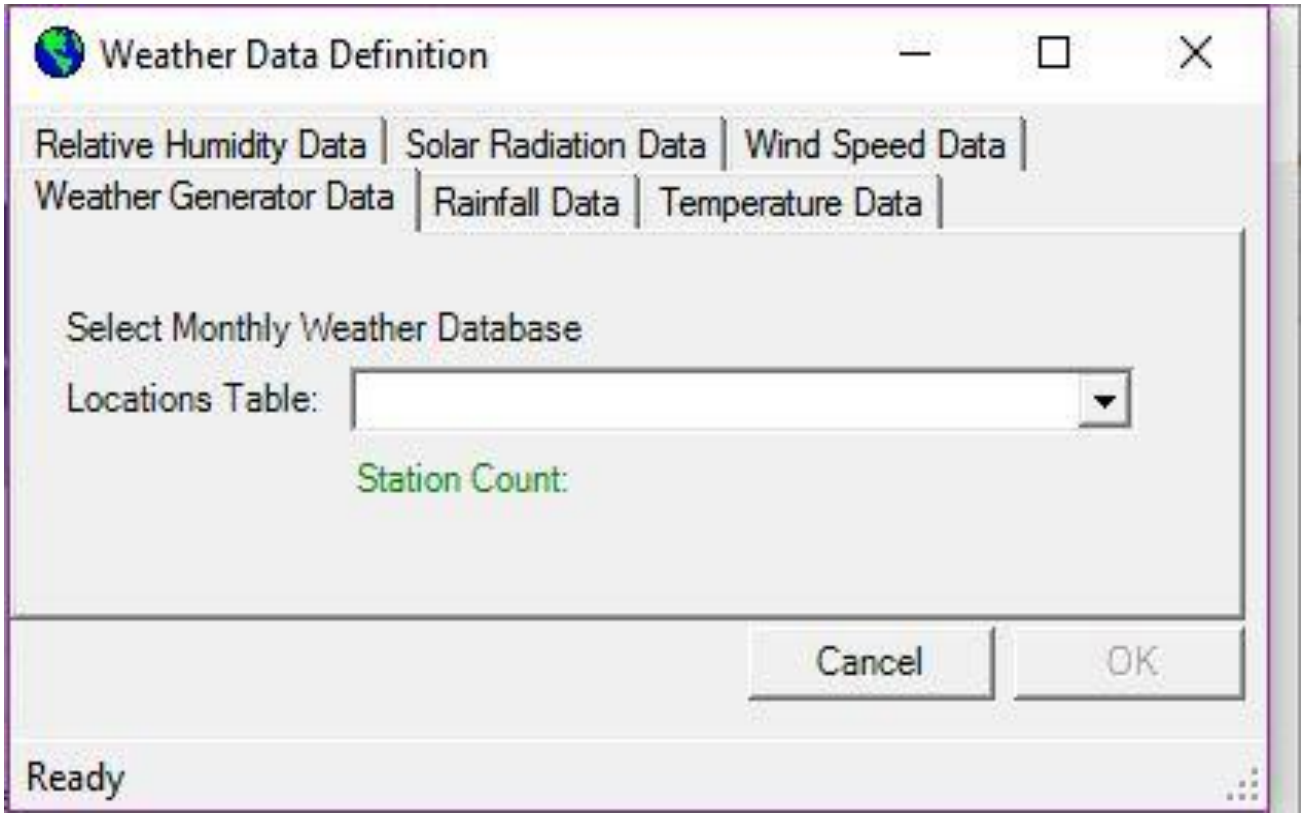

Figure 3.9 Weather data definition menu in the QSWAT program

3.5 Modelling using SWAT hydrological model

3.5.1 Model setup

Hydrological simulation was performed with the 2012 version of SWAT model through an interface between the model and QGIS desktop 2.6.1 software, QSWAT 1.3 2016. The model was set up following the guidelines laid out in (Dile *et al*., 2015), which details the use of QGIS interface of SWAT 2012 known as QSWAT. The process of running SWAT model on a QGIS interface, QSWAT, is shown in **Figure 3.10**. The model was run for a 33-year period of 1983 to 2015 but the first 3 years were used as "warm up" period to mitigate unknown initial conditions and hence were excluded from the analysis.

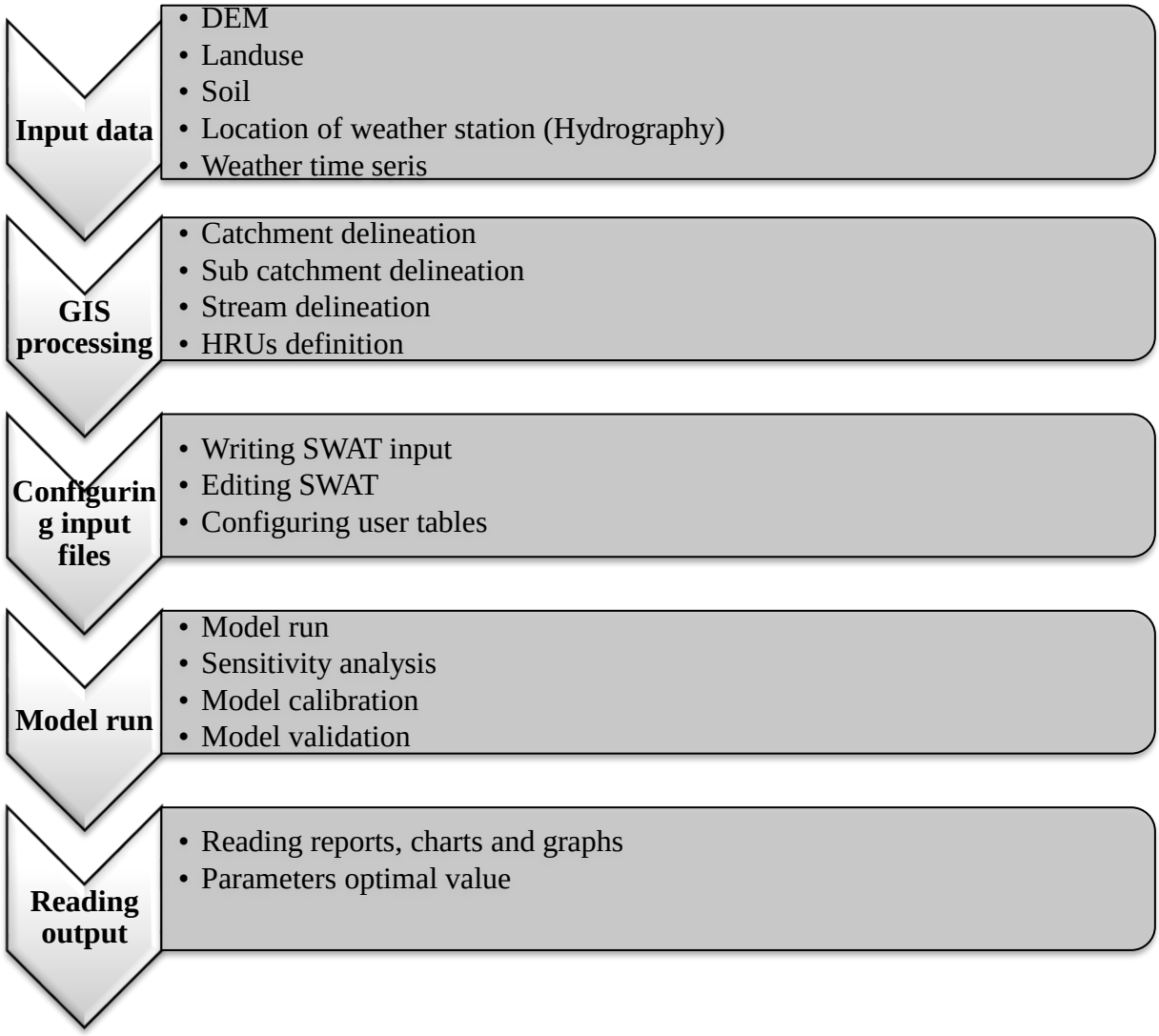

Figure 3.10 The SWAT model process flow diagram

There are three steps that a user needs to complete before the model can run, and these are: *delineating the catchment*, *Creating HRUs* and *Editing inputs and Run SWAT* (**Figure D.1** and **Figure D.2**). The following sections will be looking at the different steps detailing the five input parameters required by the model.

3.5.1.1 Delineation of catchments and sub-catchments

Delineation of the catchment and sub-catchment were done automatically using the SWAT tool whereby the catchment was sub-divided into smaller catchments and stream networks generated looking at topography, flow direction and flow accumulation (**Figure 3.11**). In delineating the catchment, a flow vector is created by filling the basins in the DEM thus increasing the elevation of basins until they overflow (Fadil *et al*., 2011). When the overflow

has occurred, flow accumulation grid is then created by numbering the cells flowing into each unit in the grid, meaning the flow accumulation is related to the flowing cells (which are part of the stream network) (Ncube, 2006). Stream networks were created automatically and the catchment outlet was modified to fit the project's requirements by adding the outlet position manually. The watershed was then created, and point sources added to each sub-catchment.

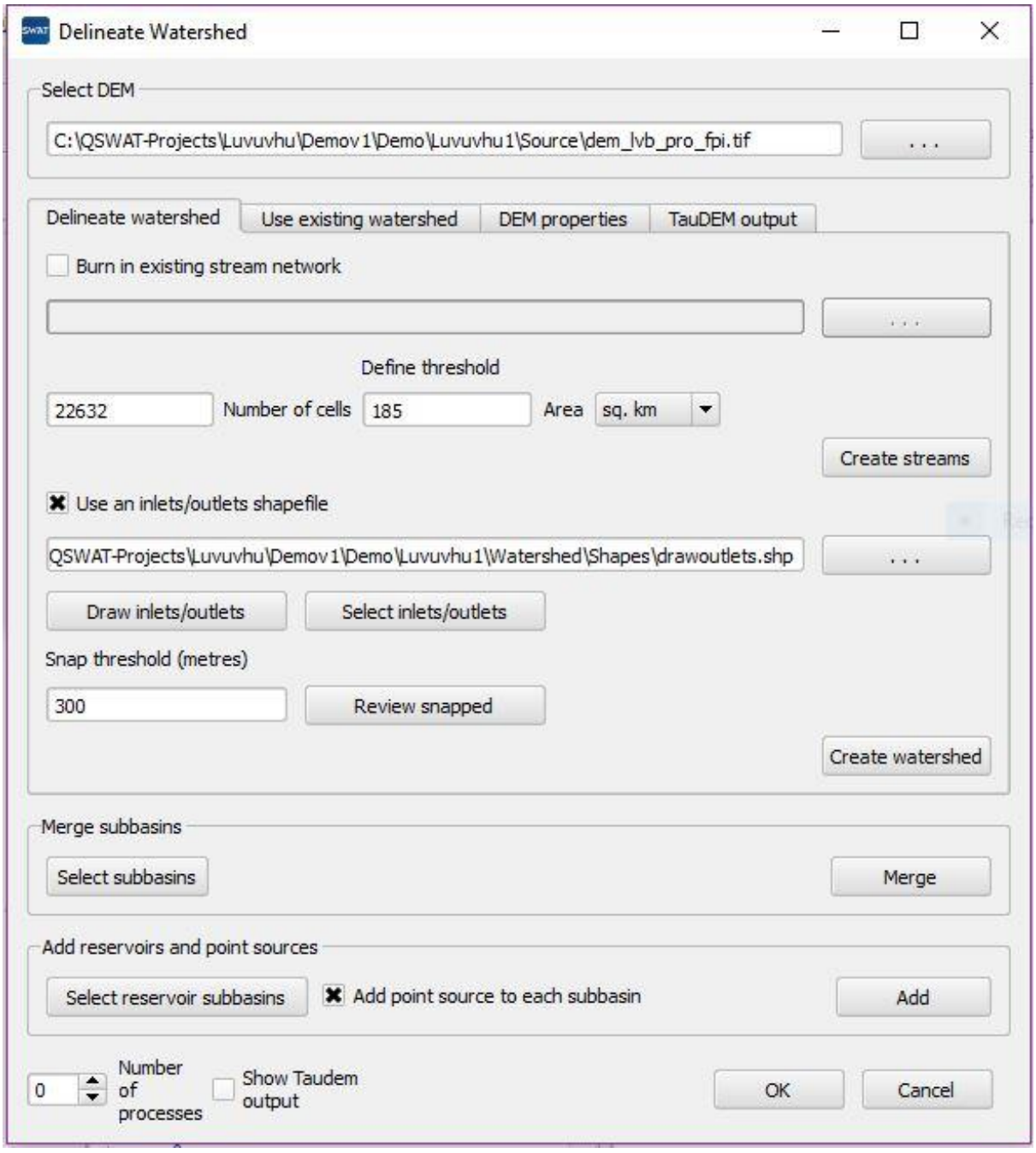

Figure 3.11 Catchment and sub-catchment delineation

3.5.1.2 Definition of land use and soil overlay

Soil and land use data are very important when it comes to the creation of HRUs. Soil and land use maps were imported into the SWAT model following the procedure expressed in (Dile *et al*., 2015). The created soil and land use tables were saved in the QSWAT project database in order to appear as options in the model drop down (**Figure 3.12**).

3.5.1.3 Hydrological response units

Having divided the catchment into several sub-catchments, the catchments were further divided into smaller units. These are the hydrological response units (HRU) which are used by the SWAT model (**Figure 3.12**) (Vazquez-Amabile *et al*., 2006; Jha, 2011).

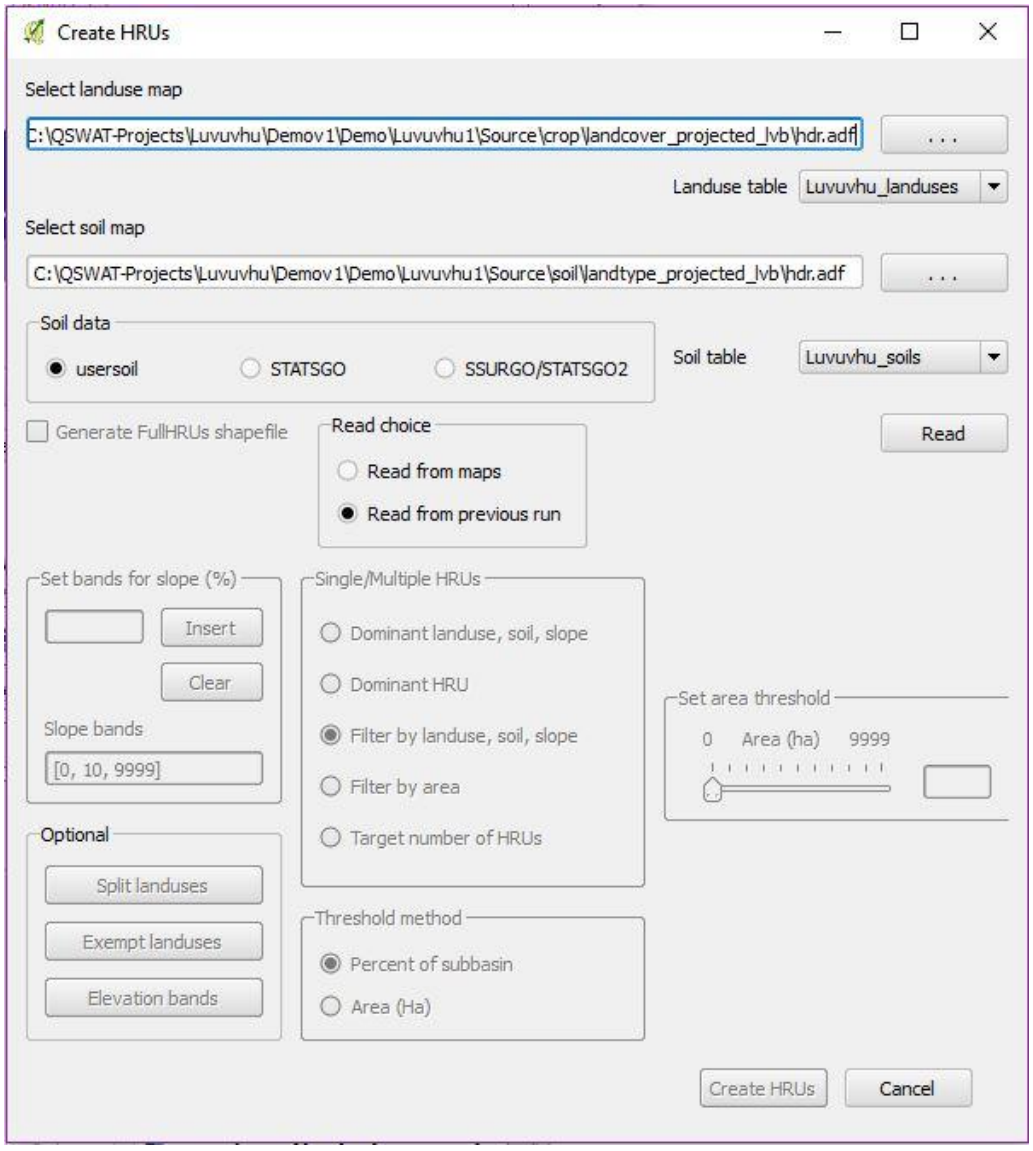

Figure 3.12 HRUs creation through land use and soil overlay definition

The SWAT model was able to read the information supplied in the land use and soil tables and also in the maps and therefore able to create the HRUs. The HRUs were created by overlaying analysis of land use, soil and slopes from information obtained from slope range, soil and land use maps and tables (Vazquez-Amabile *et al*., 2006). A threshold of 10% was recommended and selected for soil, land use and slope to divide the HRUs. This meant that if the percentage of soil and land use was less than the threshold value (10%) of the sub-catchment area it was then considered insignificant and not included in the analysis (Mutenyo *et al*., 2013). This approach defines the HRUs by creating at least one HRU per sub-catchment given the threshold value for soil and land use (Ncube, 2006). In the process of delineation, QSWAT automatically estimates the number of HRUs and stores the parameters into a SWAT sub-catchment input file.

3.5.1.4 Edit input and run SWAT

The SWAT editor was connected to the project database and SWAT reference database, which then was able to activate the "Write input tables" (**Figure 3.13** and **Figure 3.14**). Weather generator and climate data are provided through the option of "Weather stations". For each sub-catchment, the model uses observed climate data from the closest station. If there is no observed station climate data, QSWAT uses simulated data from the weather generator (Golmohammadi *et al*., 2014).

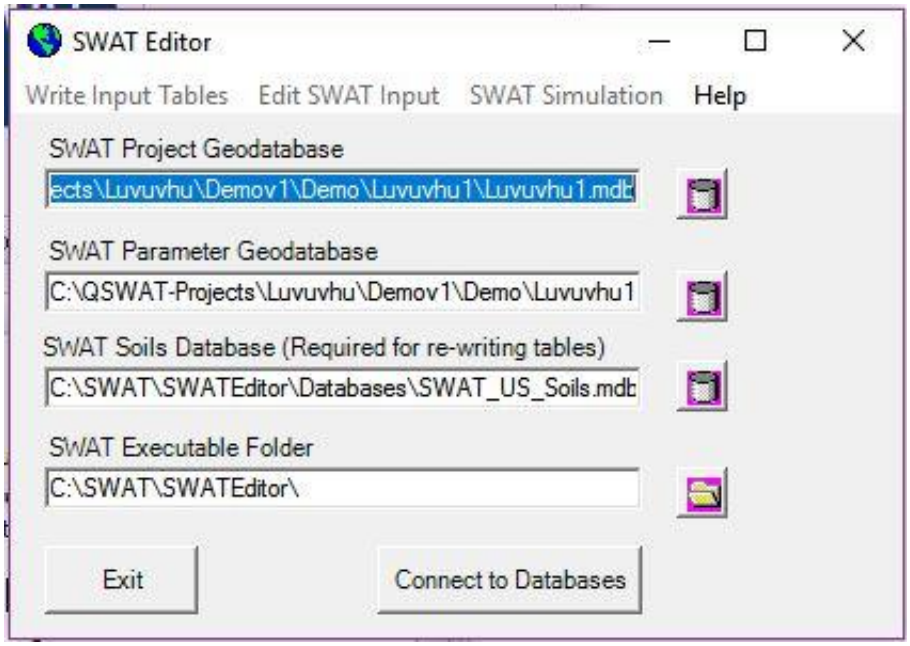

Figure 3.13 SWAT Editor input database

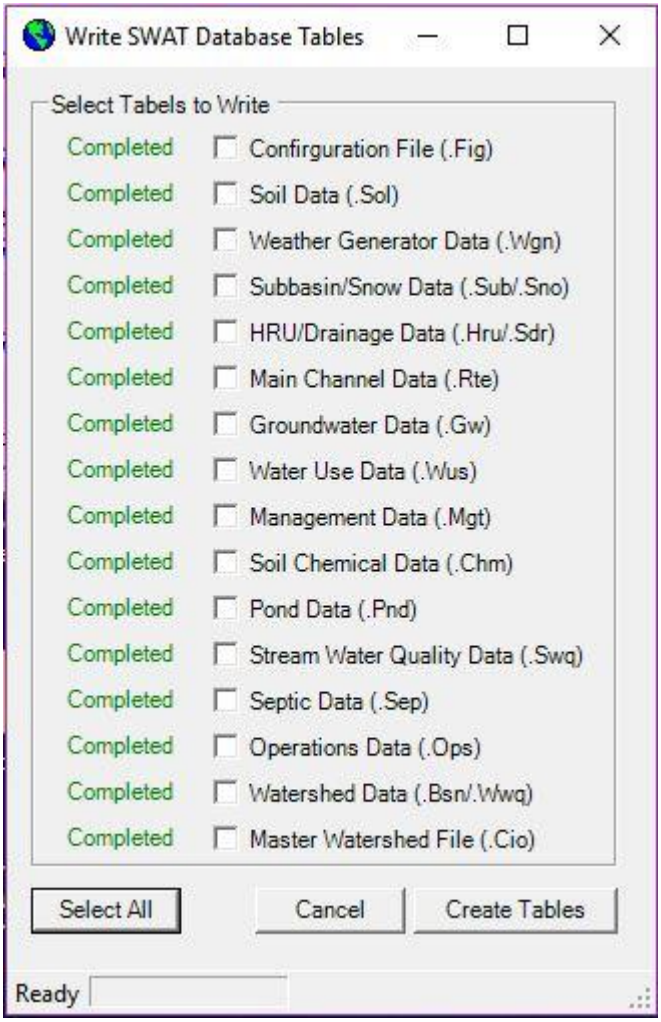

Figure 3.14 Window of complete written database tables

3.6 Sensitivity analysis, calibration and validation

3.6.1 Parameter sensitivity analysis

Before calibration and validation processes, SWAT requires that a sensitivity analysis of the most sensitive parameters for a given catchment be conducted (Mutenyo *et al*., 2013). A large number of parameter inputs influences the catchment processes (Gyamfi *et al*., 2016). Hence, it is essential to perform a sensitivity analysis test. A sensitivity analysis was conducted using the sequential uncertainty fitting (SUFI-2) algorithm to categorise main parameters that have more effect on streamflow. To determine the most sensitive parameters, the global sensitivity analysis approach was chosen. The global sensitivity analysis considers the sensitivity of one parameter in relation to other parameters which are under consideration (Arnold *et al*., 2012). The global sensitivity of surface runoff parameters was calculated using Latin hypercube

regression analyses and the minimum and maximum ranges of parameters were then fitted for calibration using the SUFI-2 uncertainty technique. The parameters were ranked according to their model sensitivity during calibration. Consistent with literature, these parameters are responsible for model calibration and parameter changes during different iterations. During sensitivity analyses, scatter plots were created and were used to display the distribution of simulations in parameter sensitivity analysis by comparing parameter values on the x-axis with the objective functions on the y-axis, value R^2 with a threshold of 0.5.

The level of significance between datasets was established by applying *t*-test and *p*-value sensitivity analyses parameters, to identify relative sensitivity of each parameter and to provide the significance of the sensitivity respectively. The *t*-test and *p*-value were used to rank the various parameters considered to have more influence on streamflow. The *t*-test gives a measure of the sensitivity of a parameter while the *p*-value gives the significance of the sensitivity of that parameter (Gyamfi *et al*., 2016). Parameters with higher *t*-test values and lower *p*-values show greater sensitivity on the streamflow (Jha, 2011).

According to past studies, **Table 3.10** depicts parameters which have been found to be sensitive to streamflow. A sensitivity analysis was conducted for each sub-catchment because parameters vary from one catchment to the other depending on geomorphological characteristics and other processes occuring in the catchment (Arnold *et al*., 2012). Initially, parameters in **Table 3.10** were considered for sensitivity analyses and final parameters were selected based on the *t*-test and *p*-value. Having accomplished the sensitivity analyses, model calibration was then carried out using the selected most sensitive parameters.

3.6.2 Calibration and validation

It is important to calibrate and validate the model in order to reduce errors (Pasi, 2014; Gyamfi *et al*., 2016). SUFI-2 was used to calibrate and validate the hydrologic setup of the model through its interface with SWAT calibration and uncertainty procedure (SWAT-CUP). The streamflow weir station A9H013 was selected to be the outlet point of the catchment. The reason for the selection was due to its location in the catchment and the availability of streamflow data, which makes it applicable for calibration and validation.

Table 3.10 Parameters considered for sensitivity analysis (Gyamfi *et al*., 2016)

Parameter name	Description
CN2	SCS runoff curve number.
ESCO	Soil evaporation compensation factor.
GWQMN	Threshold depth of water in the shallow aquifer required for return flow to occur (mm H_2O).
SOL_AWC	Soil available water storage capacity (mm H_2O/mm soil).
GW_REVAP	Groundwater revap coefficient.
RCHRG_DP	Deep aquifer percolation function.
SOL_Z	Soil depth (mm).
SURLAG	Surface runoff lag coefficient (days).
SOL_K	Soil conductivity (mm h^{-1}).
CH_K2	Effective hydraulic conductivity in the main channel (mm h^{-1}).
ALPHA_BF	Baseflow alpha factor (day).
GW_DELAY	Groundwater delay (day).
ALPHA_BNK	Baseflow alpha factor for bank storage (day).
REVAPMN	Threshold depth of water in the shallow aquifer for "revap" to occur (mm).

A split sample procedure using daily streamflow data from weir stations, A9H003, A9H006, A9H012 and A9H013 for the period 1986-2005 and 2006-2015 were used for calibration and validation respectively. Multiple simulation iterations were executed with a minimum of 300 simulations in each run.

3.6.3 Performance indices

Performance of the model in simulating the observed streamflow was judged against four objective functions. Objective functions are not universally applicable to all situations hence the choice is dictated by the objective of the particular study (Gyamfi *et al*., 2016). The goodness-of-fit and efficiency of the model were tested using four main objective functions, R^2, NSE, PBIAS, RSR and two performance indices, *P*-factor and *R*-factor. The performance of the model was judged according to findings from literature.

The formulae of these efficiency measures are as follows:

$$NSE = 1 - \frac{\sum_{i=1}^{n}(O_i - S_i)^2}{\sum_{i=1}^{n}(O_i - \bar{O})^2} \quad (3.17)$$

$$R^2 = \left[\frac{\sum_{i=1}^{n}(O_i - S_i)(S_i - \bar{S})}{(\sum_{i=1}^{n}(O_i - \bar{O})^2)^{0.5}(\sum_{i=1}^{n}(S_i - \bar{S})^2)^{0.5}}\right]^2 \quad (3.18)$$

$$PBIAS = \frac{\sum_{i=1}^{n}(O_i - S_i) \times 100}{\sum_{i=1}^{n} O_i} \quad (3.19)$$

$$RSR = \frac{\sqrt{\sum_{i=1}^{n}(O_i - S_i)^2}}{\sum_{i=1}^{n}(O_i - \bar{O})^2} \quad (3.20)$$

where O_i is observed variable, S_i is simulated variable, $\bar{O}$ is the mean observed variable, $\bar{S}$ is the mean simulated variable and n is the number of observations under consideration.

The model calibration was aimed at achieving a satisfactory model efficiency of concurrently having NSE ≥ 0.5, PBIAS ± 25 % and RSR < 0.7 (Mutenyo *et al*., 2013).

SUFI-2 assumes large parameter uncertainty and decreases this uncertainty through *P*-factor and *R*-factor performance statistics. The *P*-factor was used to quantify all the uncertainties associated with the SWAT model by bracketing an amount of measured data containing all uncertainties. SUFI-2 algorithm was used to reduce uncertainty by placing most of the observed streamflow data in the 95% band. These model uncertainties can be accounted for due to some errors in data input sources, data preparation and parameterization. Other sources of uncertainty may be the result of human and instrumental errors during data processing. Rainfall in the Luvuvhu catchment is not equally distributed due to topography variation and thus may contribute to some of the uncertainties in the model because of insufficient data availability. Furthermore, model structure may also be the source of uncertainties.

3.6.4 Flood frequency and risk analysis

Following calibration and validation, SWAT was run to simulate 30 years in order to compute flood annual exceedance probability. Flood frequency analyses were performed for all four sub-catchments for the simulated peaks. The log-normal probability distribution was used to fit the maximum annual peak data to estimate the flood frequencies. The flood magnitudes were estimated at seven different return periods of 2, 5, 10, 25, 50, 100 and 200 years. Graphical extrapolation was used to estimate the flood peaks for higher return periods. A 30-year period of data from 1986 to 2015 was used to attain the flood frequencies. The data were sorted from

highest to lowest so that a reoccurrence interval could be calculated. The reoccurrence interval was calculated using:

$$RI = \frac{n+1}{m} \tag{3.21}$$

where n is the number of years in the set, and m is the rank of discharge.

The exceedance probability of the critical value were presented in plots for the whole catchment and for the other three sub-catchments.

CHAPTER 4: RESULTS AND DISCUSSION

4.1 Results

4.1.1 Initial model run analysis

Once the SWAT model was set up, reports retrieved from the model indicated elevation ranging from 199 to 1588 m with mean of 625.21 m and standard deviation of 235.72 m. The model was initially run for four sub-catchments: sub-catchment 6, 10, 15 and 17 produced during the delineation process (**Figure 4.1**). Simulations from the four sub-catchments were compared with the observed daily flows from four weir stations chosen for the study (**Figure 4.2**).

The water balance components of the catchment were calculated using the water balance

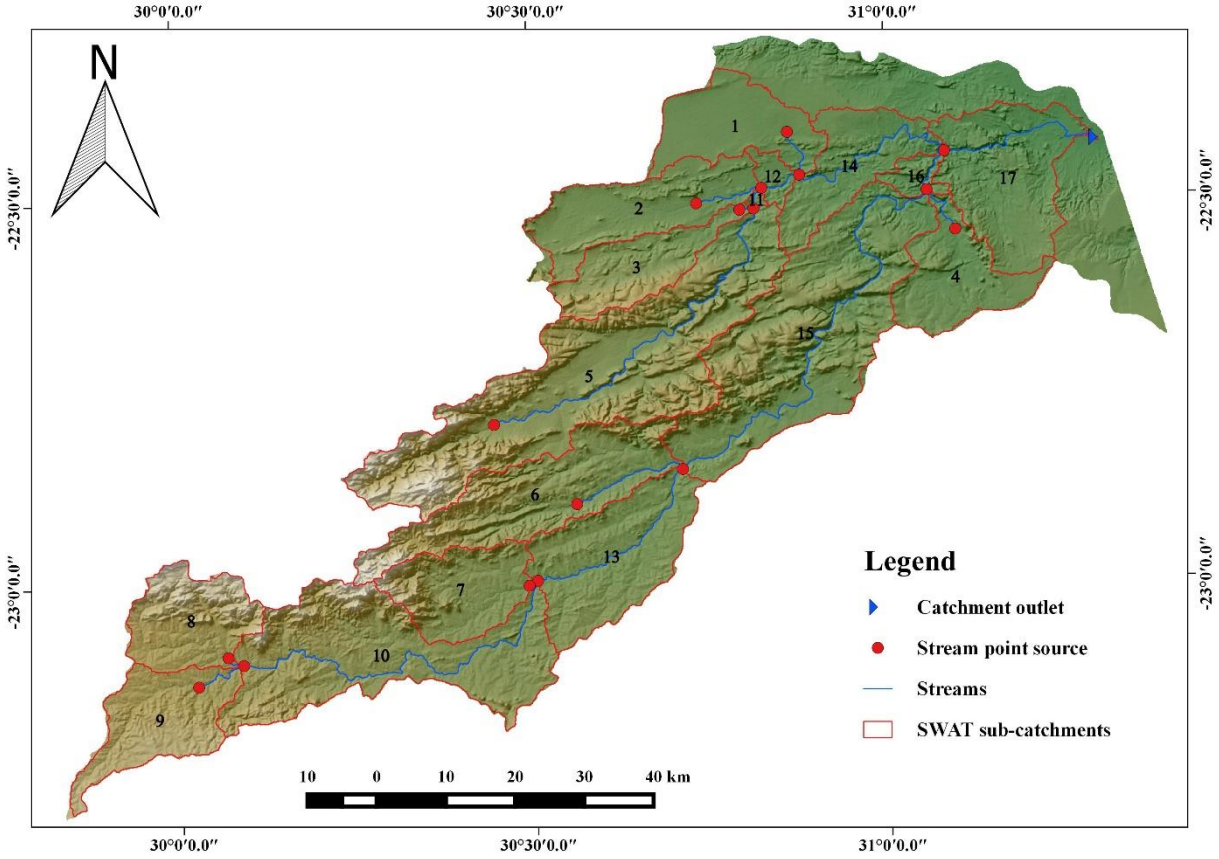

Figure 4.1 Sub-catchments delineation through QSWAT

equation of the SWAT model and the computed results were analysed in the SWAT check tool (**Table 4.1)**. The average curve number was computed to be 49.96 which meant the hydrological condition of the Luvuvhu River catchment ranged from fair to poor and therefore prone to runoff and ultimately flooding (**Table E.1**) (Pitt, 2002).

Table 4.1 Simulation details of the SWAT model set-up

General details	
Simulation length (years)	33
Warm up (years)	3
Hydrological response units	214
Sub-basins	17
Output time-step	Daily
Precipitation method	Measured
Watershed area (km^2)	5273.1
Hydrology (water balance ratio)	
Streamflow/precipitation	0.61
Baseflow/total flow	0.68
Surface run-off/total flow	0.32
Percolation/precipitation	0.42
Deep recharge/precipitation	0.02
ET/precipitation	0.34
Hydrological parameters	
Average curve number	49.96
ET and transpiration (mm)	268.4
Precipitation (mm)	780.3
PET (mm)	946.4
Surface run-off (mm)	153.18
Lateral flow (mm)	33.18
Return flow (mm)	293.45
Percolation to shallow aquifer (mm)	325.04
Recharge to deep aquifer (mm)	16.25
Re-evaporation from shallow aquifer (mm)	16.53

To evaluate the performance of the model before calibration, correlation coefficient (R), coefficient of determination (R^2), mean absolute error (MAE), mean bias error (MBE), root mean square error (RMSE) and Nash–Sutcliffe efficiency (NSE) index were used (**Table 4.2**).

Table 4.2 Statistic evaluation of simulated versus observed streamflow data before calibration.

Sub-catchments	MAE*	MBE**	RMSE***	R^2	R	NSE****
6	7.68	3.01	9.41	0.46	0.68	0.54
10	23.87	23.82	25.93	0.43	0.66	-11.05
15	36.14	25.57	58.01	0.37	0.61	0.11
17	66.51	66.06	98.80	0.30	0.55	-3.04

MAE=Mean absolute error ($m^3 s^{-1}$) **MBE=Mean bias error ($m^3 s^{-1}$) ***RMSE=Root mean square error ($m^3 s^{-1}$) ****NSE=Nash–Sutcliffe efficiency

Results reveal a significant correlation in all the sub-catchments 6, 10, 15 and 17 with R of 0.68, 0.66, 0.61 and 0.55 respectively (**Figure 4.2**). However, the coefficient of determination results for sub-catchment 6, 10, 15 and 17 reveal that in all of the sub-catchments, one cannot be certain when predicting using the model because of the R^2 of 0.46, 0.43, 0.37 and 0.30 respectively.

The regression line does not represent the data well, since the strength between the observed and simulated variables was not strong, and only less than 46% of the simulated variation can be explained by the linear relationship between observed and simulated while more than 54% remains unexplained. The RMSE imply unacceptable model results since there is larger variation than bias while the positive MBE shows that the model overestimates the observed data. There is not much difference between MAE and RMSE for sub-catchment 6 and 10 hence there was less variance in the individual errors in the sample. However, sub-catchments 15 and 17 revealed a greater difference between MAE and RMSE, which implies greater variance in the individual errors in the sample. The NSE index indicated a good model performance in sub-catchments 6 and 15 showing an NSE index of 0.54 and 0.11 respectively. Conversely, sub-catchments 10 and 17 revealed an NSE index less than zero which suggests that the observed mean was a better predictor than the model. Judging the initial model run by the above efficiency measures, it is evident that a calibration and validation procedure should be done for each of the sub-catchments to attain improved parameter estimation for improved model simulation.

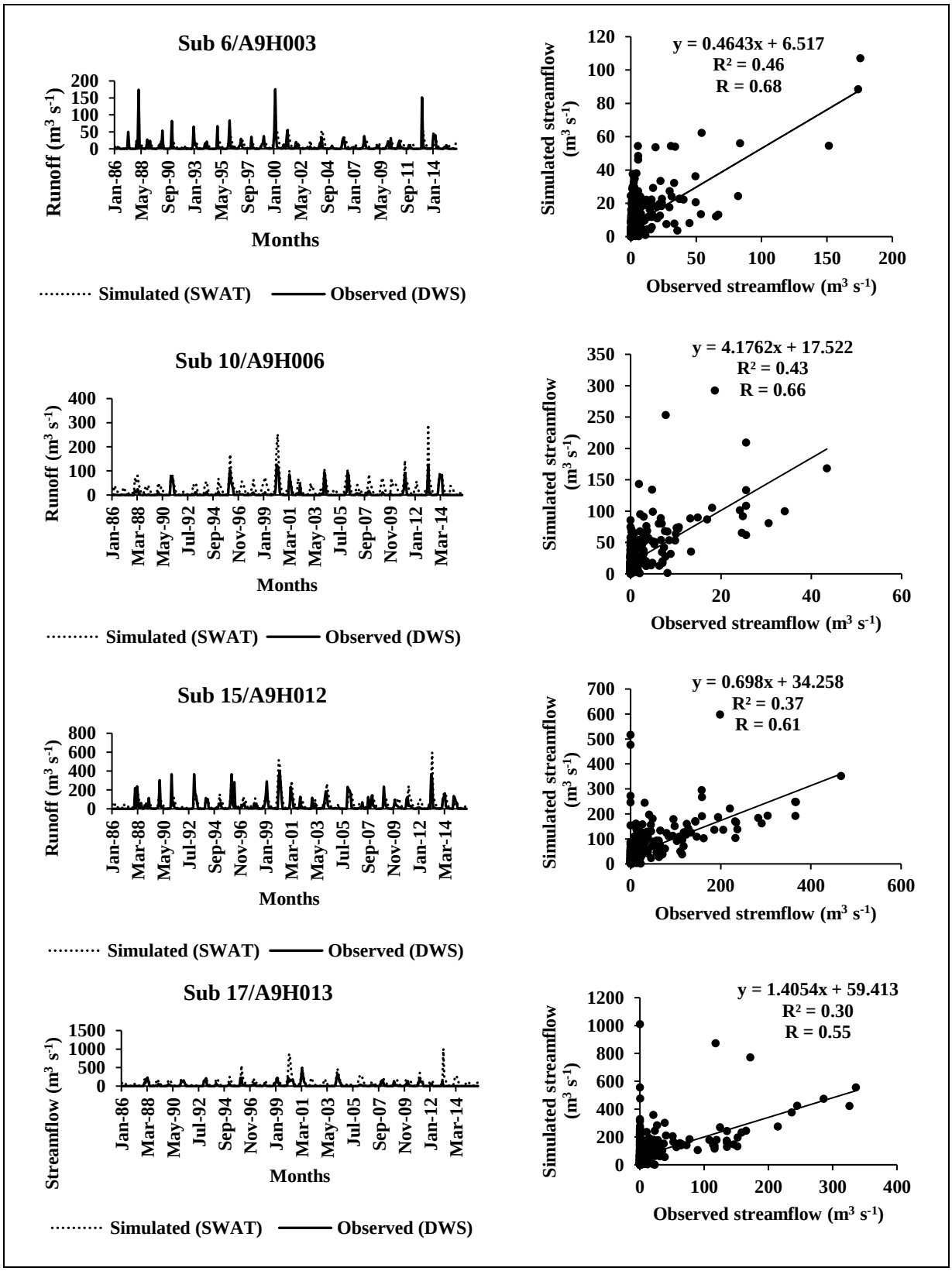

Figure 4.2 Comparison of simulated and observed daily discharge through hydrographs and regression graphs for the period 1986-2015 at stations: A9H003, A9H006, A9H012 and A9H013

4.1.2 Model calibration

SUFI-2 was applied for model sensitivity, calibration and uncertainty analysis. The model was calibrated using twelve parameters which, based on previous studies, were recorded to be the most sensitive parameters for streamflow. Over 300 simulations in five iterations were run to achieve the best model efficiency between the observed and simulated flows.

4.1.2.1 Parameter sensitivity analysis

The global sensitivity analysis based on surface runoff showed that the most sensitive parameters in SWAT hydrological modeling for the Luvuvhu river catchment are baseflow alpha factor (ALPHA_BF), initial SCS runoff curve number for moisture condition II (CN2), groundwater delay time (GW_DELAY), and saturated hydraulic conductivity (SOL_K) with $p < 0.05$ (**Figure 4.3** and **Table 4.3**). This result confirms similar studies done by Fadil *et al*. (2011), Mamo and Jain (2013) and Gyamfi *et al*. (2016) where these parameters were shown to be most sensitive to streamflow. The remaining parameters were found to have no significant effect on streamflow simulations and caused no significant changes in the model surface runoff output with $p > 0.05$. This agreed with literature with Jha (2011) confirming that great sensitivity on streamflow is when there is high *t*-test value and lower *p*-value.

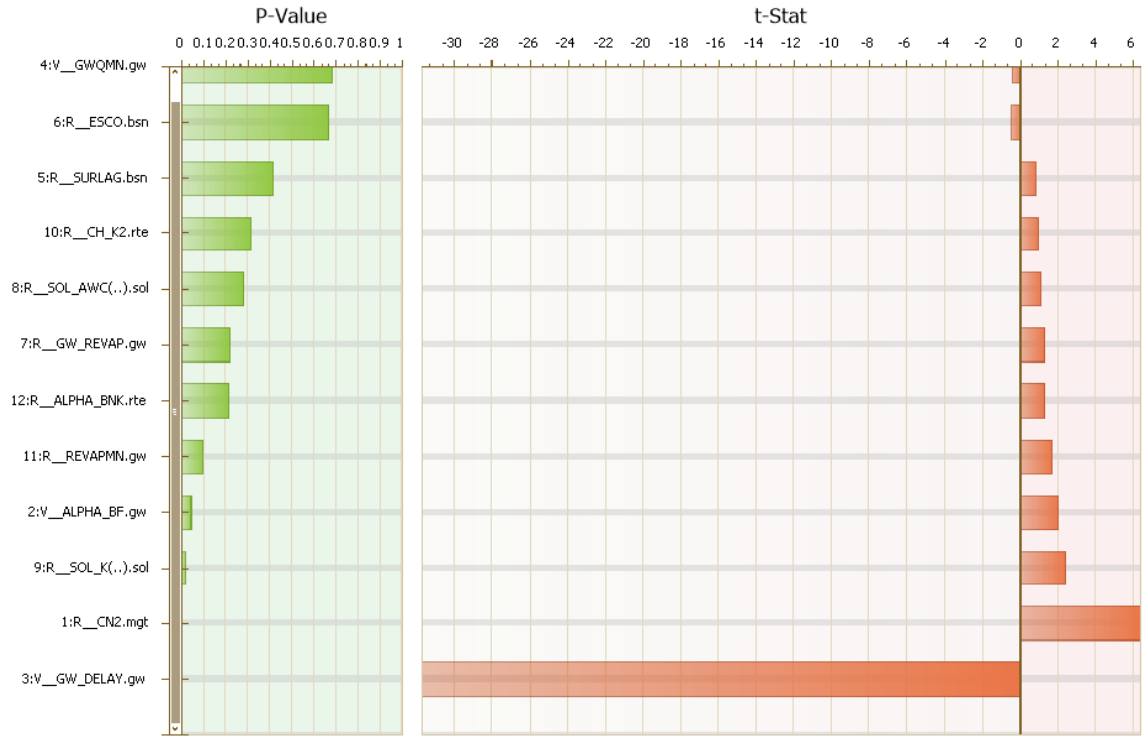

Figure 4.3: Global sensitivity analysis and ranking of SWAT parameters

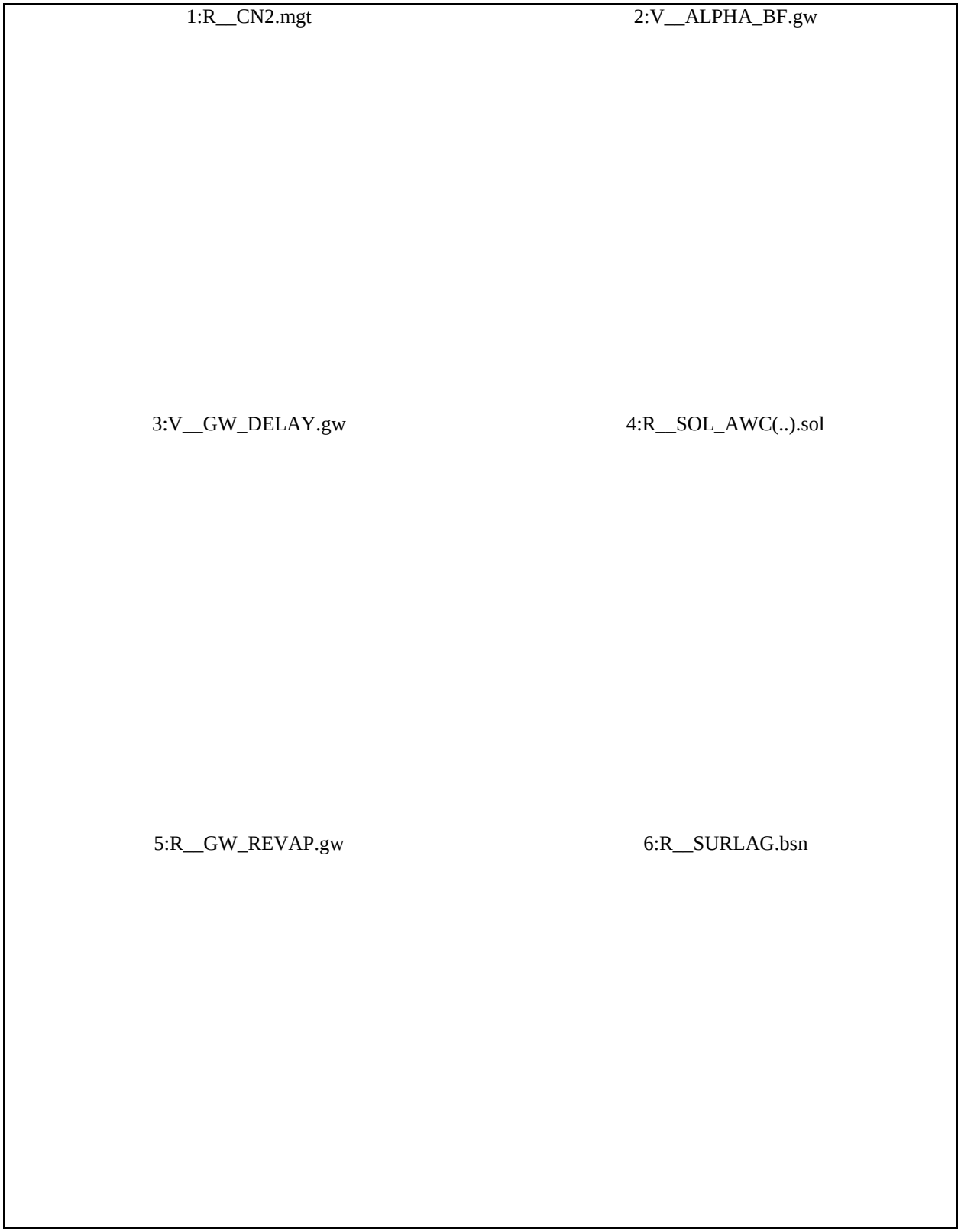

Looking at the scatter plots created during calibration, significant variation/distribution parameter values were observed in most of the parameters (

Figure E.1). However, parameters ALPHA_BF, CN2, GW_DELAY and SOL_K were more distinguishable, showing more variance than the other parameters indicating that the other

parameters were the primary source of streamflow uncertainty in the Luvuvhu River catchment. ALPHA_BF parameter forms part of the baseflow, which contributes to channel runoff and thus delay may have an effect on streamflow discharge and runoff. SOL_K is important for groundwater seepage to streamflow, while GW_DELAY is as important in know the amount time the percolated water will eventually reach the streams (van Liew *et al*., 2007; Chapuis, 2012).

4.1.2.2 Performance indices during calibration

The *P*-factor during calibration was 0.64, 0.52, 0.67, and 0.45 for sub-catchments 6, 10, 15 and 17 respectively. The model produced *R*-factor of 0.59, 1.81, 0.68 and 0.91 for sub-catchments 6, 10, 15 and 17 respectively showing good calibration results.

Performance indices results obtained (**Figure 4.4** and **Table 4.4**) for all the sub-catchments 6, 10, 15 and 17 proved to have satisfactory simulation results with an R^2 of 0.61, 0.73, 0.63 and 0.75 respectively. Results further indicated an NSE index of 0.35 and 0.66 for sub-catchments 6 and 15 respectively, which meant acceptable results, while sub-catchments 10 and 17 revealed unsatisfactory results of -16.46 and -0.36 respectively. The model revealed acceptable RSR results of 0.62, 0.56 and 0.71 for sub-catchments 6, 15 and 17 respectively while sub-catchments 10 showed unsatisfactory results of 3.23. Sub-catchments 6 and 15 showed positive PBIAS of 1.18 and 16.3 respectively, while sub-catchments 10 and 17 gave a negative PBIAS of -7.60 and -2.40 respectively.

Table 4.3 Sensitivity ranking of SWAT parameter in the Luvuvhu River catchment

Parameter	Parameter definition	Ranking	*t*-Stat	*p*-value	Minimum	Maximum	Fitted values
r__CN2.mgt	Initial SCS (Soil Conservation Service) runoff curve no. for moisture condition II	2	6.420	0.000	-0.018	0.345	0.082
r__ALPHA_BF.gw	Baseflow alpha factor (days)	4	2.050	0.040	0.499	1.498	0.943
r__GW_DELAY.gw	Groundwater delay time (days)	1	-31.740	0.000	-17.162	24.294	0.319
r__GWQMN.gw	Threshold depth of water in the shallow aquifer required for return flow to occur (mm)	12	-0.410	0.690	-2388.583	2538.583	1873.416
r__GW_REVAP.gw	Groundwater “revap” coefficient	7	1.230	0.220	0.091	0.234	0.167
r__ESCO.hru	Soil evaporation compensation factor	11	-0.440	0.660	-0.123	0.626	0.108
r__CH_K2.rte	Effective hydraulic conductivity in main channel alluvium	9	1.010	0.310	54.592	163.908	159.718
r__ALPHA_BNK.rte	Baseflow alpha factor for bank storage	6	1.250	0.210	0.127	0.709	0.658
r__SOL_K.sol	Saturated hydraulic conductivity	3	2.440	0.020	-137.606	154.218	7.819
r__SOL_AWC.sol	Available water capacity of the soil layer	8	1.090	0.270	0.484	1.453	0.889
r__SURLAG.bsn	Surface runoff lag coefficient (days)	10	0.820	0.410	-0.853	15.722	2.379
r__REVAPMN.gw	Threshold depth of water in the shallow aquifer for "revap" to occur (mm)	5	1.670	0.100	153.640	461.360	454.692

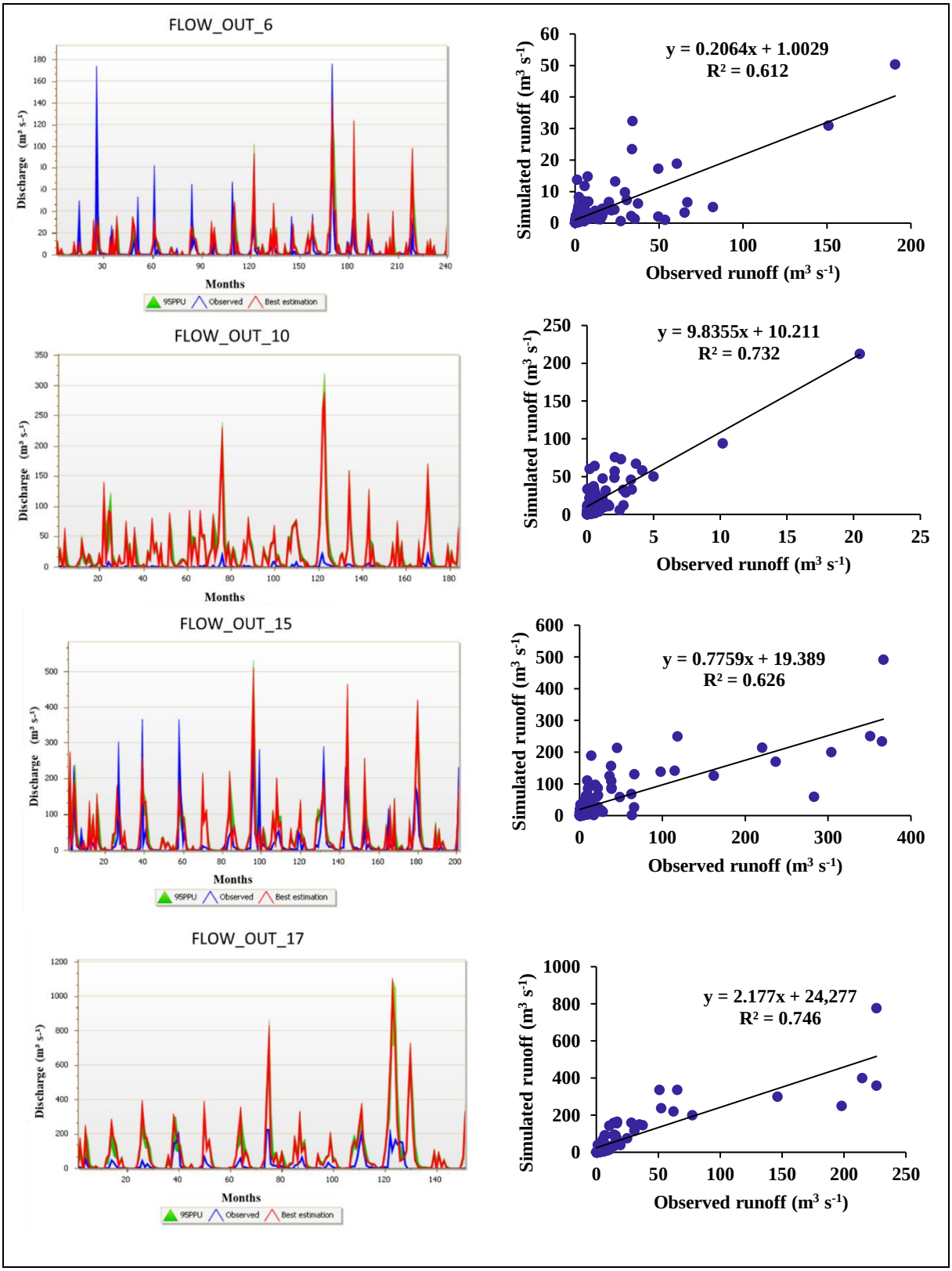

Figure 4.4 Comparison of observed and simulated streamflow for the calibration period (1986-2005) for sub-catchments 6, 10, 15 and 17

Table 4.4 Performance indices of the SWAT model during calibration

Index	*P*-factor	*R*-factor	R^2	NSE	RSR	PBIAS
FLOW_OUT_ 6	0.64	0.59	0.61	0.35	0.62	1.18
FLOW_OUT_10	0.52	1.81	0.73	-16.46	3.23	-7.60
FLOW_OUT_15	0.67	0.68	0.63	0.66	0.56	16.30
FLOW_OUT_17	0.45	0.91	0.75	-0.36	0.71	-2.10

4.1.3 Model validation

During the period 2006-2015, the *P*-factor obtained was 0.59, 0.34, 0.69 and 0.41 for sub-catchments 6, 10, 15 and 17 respectively, while the *R*-factor obtained was 0.46, 2.67, 0.53 and 0.75 for the same sub-catchments respectively. The percentage of observed data grouped together by 95% prediction uncertainty (95PPU) during validation was 59, 34, and 69 and 41 for sub-catchments 6, 10, 15 and 17 respectively, which indicates the strength of the model calibration to be satisfactory and thus satisfactory model performance.

Objective function results obtained (**Figure 4.** and **Table 4.5**) revealed an R^2 of 0.63, 0.52 and 0.62 for sub-catchment 10, 15 and 17 respectively which showed satisfactory results while sub-catchment 6 still showed unsatisfactory results with an R^2 of 0.34. NSE in sub-catchments 6, 15 and 17 gave acceptable results of 0.35, 0.48 and 0.31 respectively while sub-catchment 10 still gave unsatisfactory results of -0.45. Sub-catchment 15 showed acceptable RSR result of 0.72 while sub-catchments 6, 10 and 17 showed unacceptable RSR results of 0.86, 1.14 and 2.10 respectively. Sub-catchments 6 and 15 gave positive PBIAS of 65.0 and 19.90 respectively and negative PBIAS of -12.30 and -14.60 was observed in sub-catchments 10 and 17 respectively.

Table 4.5 Performance indices of the SWAT model during validation

Index	*P*-factor	*R*-factor	R^2	NSE	RSR	PBIAS
FLOW_OUT_ 6	0.59	0.46	0.34	0.35	0.86	65.00
FLOW_OUT_10	0.34	2.67	0.63	-0.45	1.14	-12.30
FLOW_OUT_15	0.69	0.53	0.52	0.48	0.72	19.90
FLOW_OUT_17	0.41	0.75	0.62	0.31	2.10	-14.60

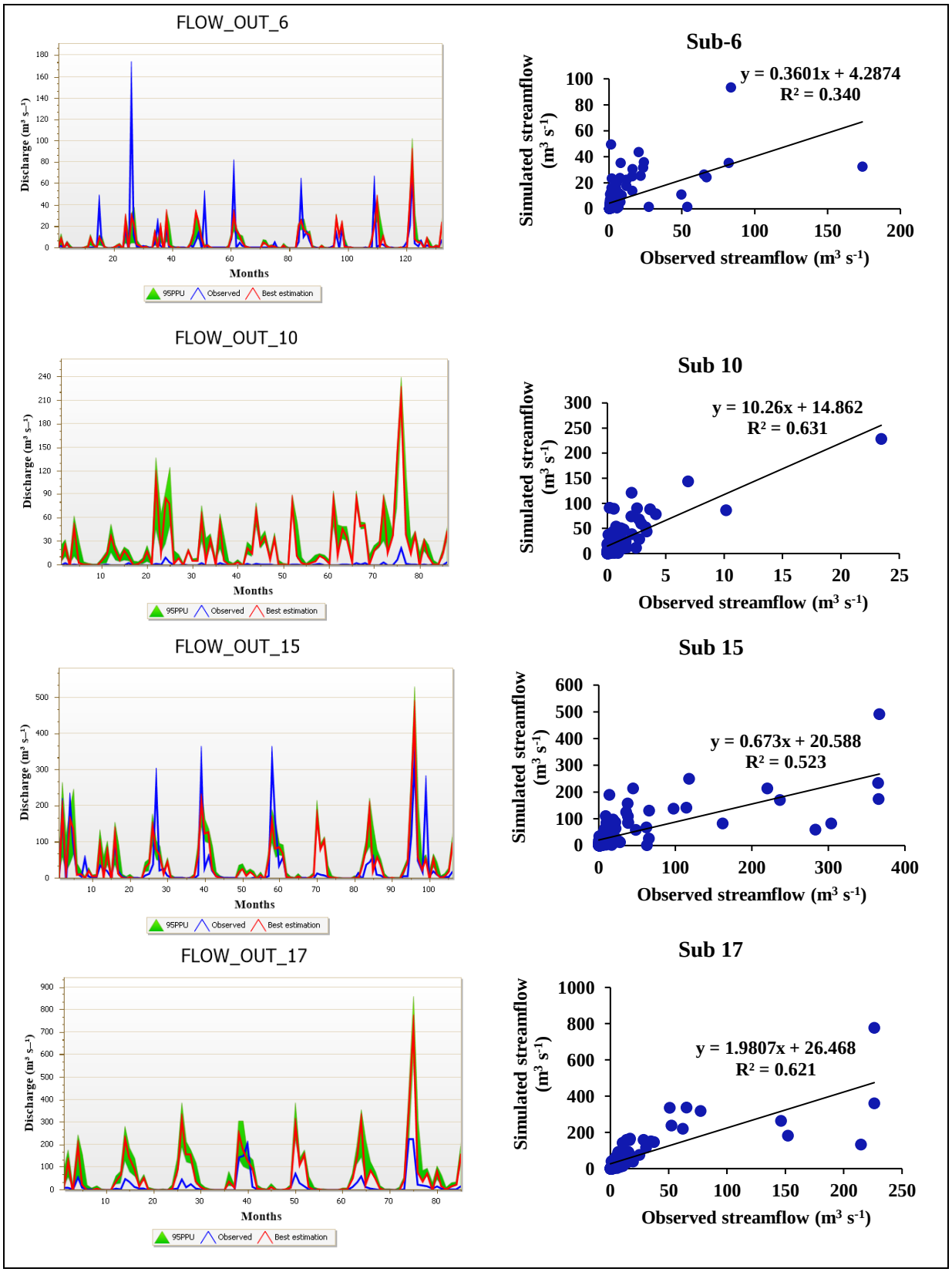

Figure 4.5 Comparison of observed and simulated streamflow for the validation period (2006-2015) for sub-catchments 6, 10, 15 and 17

4.1.4 Flood frequency analysis and design flood estimation

Flood return periods were plotted against the flood discharges in order to estimate 100- and 200-year floods (**Figure 4.6**). Sub-catchment 6 received very low flood discharges compared to sub-catchment 17, and this was expected since sub-catchment 6 had a smaller catchment area compared to sub-catchment 17. A 30-year period flood data was used, thus the 5 % and 95% confidence bound showed considerable scatter. Using the equations created from the plots for each sub-catchment, flood magnitudes for different return periods were established (**Table 4.6**). At the outlet sub-catchment 17, the 50-, 100- and 200-year flood magnitudes of 960.70, 1121.02 and 1281.35 m^3 s^{-1} respectively occur.

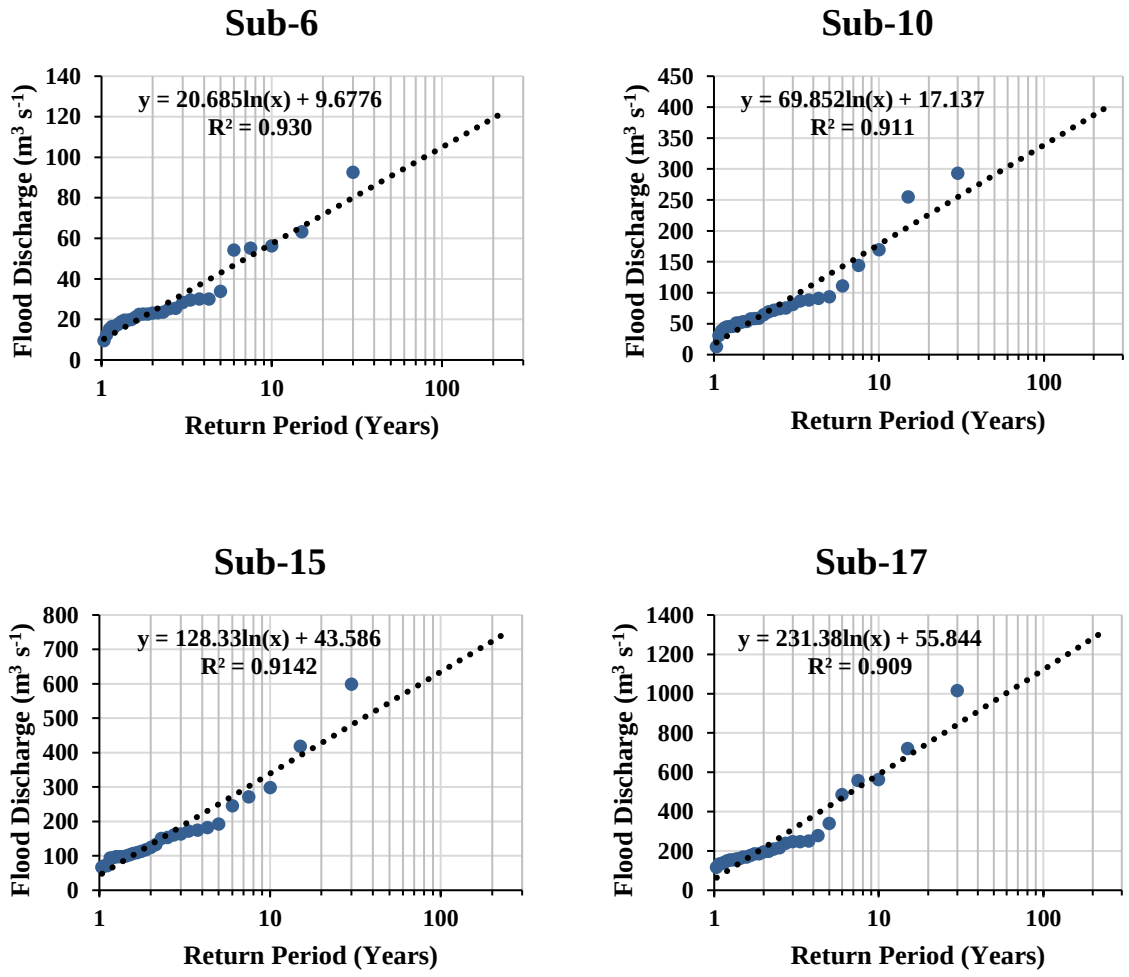

Figure 4.6 Flood return periods and the magnitude for 30-year period

Table 4.6 Sub-catchments' return periods and the estimated flood magnitudes

Return period (years)	Probability of exceedance (%)	Probability of non-exceedance (%)	Estimated flood magnitude ($m^3 s^{-1}$)			
			Sub-catchment 6 **405.2 km^2**	Sub-catchment 10 **1068 km^2**	Sub-catchment 15 **2800 km^2**	Sub-catchment 17 **5273 km^2**
2	50	50	24.02	65.56	132.54	216.17
5	20	80	42.97	129.56	250.13	428.11
10	10	90	57.31	177.98	339.08	588.43
25	4	96	76.26	241.98	456.66	800.37
50	2	98	90.60	290.40	545.62	960.70
100	1	99	104.94	338.82	634.57	1121.02
200	0.5	99.5	119.27	387.24	723.52	1281.35

Cumulative frequency distribution indicate that there is a 99.5 % chance of non-exceedance for such a 200-year flood of 1281.35 $m^3 s^{-1}$ in the catchment, which means that there is only 0.5 % chance for this flood magnitude to equal or be exceeded (**Figure 4.7**). The cumulative probability graphs in **Figure 4.7** indicate the non-exceedance probability for all possible flood magnitudes in the catchment. A 100- year flood of magnitude 1121.02 $m^3 s^{-1}$ has a 99% chance of non-exceedance, while 50-, 25-, 10-, 5-, and 2-year floods indicate a 98, 96, 90, 80 and 50% chance of them not exceeded respectively.

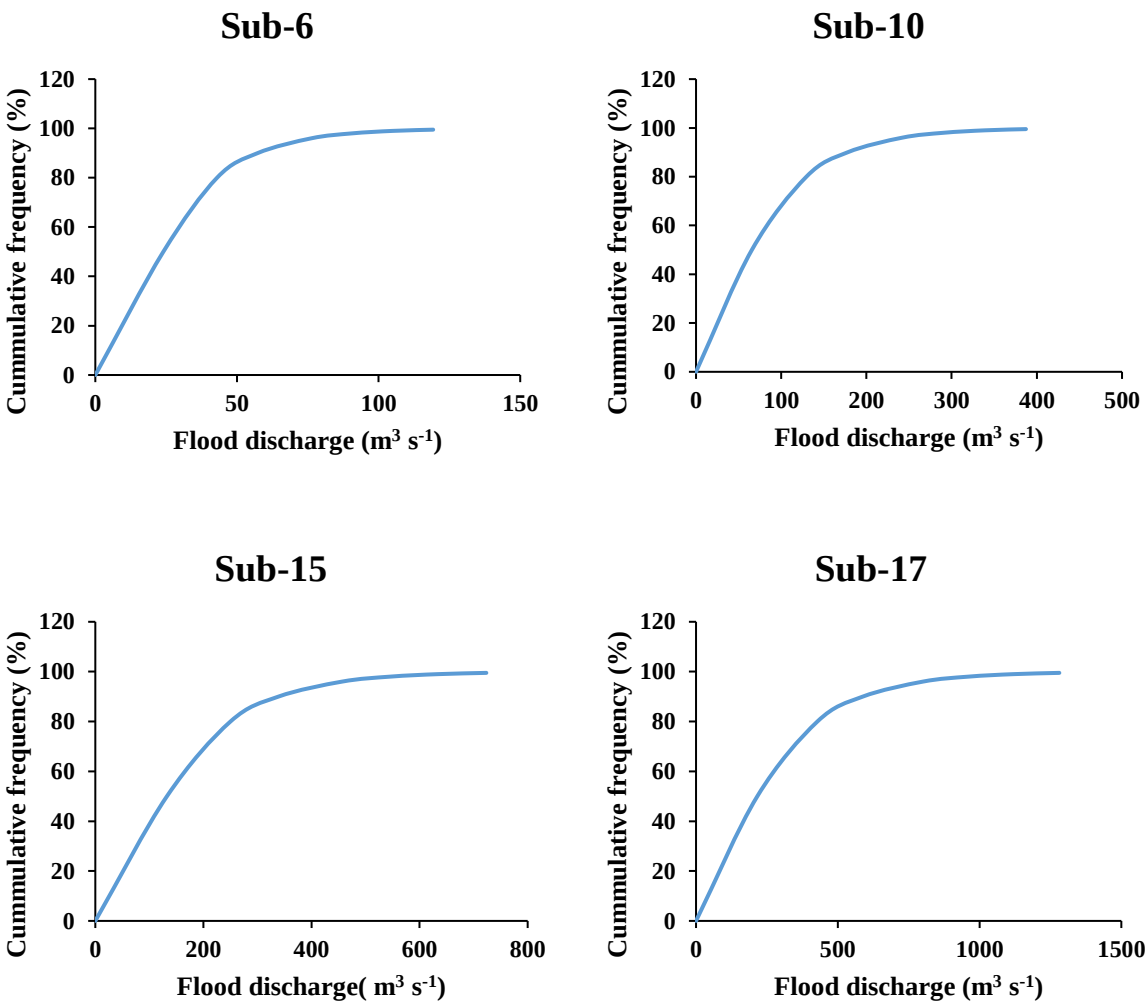

Figure 4.7 Cumulative frequency distribution for sub-catchments 6, 10, 15 and 17

4.2 Discussion

Simulating streamflow is a challenging process due to the numerous uncertainties that exist in the form of input parameter inaccuracies, processes unaccounted for by the model, and processes occurring in the catchment that are unknown to the modeller. Even more so with the lack of continuous high quality data, is a challenge that hydrologists face when modelling streamflow. The process of modelling streamflow becomes even more difficult in catchments where irregular rainfall distribution occurs, such as the Luvuvhu River catchment. Despite this, modelling efforts involving the SWAT model have been conducted in various catchment types such as agricultural land and mountainous catchments by Jha (2011) and Mutenyo *et al*. (2013) respectively and the studies proved the SWAT model is capable of simulating runoff with satisfactory results for these conditions.

Initially the model was unable to capture runoff discharge flows well. It is commonly experienced when simulating streamflow using SWAT because the model is executed through numerous parameters that interact and thus affect various processes. It is therefore a challenge to determine which parameter or parameter combination may be reducing the model's performance.

Initial simulation values were generated by SWAT, based on the general land use, soil and slope, where the peak flows were drastically overestimated. This meant that the water balance within the catchment may have been incorrect, thus contributing to the overestimation of the peak flows. Initial sensitivity analysis resulted in the choice of twelve parameters, which were used for calibration and validation. The twelves parameters were found to be more sensitive to streamflow output based on the large *t*-stat values and low *p*-values (< 0.05). After careful parameter adjustments based on SUFI-2 minimum and maximum parameter output values, parameters ALPHA_BF, CN2, GW_DELAY and SOL_K showed to be more sensitive to streamflow output. Ultimately, the model was able to simulate both peak and low flows well for both calibration and validation.

The use of SUFI-2 in SWAT-CUP to calibrate assisted in enabling adequate modelling since it incorporates almost all forms of uncertainties in the modelling processes. The model produced reasonable results of the *P*-factor during calibration and validation and the small indication of uncertainties could be due to inputs driving variables such as rainfall. Since an *R*-factor less than one generally indicates good calibration results (Rostamian *et al*., 2008), this was the case for all sub-catchments 6, 10, 15 and 17 during both calibration and validation. However, the *P*-

factor values for sub-catchments 10 and 17 were just lower than the acceptable value of 60% and according to Rostamian *et al*. (2008) this indicates that the actual uncertainty is higher than that shown, and could be improved by a higher *R*-factor value. The remainder of the sub-catchments' results indicated that most of the observed values were bracketed and were within the 95PPU boundary.

Overall, parameter ranges of the *P*-factor and *R*-factor reached desired limits, indicating substantial parameter uncertainties results, which were acceptable. Moreover, model uncertainties were falling within the permissible limits. Hence, SUFI-2 is capable of capturing the model's behaviour, with *P*-factor results indicating good model calibration strength and desirable levels of *R*-factor. For this reason, results obtained in this study demonstrate good model performance and acceptable accuracy of the model in runoff simulation. It can be concluded that SWAT simulation results were satisfactory for the simulation of runoff in the Luvuvhu catchment.

Observation functions R^2, NSE, RSR and PBIAS were analysed according to the limits placed by Moriasi *et al*. (2007) and Mutenyo *et al*. (2013) with objective functions reaching model efficiency of concurrently having an NSE index greater than 0.5, PBIAS ± 25% and an RSR < 0.7. According to this standard, the model performed well during both calibration and validation. For sub-catchments that were unable to reach these limits, such as sub-catchment 10 and 17, this could be due to the choice of objective function influencing the results (Abbaspour, 2015).

To achieve the runoff simulation, a careful and time-intensive effort of calibrating SWAT parameters to better represent catchment area was made. Once the parameters were set within a sufficient and acceptable calibration range, the model's results demonstrated the capability of the model to provide reasonable simulation of runoff.

One of the limitations of the model is the high number of parameters, which complicates the model's parameterization and calibration process, and is therefore considered SWAT model's weakness. Parameterization continues to be of importance, as highlighted in previous studies conducted and for parameterization to be more efficient and sustainable, long period quality data are needed, which however is a major obstacle in hydrological modelling. Despite results from this study being generally acceptable, the lack of datasets hinders better results and increases prediction uncertainties. Good quality data of climate and observed streamflow would

improve the ability of runoff modelling to accurately simulate flow and improve the parameterization and calibration process.

Following calibration and validation, a 30-year period of simulated flood discharge from 1986 to 2015 was used to analyse flood frequencies and estimate design flood. The data was sorted from highest to lowest and a reoccurrence interval was estimated. Through the sorting of simulated data it was evident that the highest flood flows were experienced in the years 1987/1988, 2000/2001, 2010/2011, 2013/2014, and these are years that correspond with the years Luvuvhu catchment received great flooding. The increase in flood peak frequency may be attributed to the changing land uses over the years.

Four probability plot graphs were created for the four sub-catchments using log-normal probability distribution. Sub-catchment 17 which is the outlet catchment, produced the highest flood magnitudes compared to the other catchments. This was because it covered the whole Luvuvhu catchment in area. The 100- and 200-year floods revealed flood magnitudes of 1121.02 and 1281.35 $m^3 s^{-1}$ respectively. This means that for example, in 100 years a flood of 1121.02 $m^3 s^{-1}$ will occur in any given year. This flood magnitude may occur several times in that 100-year period and may occur in two or more years consecutively. This is also the case for 200-year flood. However, it is also likely that they might not occur even once over these periods since the return period is the average time over which one expects a flood equal to or exceeding the specified magnitudes.

From the results, it is evident that the low-lying areas received more flooding during the 2000 and 2013 flood events while the mountainous areas received less flooding. This was unusual since naturally the Luvuvhu catchment receives high rainfall in the mountainous areas. However, literature confirms that low-lying areas are more prone to flooding unlike mountainous area. Furthermore, the floods were caused by tropical cyclones from Mozambique, hence results obtained can be justified.

The 2000 floods had more impact on the Limpopo province and Mozambique due to tropical cyclone Eline (Reason and Keibel, 2004). The cyclone occurred from February to March 2000, causing intense flooding, which was later recorded as the worst flood event in 50 years thus making it a 50-year flood (Heritage *et al*., 2000; Smithers *et al*., 2001). The 2013 floods started as a tropical low over Mozambique in January 2013. Later, tropical cyclone Hellen met the tropical low causing extreme rainfall and flooding in South Africa (Pringle *et al*., 2013).

The 10- and 50-year floods are regarded as high-risk floods since they occur more frequently. Knowing such magnitude will better help prepare the community and disaster management groups in the catchment. Looking at upstream (sub-catchment 10) and downstream (sub-catchment 17) sub-catchments, the log-normal distribution showed a 10-year return period with estimated flood magnitude of 177.98 $m^3 s^{-1}$ upstream and 588.43 $m^3 s^{-1}$ downstream while a 50-year flood had an estimated flood of 290.40 $m^3 s^{-1}$ upstream and 960.70 $m^3 s^{-1}$ downstream. Cumulative frequency distribution indicates that there is a 0.5 % chance for a 200-year flood to occur which means that there is a 0.5 % chance for the event to be equal to or be exceeded.

The log-normal distribution model showed high peak events which can be used as estimating limiting values for design purposes. Furthermore, the distribution performed well enough to be considered as a distribution of choice in terms of flood frequency analysis and planning in the Luvuvhu River catchment.

Results obtained in this study were based on daily data that were available. However, a study undertaken by Lee *et al*. (2017) indicated that a shorter time increment might be suitable in producing an improved estimation. Therefore, it is suggested that use of hourly data can be useful in producing approximate estimations. However this can be impractical in our study site since there are no shorter time increment data available. Nevertheless, it can still be recommended that future data collection may be done in hourly time increment for more accurate results.

The 2000 and 2013 flood disasters caught the Luvuvhu community unawares and this is because the people were not prepared for such disasters. The effects of the flooding could have been minimized through proper planning and investment management strategies. Therefore, results obtained from this study can further be used for such planning to mitigate and adapt during future flooding events. It is further recommended that there be improved transfer of knowledge system to the community and farmers of weather forecast and warnings of possible heavy rains that may lead to flooding so that people may be better prepared for such events. In planning, it is of utmost importance that planners be advised and reminded that hydrological models are guides and results are not certain. The floods may or may not occur as modelled, because there are probabilities with various uncertainties involved.

CHAPTER 5: CONCLUSIONS AND RECOMMENDATIONS FOR FURTHER RESEARCH

This study aimed at assessing the SWAT model in simulating runoff in the Luvuvhu River catchment. The catchment lies in an area vulnerable to flooding due to tropical depressions and the geographical distribution of river floodplains. This has led to catchments experiencing extreme flooding events over the past years, destroying crops and thus resulting in crop failure and reduced crop yield. A 2012 version of SWAT model was run through an interface with a QGIS desktop 2.6.1 software, QSWAT 1.3 2016. The model was chosen because it is physically based, deterministic and semi-distributed, thus capturing many physical processes occuring in the catchment.

The SWAT model's initial run was successfully implemented. The model successfully simulated streamflow and proved to be capable of capturing streamflow trends despite sub-catchment's characteristics and location. However, initial results indicated an over-estimation of observed flows in parts of the catchment, revealing unacceptable correlation coefficient results in three of the sub-catchments (sub-catchment 6, 15 and 17) while sub-catchment 10 displayed a good correlation. The evaluation of the model using the six statistical parameters R, R^2, MAE, MBE, RMSE and NSE index revealed model results that were unsatisfactory. From the initial results, it was evident that calibration and validation of the model needed to be conducted before attempting further analyses.

Calibration was conducted using twelve parameters which, based on previous studies, were recorded to be the most sensitive parameters for streamflow. Global sensitivity analyses found ALPHA_BF, CN2, GW_DELAY and SOL_K to be more distinguishable with $p < 0.05$. Performance indices results indicated that most of the observations with different parameters were grouped together by the 95PPU boundary, which signified the capability of SUFI-2 to capture the SWAT model behaviour. Following calibration and validation, SWAT simulation revealed satisfactory results for the prediction of runoff and the final parameter ranges were considered acceptable for the Luvuvhu catchment. The percentage of observed data being grouped together by 95PPU during calibration indicated the strength of the model calibration to be satisfactory, with 60 % of the data bracketed. *R*-factor results showed acceptable model calibration. Objective functions R^2, NSE index, RSR and PBIAS used to quantify the model's calibration result showed satisfactory results for both calibration and validation. It can be

concluded that the SWAT model performed well in simulating runoff in the Luvuvhu catchment after calibration and validation.

Flood frequency analyses were done, and a design flood estimation completed. This was accomplished using a 30-year period of simulated flood discharge from the SWAT model. Flood frequency analyses indicated increasing floods at greater probability of exceedance for all return periods. Focusing on sub-catchment 17 being the Luvuvhu catchment outlet, 50-, 100- and 200-year floods revealed flood magnitudes of 960.70, 1121.02 and 1281.35 $m^3 s^{-1}$ respectively. This meant that in 50 years, a flood of 960.70 $m^3 s^{-1}$ would occur in any given year. The flood may occur several times in the 50 years and may occur in two or more years consecutively. It is the case for 100- and 200-year floods as well. However, it is also likely that they might not occur even once over these periods since the return period is the average time over which one expects a flood equal to or exceeding the specified magnitudes. Cumulative frequency distribution indicates that there is a 0.5 % chance for a 200-year flood to occur which means that there is a 0.5 % chance for the event to be equal to or be exceeded. The log-normal distribution model produced good results that can be used to support planning and decision making about development, flood mitigation and adaptation during the flooding season. Hence, it can be considered as a distribution model of choice among other probability distribution models for flood frequency analysis at any point in the Luvuvhu River catchment. It is of utmost importance that planners remember that hydrological models are guides and results are not certain. The floods may or may not happen, because these are probabilities with various uncertainties involved.

5.1 Challenges

Meteorological data availability or lack thereof due to continuous missing data affected the quality and accuracy of the results. The study relied on treated patched data, which increase the inaccuracies and uncertainties in the model results. For example, in some of the weather stations, sunshine hours had to be used to estimate solar radiation. Therefore, to improve the quality of the study results, improved longer record with quality data are needed. The land cover and soil datasets are essential for SWAT model input since they both have an influence on the runoff process. Ground-truthing and soil field analyses were not done, hence relying solely on soil and land use maps for which some information was not up to date. It would be of great benefit to produce high quality results if reclassification could be done in order to have a more reliable up-to-date data bank. The model is purposed to be physically based but continues to

possess many assumptions; therefore, due to many assumptions and uncertainties it is recommended that the SWAT model be used in conjunction with other hydrological models as a conceptual model. For South Africa, the SWAT model user group support base is small. A larger user support base would encourage the exploration of possible interaction with other hydrological models already available in South Africa.

5.2 Future possibilities

There are many future research areas involving the SWAT model that need attention. Due to the size of the catchment study area, a lower resolution DEM was used which also contributed to the lack of accuracy of the results obtained. The accuracy of results would increase if a study were undertaken on a smaller, more specific sub-catchment using a much higher DEM resolution. Use of more than one weather generation model could improve the quality of generated climate data and reveal some inconsistencies that may have existed with the SWAT model. The SWAT model simulation results in the catchment may be compared with another hydrological model simulation results in order to quantify the calibration process, and this may be a possible future study. SWAT model interaction with other hydrological models may also be a good tool for future catchment planning and management purposes. The model can be used to simulate sediment loading and land use management practices, which due to the scope of the study was not undertaken.

5.3 Final comments and summary conclusions

The use of SUFI-2 in SWAT-CUP quantified the calibration and validation results well. The SWAT simulation results were satisfactory for the prediction of runoff in the catchment, proving the model to be a useful tool for simulating runoff.

The log-normal distribution model showed high peak events which can be used as estimating limiting values for design purposes and can be considered as a distribution of choice in terms of flood frequency analysis and planning in the Luvuvhu River catchment.

REFERENCES

Abbaspour KC, Yang J, Maximov I, Siber R, Bogner K, Mieleitner J, Zobrist J, Srinivasan R. 2007. Modelling hydrology and water quality in the pre-alpine/alpine Thur watershed using SWAT. Journal of Hydrology 333: 413-430.

Abbaspour KC. 2015. SWAT-CUP 2012: SWAT calibration and uncertainty programs - A user manual, Switzerland: Eawag Aquatic Research.

Aghakouchak A, Habib E. 2010. Application of a conceptual hydrological model in teaching hydrologic processes. International Journal of Engineering Education 26: 963-973.

Ahn J, Cho W, Kim T, Shin H, Heo JH. 2014. Flood frequency analysis for the annual peak flows simulated by an event-based rainfall-runoff model in an urban drainage basin. Water 6: 3841-3863.

Ailliot P, Allard D, Monbet V, Naveau P. 2015. Stochastic weather generators: an overview of weather type models. Journal de la Societe Francaise de Statistique 156: 101-113.

Alexakis DD, Hadjimitsis DG, Agapiou A. 2012. Estimating flash flood discharge in a catchment area with the use of hydraulic model and terrestrial laser scanner. Helmis CG, Nastos PT (eds.). Advances in meteorology, climatology and atmospheric physics, Springer Atmospheric Sciences. DOI 10.1007/978-3-642-29/72-2_2.

Allan RJ. 2000. ENSO and climate variability in the past 150 years. In: HF Diaz and V Markgraf, eds. El Niño and the Southern Oscillation: Multiscale variability and global and regional impacts. New York City: Cambridge University Press. pp. 3-55.

Allen RG, Pereira LS, Raes D, Smith M. 1998. Crop evaporation-Guidelines for computing crop water requirements. FAO Irrigation and Drainage Paper 56, Rome, Italy. pp 1-15.

Angstrom A. 1924. Solar and terrestrial radiation report to the international commission for solar research on actinometric investigations of solar and atmospheric radiation. Quarterly Journal of the Royal Meteorological society, 50: 121-126.

Arnold JG, Srinivasan R, Muttiah RS, Williams JR. 1998. Large area hydrologic modeling and assessment part I: model development. Journal of the American Water Resources Association 34: 73-89.

Arnold JG, Moriasi DN, Gassman PW, Abbaspour KC, White MJ, Srinivasan R, Santhi C, Harmel RD, van Griensven A, Van Liew MW, Kannan N, Jha MK. 2012. SWAT: Model use, calibration and validation. American Society of Agricultural and Biological Engineers 55: 1491-1508.

Aronica GT, Candela A, Fabio P, Santoro M. 2012. Estimation of flood inundation probabilities using global hazard indexes based on hydrodynamic variables. Physics and Chemistry of the Earth 42:119-129.

Atroosh KB, Moustafa AT. 2012. An estimation of the probability distribution of Wadi Bana Flow in the Abyan Delta of Yemen. Journal of Agricultural Science 4: 80-89.

Baker VR. 2000. Paleoflood hydrology and the estimation of extreme floods. In: Wohl EE (ed.), Inland flood hazards: Human, riparian, and aquatic communities. New York City: Cambridge University Press. pp. 359-374.

Ball JE. 2012. Estimation of design floods using continuous simulation. In: Floodplain Management Associatin National Conference, 28-31 May. Tweed Head, NSW, Australia, pp 1-16.

Beven KJ, Binley A. 1992. The future of distributed models: Model calibration and uncertainty prediction. Hydrological Processes 6: 279-298.

Beven KJ. 1997. TOPMODEL:A critique. Hydrological Processes 11: 1069-1085.

Beven KJ. 2012. Hydrological similarity, distribution functions and semi-distributed rainfall-runoff models. In: Beven KJ (ed.), Rainfall-runoff modelling: The primer. John Wiley and Sons, pp. 185-229.

Bhawan JV. 1998. Estimation of sediment yield and runoff from small watershed using WEPP model. SCAR bulletin series No. 23/97-98. India: National Institute of Hydrology.

Bowen W, Baigorria G, Barrera V, Cordova J, Muck P, Pastor R. 1998. A process-based model (WEPP) for simulating soil erosion in the Andes. Critical Infrastructure Protection (CIP) Programme Report 1997-98, National Resource Management in the Andes. pp 403-408.

Chapuis RP. 2012. Predicting the saturated hydraulic conductivity of soils: a review. Bulletin of Engineering Geology and the Environment 71:401-434.

Chetty K, Smithers J. 2005. Continuous simulation modelling for design flood estimation in South Africa: Preliminary investigations in the Thukela catchment. Physics and Chemistry of the Earth 30: 634-638.

Chen FW, Liu CW. 2012. Estimation of the spatial rainfall distribution using inverse distance weighting (IDW) in the middle of Taiwan. Paddy Water Environment 10: 209-222.

Chow VT, Maidment DR, Mays LW. 1988. Applied hydrology. Berkshire: McGraw-Hill Book Co (UK) Ltd.

Clemence BSE. 1997. A brief assessment of a weather data generator (CLIMGEN) at Southern African Sites. Water SA 23: 271-274.

Conroy WJ. Hotchkiss RH, Elliot WJ. 2006. A coupled upland-erosion and instream hydrodynamic-sediment transport model for evaluating sediment transport in forested watersheds. American Society of Agricultural and Biological Engineers 49: 1-10.

Davis C, Joubert A. 2011. Southern Africa's climate: Current state and recent historical changes. In: Davis C (ed.). Climate risk and vulnerability a handbook for southern Africa. Stellenbosch: CSIR, pp. 7-20.

Davis C (ed). 2011. Climate risk and vulnerability a handbook for southern Africa. Stellenbosch: CSIR.

de Jong van Lier Q, Sparovek G, Flanagan DC, Bloem EM, Schnug E. 2005. Runoff mapping using WEPP erosion model and GIS tools. Computers and Geosciences 31: 1270–1276.

DePue M. 2010. Flood types and characteristics. In: Annual Georgia association of floodplain management conference, 23 March, Lake Lanier Islands, Georgia, pp 1-27.

Dile Y, Srinivasan R, George C. 2015. QGIS interface for SWAT (QSWAT): User manual for QSWAT version 1.4.

Dyson LL. 2009. Heavy daily-rainfall characteristics over the Gauteng Province. Water SA 35: 627-638.

Eccel E., 2012. Estimating air humidity from temperature and precipitation measures for modelling applications. Meteorological Applications 19: 118-128.

El-Nasr AA, Arnold JG, Feyen J, Berlamont J. 2005. Modelling the hydrology of a catchment using a distributed and a semi-distributed model. Hydrological Processes 19: 573-587.

Els Z. 2011. Data availability and requirements for flood hazard mapping in South Africa. MSc dissertation, University of Stellenbosch, South Africa.

Emam AR, Kappas M, Nguyen LHK , Renchin T. 2016. Hydrological modeling in an ungauged basin of Central Vietnam using SWAT model. Journal for Hydrology and Earth System Sciences, doi:10.5194/hess-2016-44, 2016.

Etuonovbe AK. 2011. The devastating effect of flooding in Nigeria. FIG working week, 18-22 May, Mairakech, Morocco, pp 1-15.

Ezemonye MN, Emeribe CN. 2011. Flood characteristics and management adaptation in parts of the IMO river system. Ethiopian Journal of Environmental Studies and Management 4: 56-64.

Fadil A, Rhinane H, Kaoukaya A, Kharchaf Y, Bachir OA. 2011. Hydrologic modelling of the Bouregreg watershed (Morocco) using GIS and SWAT model. Journal of Geographic Information System 3: 279-289.

Famiglietti JS, Wood EF, Sivapalan M, Thongs DI. 1992. A catchment scale water balance model for FIFE. Journal of Geophysical Research 97:18997-19007.

Fennessey LAJ, Hawkins RH. 2001. The NRCS curve number, a new look at an old tool. In: Proceedings of the 2001 Pennsylvania stormwater management symposium. 17-18 October. Pennsylvania, pp 1-16.

Franchini M, Wendling J, Obled C, Todini E. 1996. Physical interpretation and sensitivity analysis of the TOPMODEL. Journal of Hydrology 175: 293-338.

Gamage SHPW, Hewa GA, Beecham S. 2013. Probability distributions for explaining hydrological losses in South Australian catchments. Hydrology and Earth System Science 17: 4541-4553.

Garrison E. 2012. Asia geospatial forum: Introduction study area methodology expectation related issues primary results. In: 11th Annual Asian Conference and Exhibition on Geospatial Technologies and its Applications, 17-19 September, Asia Geospatial Forum.

Gassman PW, Reyes MR, Green CH, Arnold JG. 2007. The soil and water assessment tool: Historical development, applications and future research direction. American Society of Agricultural and Biological Engineers 50: 1211-1250.

Gassman PW, Sadeghi AM, Srinivasan R. 2014. Applications of the SWAT model special section: Overview and insights. Journal of Environmental Quality 43: 1-8.

Gaur A. 2013. Climate change impact on flood hazard in the Grand River basin, Ontario, Canada. MSc.Eng. dissertation, University of Western Ontario. Canada.

Gayathri KD, Ganasri BP, Dwarakish GS. 2015. A review on hydrological models. Aquatic Procedia 4: 1001-1007.

Geoscience Australia, 2013. Where do floods occur? [Online] Available at: http://www.ga.gov.au/hazards/flood/flood-basics/where.html [Accessed 06 05 2014].

Gericke OJ, du Plessis JA. 2013. Development of a customised design flood estimation tool to estimate floods in gauged and ungauged catchments. Water SA 39: 67-94.

Geyer CJ. 1992. Practical Markov chain Monte Carlo. Statistical Science 7: 473-511.

Gichere SK, Olado G, Anyona DN, Matano AS, Dida GO, Abuom PO, Amayi J, Ofulla AVO. 2013. Effects of Drought and Floods on Crop and Animal Losses and Socio-economic Status of Households in the Lake Victoria Basin of Kenya. Journal of Emerging Trends in Economics and Management Sciences 4: 31-41.

Golmohammadi G, Prasher S, Madani A, Rudra R. 2014. Evaluating three hydrological distributed watershed models: MIKE-SHE, APEX, SWAT. Hydrology 1: 20-39.

Gyamfi C, Ndamuka JM, Salim RW. 2016. Application of SWAT model to the Olifants basin: calibration, validation and uncertainty analysis. Journal of Water Resource and Protection 8: 397-410.

Hall R. 2008. Land restitution/ redestribution of large scale enterprises: Overview of issues faced by beneficiary communities. In: Trade and Industrial Policy Strategies Forum, October, Institute for Poverty, Land and Agrarian Studies, Cape Town, South Africa.

Hart NCG, Reason CJC, Fauchereau N. 2013. Cloud bands over southern Africa: seasonality, contribution to rainfall variability and modulation by the MJO. Climate Dynamics, 41: 1199-1212.

Hastings WK. 1970. Monte Carlo sampling methods using Markov chains and their applications. Biometrika 57: 97-109.

Hayhoe HN, Stewart DW. 1996. Evaluation of CLIGEN and WXGEN weather data generators under Canadian conditions. Canadian Water Resources Journal 21: 53-67.

Hirschboeck KK, Ely LL, Maddox RA. 2000. Hydroclimatology of meteorologic floods. In: EE Wohl (eds), Inland Flood Hazard: Human, Riparian, and Aquatic Communities. New York, Cambridge University Press, USA. pp. 39-68.

Jewitt GPW, Garratt JA, Calder IR, Fuller L. 2004. Water resources planning and modelling tools for the assessment of land use change in the Luvuvhu Catchment, South Africa. Physics and Chemistry of the Earth 29: 1233-1241.

Jha MK. 2011. Evaluating hydrologic response of an agricultural watershed for watershed analysis. Water 3: 604-617.

Kane RP. 2009. Periodicities, ENSO effects and trends of some South African rainfall series: An update. South African Journal of Science 105: 199-207.

Kang Y, Khan S, Ma X. 2009. Climate change impacts on crop yield, crop water productivity and food security – A review. Progress in Natural Science 19: 1665-1674.

Karkanis PG. 1983. Determining field capacity and wilting point using soil saturation by capillary rise. Canadian Agricultural Engineering 25: 19-21.

Kay AL, Davies HN, Bell VA, Jones RG. 2009. Comparison of uncertainty sources for climate change impacts: flood frequency in England. Climatic Change 92: 41-63.

Khalid K, Ali MF, Abd Rahman NF, Mispan MR. 2016. Application on one-at-a-time sensitivity analysis of semi-distributed hydrological model in tropical watershed. IACSIT International Journal of Engineering and Technology 8: 132-136.

Kozlovac JP. 1995. Adventures in flood control: The Johnstown, Pennsylvania story. In: Urban Areas as Environment, 19 April.

Krzhizhanovskaya VV, Shirshov GS, Melnikova NB, Belleman RG, Rusadi FI, Broekhuijsen BJ, Gouldby BP, Lhomme J, Balis B, Bubak M, Pyayt AL, Mokhov II, Ozhigin AV, Lang B, Meijer RJ. 2011. Flood early warning system: design, implementation and computational modules. Procedia Computer and Science 4: 106-115.

Kuhn C. 2014. Modelling rainfall-runoff using SWAT in a small urban wetland: Test of scale for the soil and water assessment tool hydrology model. Watershed Cycles and Process Report No. FES 724, Yale University of Forestry and Environmental Studies, Spring. pp 1-19.

Laflen JM, Flanagan DC, Ascough II JC, Weltz MA, Stone JJ. 1994. The WEPP model and its applicability for predicting erosion on rangelands. Soil Science Society of America 38: 11-22.

Latha JC, Saravanan S, Palanichamy K. 2010. A Semi – distributed water balance model for Amaravathi River basin using remote sensing and GIS. International Journal of Geomatics and Geosciences 1: 252-263.

Lauer J. 2008. Flooding impacts on corn growth and yield. Field Crops 28: 49-56.

Leavesley GH, Lichty RW, Troutman BM, Saindon LG. 1983. Precipitation- runoff modelling system: User's manual, Denver, USA.

Liersch S. 2003. The program pcpSTAT-SWAT user manual. Berlin.

Liu X, Li J. 2008. Application of SCS model in estimation of runoff from small watershed in Loess plateau of China. China Geography and Science 18: 235-241.

Lundin LC, Bergstrom S, Eriksson E, Seibert J. 2000. Hydrological models and modelling (2nd edn). In: LC. Lundin (ed), Sustainable water management in the baltic sea basin. Sweden, Uppsala University pp.129-140.

Mamo KHM, Jain MK. 2013. Runoff and sediment modeling using SWAT in Gumera catchment, Ethiopia. Open Journal of Modern Hydrology 3: 196-205.

Manaswi CM, Thawait AK. 2014. Application of soil and water assessment tool for runoff modeling of Karam River basin in Madhya Pradesh. International Journal of Scientific Engineering and Technology 3: 529-532.

Maré HG, Mwaka B, Sinha P. 2007. Development of simplified drought operating rules. In: Proceedings of the 13th SANCIAHS Symposium, 6-7 September, Cape Town, South Africa. pp 1-10.

Masereka EM, Otieno FAO, Ochieng GM, Snyman J. 2015. Best fit and selection of probability distribution models for frequency analysis of extreme mean annual rainfall events. International Journal of Engineering Research and Development 11: 34-53.

McCuen RH. 2003. Data, statistics and modeling. In: RH. Mccuen, (ed.). Modeling hydrologic change. New York, USA: Lewis publishers, pp. 1-7.

McCuen RH. 2003. Modeling change. In: R. H. McCuen, (ed.). Modeling hydrologic change. New York,USA: Lewis publishers, pp. 247-288.

McCuen RH. 2003. Hydrologic simulation. In: RH. McCuen, (ed.). Modeling hydrologic change. New York, USA: Lewis Publishers, pp. 293-328.

McKague K, Rudra R, Ogilvie J. 2003. ClimGen – A convenient weather generation tool for Canadian climate stations. In: Proceeedings CSAE/SCGR Meeting, 6-9 July, Montreal, Quebec. pp 03-118.

McKague K, Rudra R, Ogilvie J, Ahmed I, Gharabaghi B. 2005. Evaluation of weather generator ClimGen for southern Ontario. Canadian Water Resources Journal 30: 315-330.

Metropolis N, Rosenbluth AW, Rosenbluth MN, Teller AH, Teller E. 1953. Equation of state calculations by fast computing machines. Journal of Chemical Physics 21: 1087-1092.

Millington N, Das S, Simonovic SP. 2011. The Comparison of GEV, Log-Pearson Type 3 and Gumbel Distributions in the Upper Thames River Watershed under Global Climate Models. Water Resource Research Report No. 077. Canada: Water Resource Research.

Moeletsi ME, Walker S, Landman WA. 2011. ENSO and implications on rainfall characteristics with reference to maize production in the Free State Province of South Africa. Physics and Chemistry of the Earth 36: 715-726.

Moeletsi ME, Shabalala ZP, De Nysschen G, Walker S. 2016. Evaluation of an inverse distance weighting method for patching daily and dekadal rainfall over the Free State Province, South Africa. Water SA 42: 466-474.

Montgomery DC, Peck EA, Vining G. 2006. Introduction to linear regression analysis (4th edn). New Jersey: John Wiley and Sons, Inc.

Moodley K. 2014. Ethical concerns in disaster research- A South African perspective. In: D. P. O'Mathuna, B. Gordijn & M. Clarke, (eds.). Disater bioethics: Normative issues when nothing is normal. Dordretcht, South Africa: Springer Science, pp. 191-208.

Moriasi DN, Arnold JG, Van Liew MW, Bingner RL, Harmel RD, Veith TL. 2007. Model evaluation guidelines for systematic quantification of accuracy in watershed simulations. American Society of Agricultral and Biological Engineers 50: 885-900.

Muinga MG. 2004. Flood Assessment and Zonation in the Lower Limpopo, Mozambique. MSc dissertation. Institute for Geo-Information Science and Earth Observation, Enschede, Netherlands.

Mutenyo I, Nejadhashemi AP, Woznicki SA, Giri S. 2013. Evaluation of SWAT perfomance on a mountainous watershed in tropical Africa. Hydrology Current Research, Issue S14: 001. doi:10.4172/2157-7589.S14-001

Muthuwatta LP. 2004. Long term rainfall-runoff lake level modelling of the lake Naivasha basin, Kenya. MSc dissertation, University of the Netherlands, Netherlands.

Mzezewa J, Misi T, Van-Rensburg LD. 2010. Characterisation of rainfall at a semi-arid ecotope in the Limpopo Province (South Africa) and its implications for sustainable crop production. Water SA 36: 19-26.

Narsimlu B, Gosain AK, Chaha BR, Singh SK, Srivastava PK. 2015. SWAT model calibration and uncertainty analysis for streamflow prediction in the Kunwari River basin, India, using sequential uncertainty fitting. Environmental Processes 2: 79-95.

Ncube M. 2006. The impact of land cover and land use on the hydrologic response in the Olifants, Johannesburg. MSc dissertation, University of Witwatersrand, South Africa.

Norouzi G, Taslimi M. 2012. The Impact of Flood Damages on Production of Iran's Agricultural Sector. Middle-East Journal of Scientific Research 12: 921-926.

Nourani V, Roughani A, Gebremichael M. 2011. Topmodel capability for rainfall-runoff modelling of the Ammameh watershed at different time scales using different terrain algorithms. Journal of Urban and Environmental Engineering 5: 1-14.

O'Connell EO, Ewen J, O'Donnell G, Quinn P. 2007. Is there a link between agricultural land-use management and flooding? Hydrology and Earth System Sciences 11:96-107.

Pasi JM. 2014. Modelling the impacts of increased air temperature on maize yields in selected area of the South African highveld using the Cropsyst model. MSc dissertation, University of KwaZulu-Natal, South Africa.

Pechlivanidis IG, Jackson BM, Mcintyre NR, Whether HS. 2011. Catchment scale hydrological modelling: A review of model types, calibration approaches and uncertainty analysis methods in the context of recent developments in technology and applications. Global Nest Journal 13: 193-214.

Pieri L, Bittelli M, Wu JQ, Dun S, Flanagan DC, Pisa PR, Ventura F, Salvatorelli F. 2007. Using the water erosion prediction project (WEPP) model to simulate field-observed runoff and erosion in the Apennines Mountain range, Italy. Journal of Hydrology 336: 84-97.

Pilgrim DH, Chapman TG, Doran DG. 1988. Problems of rainfall-runoff modelling in arid and semiarid regions. Hydrological Sciences Journal 33: 379-400.

Pitt R. 2002. Regional rainfall conditions and site hydrology for construction site erosion evaluations. [Online] Available at: http://rpitt.eng.ua.edu/Workshop/WSErorionControl/Module4/Module4.htm [Accessed 16 11 2016].

Ponce VM, Hawkins RH. 1996. Runoff curve number: Has it reached maturity. Journal of Hydrologic Engineering 1: 11-19.

Praskievicz S, Chang H. 2009. A review of hydrological modelling of basin-scale climate change and urban development impacts. Progress in Physical Geography 33: 650-671.

Pudasaini M, Shrestha S, Riley S. 2004. Application of water erosion prediction project (WEPP) to estimate soil erosion from single storm rainfall events from construction sites. In: 3rd Australian New Zealand Soils Conference, 5-9 December, University of Sydney, Australia. pp 1-7.

Raghunath HM. 2006. Hydrology: Principles, analysis and design (2nd edn). New Delhi: New Age International.

Ramirez JA. 2000. Prediction and Modelling of Flood Hydrology and Hydroulics. In: EE Wohl, (ed.). Inland Flood Hazards: Human, Riparian and Aquatic Communities. New York, USA: Cambridge University Press, pp. 293-329.

Rasiuba TC. 2007. Water budget, water use efficiency in agriculture in Olifants catchment, Johannesburg. MSc dissertation, University of Witwatersrand, South Africa.

Refsgaard JC. 1996. Terminology, modelling protocol and classification of hydrological model codes. In: MB Abbott, JC Refsgaard, (eds.). Distributed hydrological modelling. Netherlands: Kluwer Academic Publishers, pp. 17-39.

Refsgaard JC, Abbott MB. 1996. The role of distributed hydrological modelling in water resource management. In: MB Abbott, JC Refsgaard, (eds.). Distributed hydrological modelling. Netherlands: Kluwer Academic Publishers, pp. 55-69.

Refsgaard JC, Storm B. 1996. Construction, calibration and validation of hydrological models. In: MB Abbott, JC Refsgaard, (eds.). Distributed hydrological modeling. The Netherlands: Kluwer Academic Publishers, pp. 41-45.

Rogger M, Kohl B, Pirkl H, Viglione A, Kommaa J, Kirnbauer R, Merz R, Blöschl G. 2012. Runoff models and flood frequency statistics for design flood estimation in Austria – Do they tell a consistent story? Journal of Hydrology 456: 30–43.

Rostamian R, Jaleh A, Afyuni MJ, Mousavi SF, Heidarpour M, Jalalian A, Abbaspour KC. 2008. Application of a SWAT model for estimating runoff and sediment in two mountainous basins in central Iran. Hydrological Sciences Journal 53: 977-988.

Safeeq M, Fares A. 2011. Accuracy evaluation of ClimGen weather generator and daily to hourly disaggregation methods in tropical conditions. Theoretical and Applied Climatology 106: 321-341.

Sauer J. 2011. Natural disasters and agriculture: Individual risk preferences towards flooding. In: The EAAE 2011 Congress Change and Uncertainty, 30 August- 2 Spetember, Zurich, Switzerland. pp 1-15.

Schulze RE. 1998. Hydrological Modelling: Concepts and Practice, Netherlands: International Institute of Infrastructural, Hydraulic and Environmental Engineering, Delft, The Netherlands. pp 134.

Seibert J. 1999. Conceptual runoff models-fiction or representation of reality? PhD thesis, Acta Universitatis Upsaliensis, Uppsala, Sweden. ISBN 91-554-4402-4.

Silveira L, Charbonnier F, Genta JL. 2000. The antecedent soil moisture condition of the curve number procedure. Hydrological Sciences Journal 4: 3-12.

Singh V, Bankar N, Salunk SS, Bera AK, Sharma JR. 2013. Hydrological stream flow modelling on Tungabhadra catchment: parameterization and uncertainty analysis using SWAT CUP. Current Science 104: 1187-1199.

Singo LR, Kundu PM, Odiyo JO, Mathivha FI, Nkuna TR. 2012. Flood frequency analysis of annual maximum stream flows for Luvuvhu River catchment, Limpopo Province, South Africa. In: 16th SANCIAHS National Hydrology Symposium, University of Pretoria, South Africa, 1-3 October. Session 2C.

Smith, 2001. Environmental hazards: Assessing risk and reducing disaster (3rd edn). London/New York: Routledge Physical Environment Series.

Smithers JC, Schulze RE, Kienzle S. 1997. Design flood estimation using a modelling approach: a case study using the ACRU model. Sustainability of Water Resources Under Increasing Uncertainty 240: 365-375.

Smithers JC, Schulze RE. 2001. Design rainfall estimation: A review with reference to practices in South Africa. In: Proceedings 10th South African National Hydrology Symposium, 26-28 September, School of BEEH, Univeresity of KwaZulu Natal, Pietermaritzburg, South Africa.

Smithers JC. 2012. Methods for design flood estimation in South Africa: Review. Water SA 38: 633-646.

Smithers JC, Chetty KT, Frezqhi MS, Knoesen DM. 2013. Development and assessment of a daily time step continuous simulation modelling approach for design flood estimation of ungauged locations: ACRU model and Thukela catchment case study. Water SA 39: 467-476.

Soulis KX, Valiantzas JD. 2012. SCS-CN parameter determination using rainfall-runoff data in heterogeneous watersheds- the two-CN system aproach. Hydrology and Earth System Science 16: 1001-1015.

Stedinger JR. 2000. Flood frequency analysis and statistical estimation of flood risk. In: Wohl EE (ed.), Inland flood hazards: Human, riparian, and aquatic communities. New York City: Cambridge University Press. pp. 334-355.

Syaukat Y. 2011. The impact of climate change on food production and security and its adaptation programs in Indonesia. Journal of the International Society for Southeast Asian Agricultural Science 17: 40-51.

Szezesniak M, Piniewski M. 2015. Improvement of hydrological simulations by applying daily precipitation interpolation schemes in meso-scale catchment. Water 7: 747-779.

Tadross M, Suarez P, Lotsch A, Hachigonta S, Mdoka M, Unganai L, Lucio F, Kamdonyo D, Muchinda M. 2009. Growing-season rainfall and scenarios of future change in southeast Africa: Implications for cultivating maize. Climate Research 40: 147-161.

Tarboton DG (ed.). 2003. Simulation of runoff generation in hydrologic models. In: Rainfall-ruoff processes. Utah State University. pp 6(1-17).

Tennant WJ, Hewitson BC. 2002. Intra-seasonal rainfall characteristics and their importance to the seasonal prediction problem. International Journal of Climatology 22: 1033-1048.

Tessema SM. 2011. Hydrological modelling as a tool for sustainable water rresources management: A case study of the Awash river basin. MSc dissertation, Royal Institute of Technology (KTH), Stockholm, Sweden.

Tingem M, Rivington M, Azam-Ali S, Colls J. 2007. Assessment of the ClimGen stochastic weather generator at Cameroon sites. African Journal of Environmental Science and Technology 1: 86-92.

Todini E. 2007. Hydrological catchment modelling: past, present and future. Hydrology and Earth System Science 11: 468-482.

Trenberth KE. 2011. Changes in precipitation with climate change. Climate Research 47: 123-138.

Tshikolomo K, Walker S, Nesamvuni A. 2013. Prospect for Developing Water Storage through Analysis of Runoff and Storage Capacity of Limpopo and Luvuvhu-Letaba Water Management Areas of South Africa. International Journal of Applied Science and Technology 3: 70-79.

van Griensven A, Meixner T. 2006. Methods to quantify and identify the sources of uncertainty for river basin water quality models. Water Science and Technology 53: 51-59.

van Liew MW, Veith TL, Bosch DD, Arnold JG. 2007. Sustainability of SWAT for the conservation effects assessment project: Comparison on USDA agricultural research service watersheds. Journal of Hydrologic Engineering 12: 173-189.

Vazquez-Amabile G, Engel BA, Flanagan DC. 2006. Modeling and risk analysis of nonpoint-source pollution caused by Atrazine using SWAT. American Society of Agricultural and Biological Engineers 49: 667-678.

Viessman WJ, Lewis GL, Knapp JW. 1989. Frequency Analysis. In: WJ Viessman, GL Lewis, JW Knapp, (eds.). Introduction to Hydrology (3rd edn.). New York: Harper and Row Publishers, pp. 721-754.

Viessman WJ, Lewis GL, Knapp JW. 1989. Hydrologic modelling. In: WJ Viessman, GL Lewis, JW Knapp, eds. Introduction to Hydrology (3rd edn.). New York: Harper and Row Publishers, pp. 491-670.

Viviroli D, Mittelbach H, Gurtz J, Weingartner R. 2009. Continuous simulation for flood estimation in ungauged mesoscale catchment of Switzerland- Part II: Parameter regionalisation and flood estimation results. Journal of Hydrology 377: 208-225.

Waghaye AM, Siddenki V, Kumari N. 2015. Design rainfall estimation using probabilistic approach for Adilabad district of Telangana. International Journal of Advanced Scientific and Technical Research 2: 301-318.

Walker JF, Krug WR. 2003. Flood-frequency characteristics of Wisconsin streams. Water Resource Investigation Report No. 03-4250. Wisconsin Department of Transportation, Reston , Virginia. pp 1-37.

Warburton ML, Schulze RE, Jewitt GPW. 2010. Confirmation of ACRU model results for applications in land use and climate change studies. Hydrology and Earth System Science 14: 2399–2414.

Wetterhall F, Winsenius HC, Dutra E, Werner M, Pappenberger E. 2015. Seasonal predictions of agro-meteorological drought indicators for the Limpopo basin. Hydrology and Earth Sysetem Sciences 19: 2577-2586.

Woessner WW. 2012. Formulating, applying and constraining hydrological models: Modeling 101. In: Water Center and School of Natural Resources Seminar, University of Nebraska, USA. pp 1-65.

Wu JQ. 2011. WEPP: A physically-oriented hydrology and erosion model for watershed assessment, management, and conservation. In: 2011 University of Washington Water Symposium, 18 April, University of Washington, Seattle. p 38.

Xiao B, Wang QH, Fan J, Han FP, Dai QH. 2011. Application of the SCS-CN model to runoff estimation in a Small Watershed with high spatial heterogeneity. Pedosphere 21: 738-749.

Xie X, Gu W, Wang B, Yang Q. 2012. Risk assessement of rainstorm and flood disaster based on multi-index. Communications in Information Science and Management Engineering 2: 10-16.

Xu C. 2002. Text Book of Hydrological Models. Xu C (ed.). Uppsala (Sweden): Uppsala University Department of Earth Sciences Hydrology.

Ye W, Bates BC, Viney NR, Sivapalan M, Jakeman AJ. 1997. Performance of conceptual rainfall-runoff models in low-yielding ephemeral catchments. Water Resource Research 33: 153-166.

Zhang L. Walker GR, Dawes WR. 2002. Water balance modelling: concepts and applications. Regional Water and Soil Assessment for Managing Sustainable Agriculture in China and Australia 84: 31-47.

Zuma BM, Luyt CD, Chirenda T, Tandlich R. 2012. Flood disaster management in South Africa: Legislative framework and current challenges. In: proceedings from the 2012 International Conference on Applied Life Sciences (ICALS2012), 10-12 September, Konya, Turkey. pp 127-132.

APPENDIX A

PARAMETERISATION USING SUFI-2 ALGORITHM

Table A.1: Parameter definitions and initial ranges used in SUFI-2 (Szezesniak and Piniewski, 2015)

Name	Lower Limit	Upper Limit	Definition
ESCO.hru	0.7	1	Soil evaporation compensation factor
SOL_AWC.sol	-0.4	0.4	Available water capacity of the soil layer
SOL_K.sol	-0.9	2	Saturated hydraulic conductivity
ALPHA_BF.gw	-0.9	2	Baseflow alpha factor (days)
GW_DELAY.gw	50	400	Groundwater delay time (days)
GWQMN.gw	0	1000	Threshold depth of water in the shallow aquifer required for return flow to occur
GW_REVAP.gw	0.02	0.2	Groundwater “revap” coefficient
CN2.mgt	-0.15	0.15	Initial SCS (Soil Conservation Service) runoff curve no. for moisture condition II
SURLAG.bsn	0.3	3	Surface runoff lag coefficient
REVAPMN	0	500	Threshold depth of water in the shallow aquifer for "revap" to occur (mm)
CH_K2	-0.01	500	Effective hydraulic conductivity in main channel alluvium
ALPHA_BNK	0	1	Baseflow alpha factor for bank storage

APPENDIX B

TABLES USED TO CALCULATE FOR SOLAR RADIATION

Table B.1 Angot's values of daily short-wave radiation flux R_A at the outer limit of the atmosphere in g cal cm^{-2}* as a function of the month of the year and the latitude (Source: adapted from Ncube, 2006).

LAT (DEG)	JAN	FEB	MAR	APR	MAY	JUN	JUL	AUG	SEP	OCT	NOV	DEC
N 90	0	0	55	518	903	1077	944	605	136	0	0	0
80	0	3	143	518	875	1060	930	600	219	17	0	0
60	86	234	424	687	866	983	892	714	494	258	113	55
40	358	538	663	847	930	1001	941	843	719	528	397	318
20	631	795	821	914	912	947	912	887	856	740	666	599
Equator	844	963	878	876	803	803	792	820	891	866	873	829
20	970	1020	832	737	608	580	588	680	820	892	986	978
40	998	963	686	515	358	308	333	453	648	817	994	1033
60	947	802	459	240	95	50	77	187	403	648	920	1013
80	981	649	181	9	0	0	0	0	113	459	917	1094
S 90	995	656	92	0	0	0	0	0	30	447	932	1110

*** 1 g cal m^{-2} = 0.0419 MJ m^{-2}**

Table B.2 Mean daylength (h) for different months and latitudes (Source: Ncube, 2006).

LATITUDE (° SOUTH)	JUL	AUG	SEP	OCT	NOV	DEC	JAN	FEB	MAR	APR	MAY	JUN
50	8.5	10.1	11.8	13.8	15.4	16.3	15.9	14.5	12.7	10.8	9.1	8.1
48	8.8	10.2	11.8	13.6	15.2	16.0	15.6	14.3	12.6	10.9	9.3	8.3
46	9.1	10.4	11.9	13.5	14.9	15.7	15.4	14.2	12.6	10.9	9.5	8.7
44	9.3	10.5	11.9	13.4	14.7	15.4	15.2	14.0	12.6	11.0	9.7	8.9

42	9.4	10.6	11.9	13.4	14.6	15.2	14.9	13.9	12.5	11.1	9.8	9.1
40	9.6	10.7	11.9	13.3	14.4	15.0	14.7	13.7	12.5	11.2	10.0	9.3
35	10.1	11.0	11.9	13.1	14.0	14.5	14.3	13.5	12.4	11.3	10.3	9.8
30	10.4	11.1	12.0	12.9	13.6	14.0	13.9	13.2	12.4	11.5	10.6	10.2
25	10.7	11.3	12.0	12.7	13.3	13.7	13.5	13.0	12.3	11.6	10.9	10.6
20	11.0	11.5	12.0	12.6	13.1	13.3	13.2	12.8	12.3	11.7	11.2	10.9
15	11.3	11.6	12.0	12.5	12.8	13.0	12.9	12.6	12.2	11.8	11.4	11.2
10	11.6	11.8	12.0	12.3	13.6	12.7	12.6	12.4	12.1	11.8	11.6	11.5
5	11.8	11.9	12.0	12.2	12.3	12.4	12.3	12.3	12.1	12.0	11.9	11.8
0	12.1	12.1	12.1	12.1	12.1	12.1	12.1	12.1	12.1	12.1	12.1	12.1

SOIL AND LAND USE TABLES CREATED FOR SWAT MODEL

Table B.3: Soil properties and classification for Luvuvhu River catchment

SNAM	HYDGRP	TEXTURE	SOL_BD1	SOL_AWC1	SOL_K1	SOL_CBN1
Fb359	A	LS	1.24	0.013327	0.0156	0.61
Fc484	A	LS	1.24	0.013327	0.0156	0.61
Ae267	A	LS	1.24	0.013327	0.0156	0.61
Ia113	A	S	1.25	0.017587	0.0176	0.71
Ae268	A	LS	1.24	0.013327	0.0156	0.61
Fc485	A	SL	1.19	0.03343	0.00347	0.71
Ib315	A	LS	1.24	0.013327	0.0156	0.61
Ea206	C	SCL	1.3	0.041541	0.00063	0.19
Fc729	A	LS	1.24	0.013327	0.0156	0.61
Fc728	A	SL	1.19	0.03343	0.00347	0.71
Ae332	A	LS	1.24	0.013327	0.0156	0.61
Fc486	A	SL	1.19	0.03343	0.00347	0.71
Fb499	A	SL	1.19	0.03343	0.00347	0.71
Fc488	A	SL	1.19	0.03343	0.00347	0.71
Fc487	A	SL	1.19	0.03343	0.00347	0.71
Ae331	A	LS	1.24	0.013327	0.0156	0.61

Fb498	A	LS	1.24	0.013327	0.0156	0.61
Ib313	A	LS	1.24	0.013327	0.0156	0.61
Ac164	A	LS	1.24	0.013327	0.0156	0.61
Bc47	A	LS	1.24	0.013327	0.0156	0.61
Ib442	A	SL	1.19	0.03343	0.00347	0.71
Ah109	A	LS	1.24	0.013327	0.0156	0.61
Fb358	A	LS	1.24	0.013327	0.0156	0.61
Ab181	A	LS	1.24	0.013327	0.0156	0.61
Ea161	C	SCL	1.3	0.041541	0.00063	0.19
Ae330	A	SL	1.19	0.03343	0.00347	0.71
Ba62	A	SL	1.19	0.03343	0.00347	0.71
Ib443	A	SL	1.19	0.03343	0.00347	0.71
Dc51	C	SCL	1.3	0.041541	0.00063	0.19
Ba60	A	LS	1.24	0.013327	0.0156	0.61
Ca93	A	SL	1.19	0.03343	0.00347	0.71
Ae329	A	SL	1.19	0.03343	0.00347	0.71
Ba61	A	LS	1.24	0.013327	0.0156	0.61
Bd56	A	SL	1.19	0.03343	0.00347	0.71
Ib441	A	SL	1.19	0.03343	0.00347	0.71
Ea205	A	SL	1.19	0.03343	0.00347	0.71
Ab178	A	SL	1.19	0.03343	0.00347	0.71
Ab180	C	SCL	1.3	0.041541	0.00063	0.19
Fb496	A	SL	1.19	0.03343	0.00347	0.71
Fa756	A	SL	1.19	0.03343	0.00347	0.71
Ab177	D	SC	1.3	0.020626	0.000217	0.38
Ae328	A	SL	1.19	0.03343	0.00347	0.71
Ab179	A	SL	1.19	0.03343	0.00347	0.71
Water	D	C	0	0	260	0
Ib304	A	LS	1.24	0.013327	0.0156	0.61
Bb128	A	LS	1.24	0.013327	0.0156	0.61
Ib440	A	LS	1.24	0.013327	0.0156	0.61
Ab173	D	SC	1.3	0.020626	0.000217	0.38
Ab109	C	SCL	1.3	0.041541	0.00063	0.19
Ab111	C	SCL	1.3	0.041541	0.00063	0.19

Ab108	C	SCL	1.3	0.041541	0.00063	0.19
Ab151	A	SL	1.19	0.03343	0.00347	0.71
Fa535	A	SL	1.19	0.03343	0.00347	0.71
Ab107	C	SCL	1.3	0.041541	0.00063	0.19
Ae291	C	SCL	1.3	0.041541	0.00063	0.19
Ae260	C	SCL	1.3	0.041541	0.00063	0.19
Fa308	A	SL	1.19	0.03343	0.00347	0.71
Bd48	A	LS	1.24	0.013327	0.0156	0.61
Ca102	A	SL	1.19	0.03343	0.00347	0.71
Bc48	A	LS	1.24	0.013327	0.0156	0.61
Bc54	A	SL	1.19	0.03343	0.00347	0.71
Fa331	A	SL	1.19	0.03343	0.00347	0.71
Fa396	A	LS	1.24	0.013327	0.0156	0.61
Ca91	A	SL	1.19	0.03343	0.00347	0.71
Fa306	A	LS	1.24	0.013327	0.0156	0.61
Fa754	A	SL	1.19	0.03343	0.00347	0.71
Ab174	C	SCL	1.3	0.041541	0.00063	0.19
Ab175	C	SCL	1.3	0.041541	0.00063	0.19
Bc50	A	LS	1.24	0.013327	0.0156	0.61

APPENDIX C

WATERSHED SOIL INFORMATION

Table C.1 Soil hydrological input parameters for different textural classes (Source: Ncube, 2006)

Soil texture class	Horizon	Typical percentages of:				Bulk density (Mg m^{-3})	Effective porosity (m^3 m^{-3})
		Clay	Silt	Sand	Organic Carbon		
Clay	Topsoil	50	37	13	0.38	1.21	0.536
	Subsoil					1.37	0.470
Loam	Topsoil	18	25	57	0.52	1.18	0.512
	Subsoil					1.42	0.464
Sand	Topsoil	3	4	93	0.71	1.25	0.452
	Subsoil					1.50	0.430
Loamy sand	Topsoil	7	7	86	0.61	1.24	0.457
	Subsoil					1.51	0.432
Sandy loam	Topsoil	10	15	75	0.71	1.19	0.505
	Subsoil					1.46	0.448
Silty loam	Topsoil	18	55	27	0.58	1.07	0.527
	Subsoil					1.34	0.495
Sandy clay loam	Topsoil	27	8	65	0.19	1.30	0.486
	Subsoil					1.58	0.393
Clay loam	Topsoil	32	22	46	0.10	1.17	0.497
	Subsoil					1.41	0.451

Silty clay loam	Topsoil	33	46	51	0.13	1.23	0.509
	Subsoil					1.40	0.469
Sandy clay	Topsoil	40	5	55	0.38	1.30	0.430
	Subsoil					1.53	0.423
Silty clay	Topsoil	50	37	13	0.38	1.22	0.531
	Subsoil					1.38	0.476

Table C.2 Land types with spatial information and soil patterns

Broad soil pattern code	DESCRIPTION
Aa	Freely drained, red and yellow apedal soils with humic topsoils comprise >40% of the land type
Ab	Freely drained, red and yellow, dystrophic/mesotrophic, apedal soils comprise >40% of the land type (yellow soils <10%)
Ac	Freely drained, red and yellow, dystrophic/mesotrophic, apedal soils comprise >40% of the land type (red and yellow soils each >10%)
Ad	Freely drained, red and yellow, dystrophic/mesotrophic, apedal soils comprise >40% of the land type (red soils comprise <10%)
Ae	Freely drained, red, eutrophic, apedal soils comprise >40% of the land type (yellow soils comprise <10%)
Af	Freely drained, red, eutrophic, apedal soils comprise >40% of the land type (yellow soils comprise <10%); with dunes
Ag	Freely drained, shallow (<300 mm deep), red, eutrophic, apedal soils comprise >40% of the land type (yellow soils comprise <10%)
Ah	Freely drained, red and yellow, eutrophic, apedal soils comprise >40% of the land type (red and yellow soils each comprise >10%)
Ai	Freely drained, yellow, eutrophic, apedal soils comprise >40% of the land type (red soils comprise <10%)

Ba	Red and yellow, dystrophic/mesotrophic, apedal soils with plinthic subsoils (plinthic soils comprise >10% of land type, red soils comprise >33% of land type)
Bb	Red and yellow, dystrophic/mesotrophic, apedal soils with plinthic subsoils (plinthic soils comprise >10% of land type, red soils comprise <33% of land type)
Bc	Red and yellow, eutrophic, apedal soils with plinthic subsoils (plinthic soils comprise >10% of land type, red soils comprise >33% of land type)
Bd	Red and yellow, eutrophic, apedal soils with plinthic subsoils (plinthic soils comprise>10% of land type, red soils comprise <33% of land type)
Ca	Land type qualifies as Ba-Bd, but >10% occupied by upland duplex/margalitic soils
Da	Duplex soils (sandier topsoil abruptly overlying more clayey subsoil) comprise >50% of land type; >50% of duplex soils have red B horizons
Db	Duplex soils (sandier topsoil abruptly overlying more clayey subsoil) comprise >50% of land type; <50% of duplex soils have non-red B horizons
Dc	Either red or non-red duplex soils (sandier topsoil abruptly overlying more clayey subsoil) comprise >50% of land type; plus >10% occupied by black or red clays
Ea	Black or red clays comprise >50% of land type
Fa	Shallow soils (Mispah and Glenrosa forms) predominate; little or no lime in landscape
Fb	Shallow soils (Mispah and Glenrosa forms) predominate; usually lime in some of the bottomlands in landscape
Fc	Shallow soils (Mispah and Glenrosa forms) predominate; usually lime throughout much of landscape
Ga	Podzols occur (comprise >10% of land type); dominantly deep
Gb	Podzols occur (comprise >10% of land type); dominantly shallow
Ha	Deep grey sands dominant (comprise >80% of land type)
Hb	Deep grey sands sub dominant (comprise >20% of land type)
Ia	Deep alluvial soils comprise >60% of land type
Ib	Rock outcrops comprise >60% of land type
Ic	Rock outcrops comprise >80% of land type

Table C.3 Average depth and average clay class that define different land types

AVR_DEPTH_CLASS	Dominant depth class of land type
D1	Percentage of Land Type with very shallow soils (≤300 mm)
D2	Percentage of Land Type with shallow soils (300-600 mm)
D3	Percentage of Land Type with mod. deep soils (601-900 mm)
D4	Percentage of Land Type with deep soils (901-1200 mm)
D5	Percentage of Land Type with very deep soils (>1200 mm)
AVR_CLAY_CLASS	**Average topsoil clay percentage of land type**
C1	Percentage of Land Type with sandy soils (≤6%)
C2	Percentage of Land Type with loamy sand soils (6.1-15%)
C3	Percentage of Land Type with sandy loam soils (15.1-25%)
C4	Percentage of Land Type with sandy clay loam soils (25.1-35%)
C5	Percentage of Land Type with sandy clay /clay soils (35.1-55%)
C6	Percentage of Land Type with very clayey soils (>55%)

Table C.4 Description of hydrologic soil groups according to soil texture classes

HSG	Soil Textures
A	Sand, loamy sand, or sandy loam
B	Sandy clay loam
C	Silt loam or loam
D	Clay loam, silty clay loam, sandy clay, silty clay, or clay

APPENDIX D

SWAT MODEL SET UP AND PROCESS

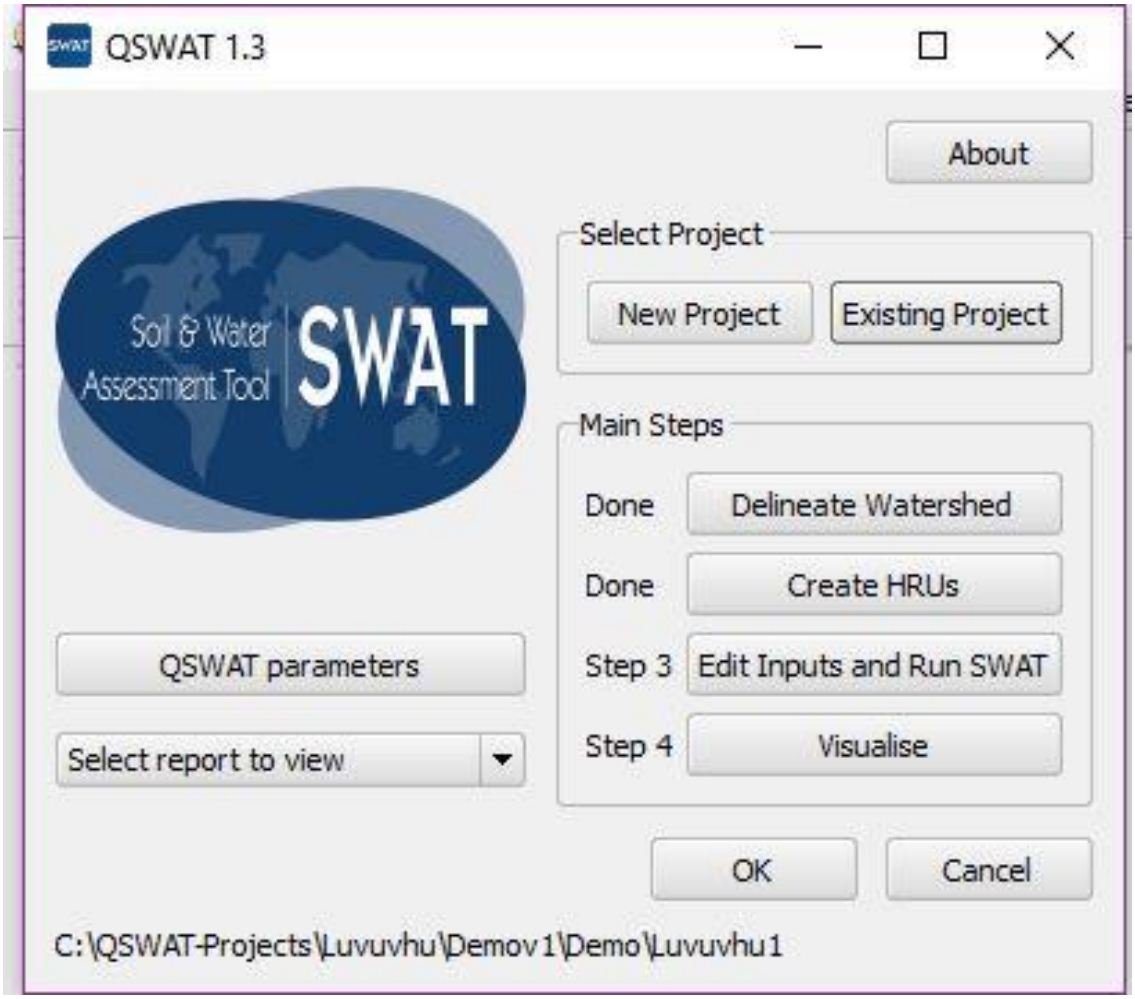

Figure D.1 Model setup interface window in the QSWAT program

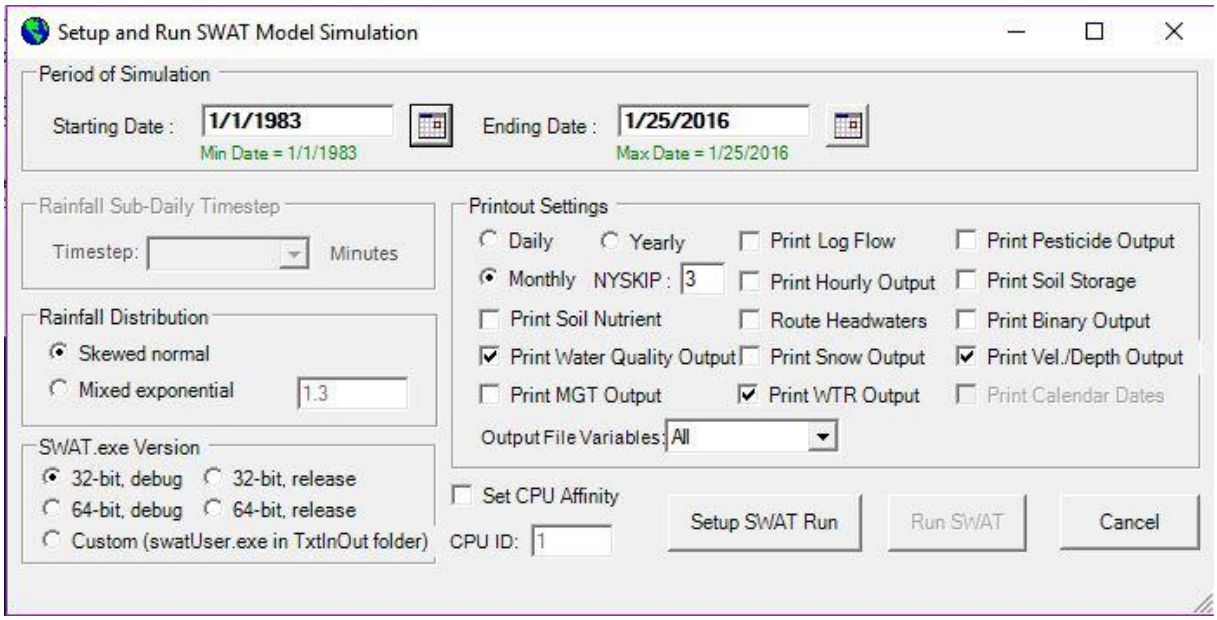

Figure D.2 SWAT model simulation and run window

APPENDIX E

SELECTION OF CURVE NUMBER AND CHARACTERISATION, AND SENSITIVITY ANALYSIS

Table E.1 Representative curve number values for pasture, grassland and woods

Cover description		Curve numbers for hydrologic soil group			
Cover type	Hydrologic condition	A	B	C	D
Pasture, grassland, or range—continuous forage for grazing. [2]	Poor	68	79	86	89
	Fair	49	69	79	84
	Good	39	61	74	80
Meadow—continuous grass, protected from grazing and generally mowed for hay.	—	30	58	71	78
Brush—brush-weed-grass mixture with brush the major element. [3]	Poor	48	67	77	83
	Fair	35	56	70	77
	Good	30 [4]	48	65	73
Woods—grass combination (orchard or tree farm). [5]	Poor	57	73	82	86
	Fair	43	65	76	82
	Good	32	58	72	79
Woods. [6]	Poor	45	66	77	83
	Fair	36	60	73	79
	Good	30 [4]	55	70	77
Farmsteads—buildings, lanes, driveways, and surrounding lots.	—	59	74	82	86

[1] Average runoff condition, and $I_a = 0.2S$.

[2] *Poor:* <50% ground cover or heavily grazed with no mulch.
Fair: 50 to 75% ground cover and not heavily grazed.
Good: > 75% ground cover and lightly or only occasionally grazed.

[3] *Poor:* <50% ground cover.
Fair: 50 to 75% ground cover.
Good: >75% ground cover.

[4] Actual curve number is less than 30; use CN = 30 for runoff computations.

[5] CN's shown were computed for areas with 50% woods and 50% grass (pasture) cover. Other combinations of conditions may be computed from the CN's for woods and pasture.

[6] *Poor:* Forest litter, small trees, and brush are destroyed by heavy grazing or regular burning.
Fair: Woods are grazed but not burned, and some forest litter covers the soil.
Good: Woods are protected from grazing, and litter and brush adequately cover the soil.

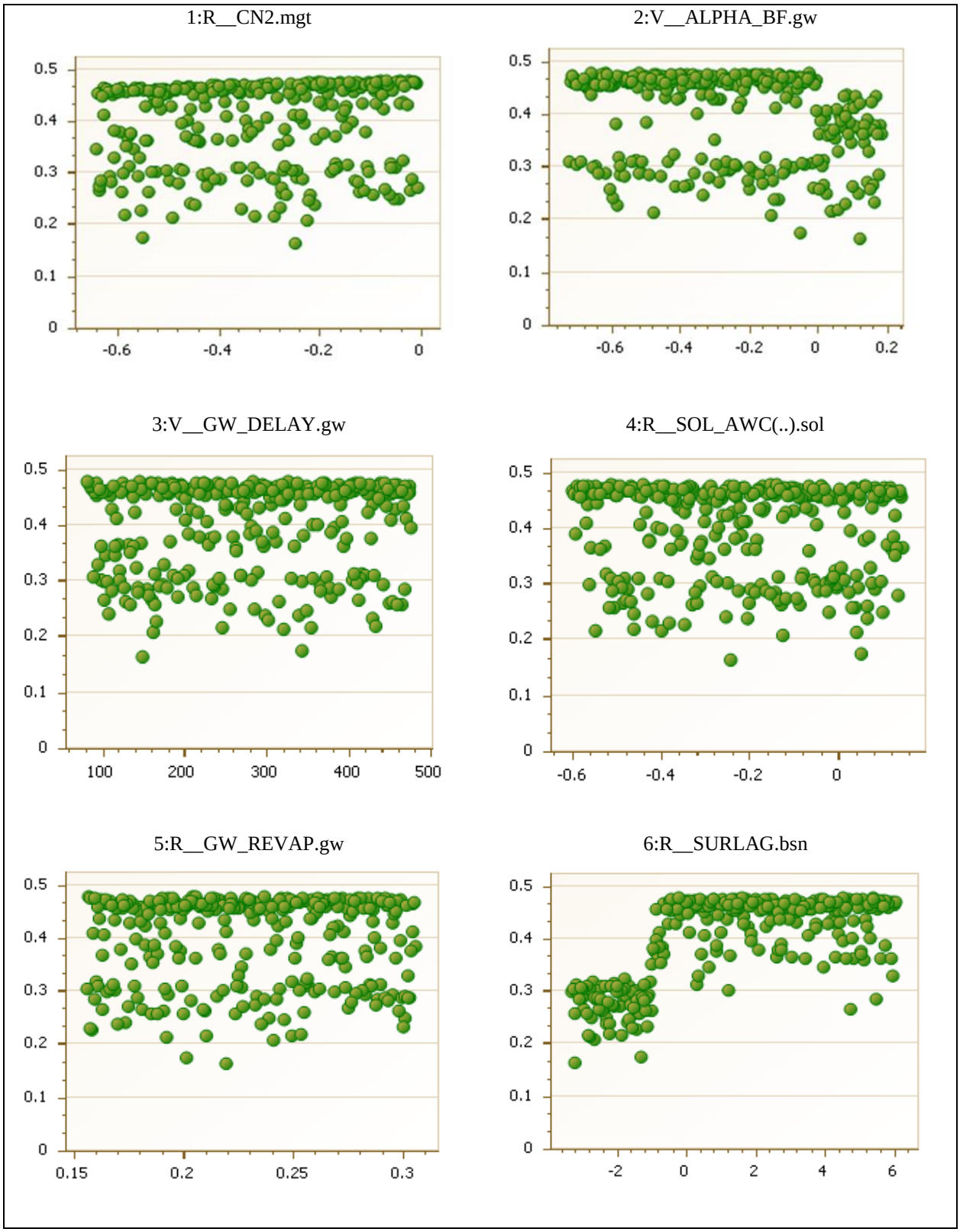

Figure E.1 Scatter plots of sensitive parameters showing the sensitivity of model parameters for streamflow discharge

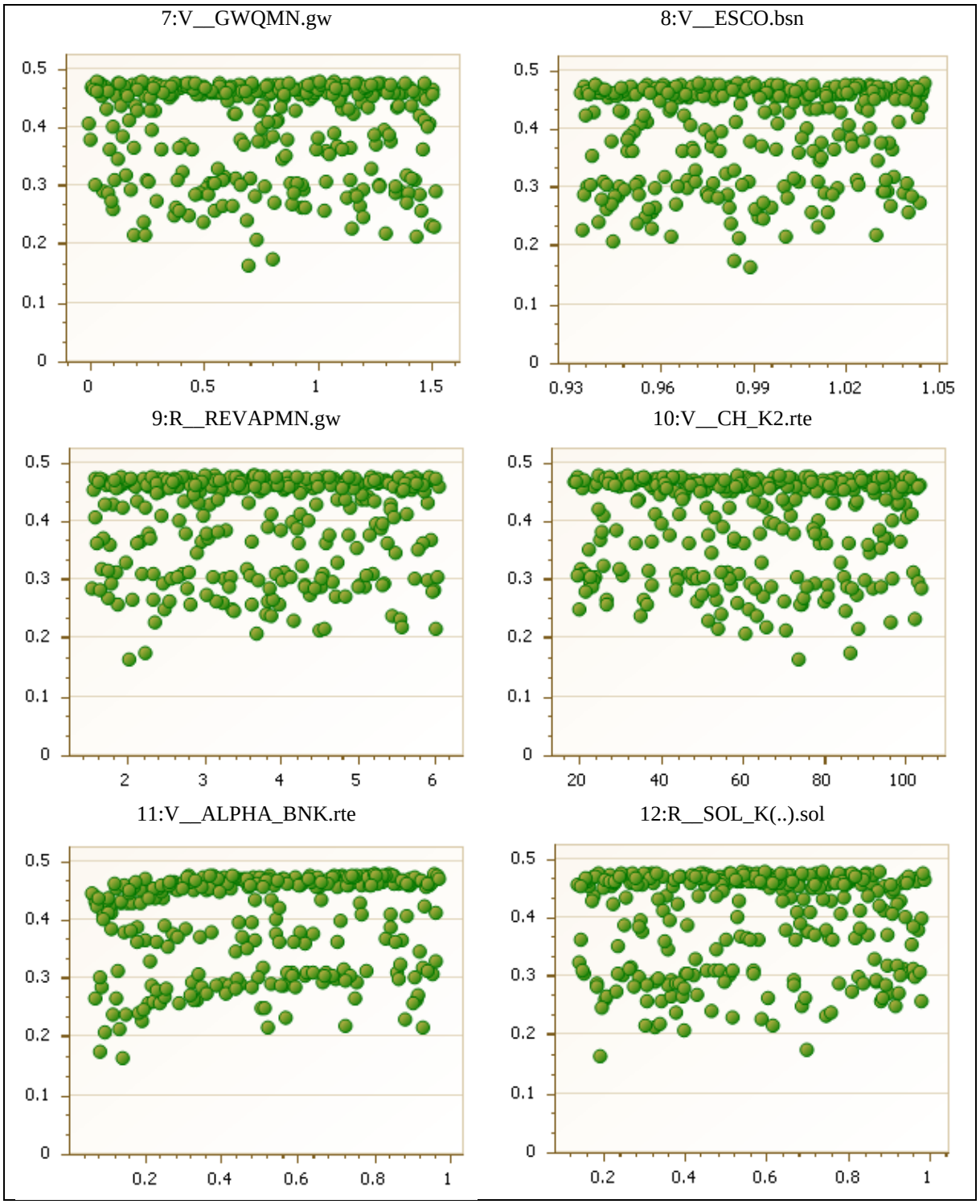

Figure E.1 (Continued) Scatter plots of sensitive parameters showing the sensitivity of model parameters for streamflow discharge continued